ON THERMAL CONVECTIVE INSTABILITY IN ROTATING FLUIDS

A THESIS SUBMITTED TO THE UNIVERSITY OF KWAZULU-NATAL
FOR THE DEGREE OF DOCTOR OF PHILOSOPHY OF SCIENCE
IN THE COLLEGE OF AGRICULTURE, ENGINEERING & SCIENCE

By

Osman.A.I. Noreldin

School of Mathematics, Statistics & Computer Science

December 2018

Contents

Abstract

The study of the impact of fluid rotation and a magnetic field in the development of Rayleigh-Bénard convective instabilities in a fluid is important due to the wide range of settings where these occur naturally such as in astrophysical and geophysical flows. In this thesis we investigate the development of Rayleigh-Bénard convective instabilities in four different flow settings, such as in a rotating horizontal layer and in an inclined cavity, using analytical and numerical techniques to solve the flow equations. The numerical methods of particular interest include the multidomain spectral collocation method.

We first study the onset of instability in a horizontal porous layer of a cross diffusive nanofluid flow using the Darcy model, with stress-free conditions and zero nanoparticle flux at the boundary. We consider linear regimes, and use normal mode analysis and the Galerkin method to solve the evolution equations. The influence of important parameters on the critical Rayleigh number is investigated. We show, among other results, that increasing the magnetic field parameter, the Darcy and the nanofluid Lewis numbers delay the onset of flow instabilities.

For weakly nonlinear stability analysis of the convective flow, we assume zero nanoparticle flux at the wall. A truncated Fourier series is used to reduce the flow equations to a Lorenz-type system of nonlinear evolution equations that describe the growth of the convection amplitudes in the nanofluid flow. These equations are solved using the multidomain spectral collocation method,

and solutions are obtained as sets of trajectories in the phase plane. Some novel bifurcations are obtained, and their sensitivity to the Rayleigh number analysed. The influence of the parameters such as the Dufour and Soret parameters on heat and mass transport are investigated. We further study thermal instability in double-diffusive convection in an inclined open square cavity subjected to an inclined magnetic field. Using a truncated Fourier series, we obtain a multi-dimensional trapping region for the convection amplitudes. The changes in heat and mass transport are investigated for different physical parameters, such as the magnetic field, Prandtl, and Lewis numbers. The magnetic field and Lewis number are found to increase heat and mass transport.

The study further investigates thermo-convective instability in a rotating ferromagnetic fluid with temperature modulation at the boundaries. Using the weakly nonlinear stability theory, the impact of certain physical parameters such as the Taylor number, magnetization parameter and the ratio of the magnetic force to buoyancy are analyzed. The heat transfer for in-phase and out-of-phase convective oscillations is analyzed.

In this study, we determine the criteria for the onset of convective instabilities in terms of certain physical parameters such as the Hartman, Darcy and Taylor numbers. We show that increasing these parameters has the effect of delaying the onset of convective instabilities and to increase heat and mass transport in the fluid flow. However, parameters such as the Dufour and Soret parameters have the effect of, respectively, reducing and increasing the critical Rayleigh number for the onset of instabilities.

Declaration 1-Plagiarism

I, Osman. A.I. Noreldin, declare that the research reported in this thesis, except where otherwise indicated, is my original research. This thesis has not been submitted for any degree or examination at any other university. This thesis does not contain other persons' data, pictures, graphs or other information, unless specifically acknowledged as being sourced from other persons. This thesis does not contain other persons' writing, unless specifically acknowledged as being sourced from other researchers. Where other written sources have been quoted, then their words have been re-written but the general information attributed to them has been referenced, or where their exact words have been used, then their writing has been placed in italics and referenced. This thesis does not contain text, graphics or tables copied and pasted from the internet, unless specifically acknowledged, and the source being detailed in the thesis and in the reference sections.

Signature: ....

Osman.A.I. Noreldin Date

Signature: ....

Prof. P. Sibanda Date

Declaration 2: Publications

1 Noreldin I. A O., Mondal S., Sibanda P. (2019). Onset of instability in a horizontal porous layer of a cross diffusive nanofluid flow. Paper presented at International Conference Numerical Heat Transfer and Fluid Flow at: NIT Warangal, India Under review in Numerical Heat Transfer and Fluid Flow Lecture Notes, Mechanical Engineering, SBN 978-981-13-1902-0.
I formulated the flow problem and drafted the manuscript. This paper appears as Chapter 2.

2 Noreldin I. A O., Sibanda P., Mondal S. (2018). Weakly Nonlinear Stability Analysis of a Nanofluid in a Horizontal Porous Layer Using a Multi-domain Spectral Collocation Method. In: Complexity in Biological and Physical Systems-Bifurcations, Solitons and Fractals,In IntechOpen, http://dx.doi.org/10.5772/intechopen.71066
I formulated the flow and obtained the numerical solution of the amplitude evolution equations and drafted the manuscript. This paper appears as Chapter 3.

3 Noreldin I. A O., Mondal S., Sibanda P. (2018). Thermal instability of double-diffusive natural convection in an inclined open square cavity. Acta Technica (3): 385- 406.
I formulated the flow problem, found the numerical solution of the amplitude convection equations and drafted the manuscript. This paper appears as Chapter 4.

4 Noreldin I. A O. and Sibanda P. (2018).Thermo-convective instability in a rotating ferromagnetic fluid layer with temperature modulation. Open Phys 16:868-888.
I formulated the flow problem, found the numerical solution of the amplitude convection equations and drafted the manuscript. This paper appears as Chapter 5.

Signature: ....

Osman. A. I. Noreldin   Date

Disclaimer

This document describes work undertaken as a PhD programme of study at the School of Mathematics, Statistics, & Computer Science, University of KwaZulu-Natal, from August 2015 to December 2018. All views and opinions expressed herein remain the sole responsibility of the author, and do not necessarily represent those of the institution.

Signature: ....

Osman.A.I. Noreldin Date

Acknowledgments

I would like to express my sincere gratitude to my supervisor Prof Precious Sibanda for his support.

My sincere thanks to Prof Sandile Motsa who introduced me to spectral collocation methods. I am also grateful to Dr Sabyasachi Mondal for the fruitful collaboration. My sincere thank you to my lovely wife Amna and my son Muaid.

I would also like to thank the School of Mathematics, Statistics and Computer Science administration and technical staff, Christel, Bev, Zibuyile, Sandile and others. I would also like to extend my gratitude to all my colleagues and friends for their support and guidance.

Last but not least, I would like to thank my family: my mother and my brothers and sisters for supporting me spiritually throughout this journey.

Dedication

This study is dedicated to my mother, my beloved wife and my son who have supported me all the way since the beginning of my studies. It is also dedicated to all the Sudanese who live in refugee camps until the dawn of a new era in which they can live in freedom. Finally, this study is dedicated to all those who believe in the richness of education.

Chapter 1

Introduction

1.1 Background and Motivation

This study is concerned with the growth of instabilities due to the flow and rotation of fluids subjected to various external stimuli, such as an applied magnetic field and temperature modulation. The study follows the theoretical framework for the Rayleigh-Bénard convection in hydrodynamic and hydromagnetic flows and the problem of the onset of thermal convective instability in a horizontal layer of fluid [1]. The flow is due to the development of convective instability if the static vertical temperature gradient is large. In such flows convection enhances the rate of heat and mass transfer through the fluid layer compared to the case of simple molecular conduction. The magnitude of the heat and mass flux in convective fluids is thus much higher than the heat and mass flux due to thermal conduction.

Rayleigh-Bénard convection problems play an important role in nature in a wide variety of situations such as in astrophysical and geophysical flows [2]. Important common examples include the warming of the atmosphere and oceans through convection currents, the dynamo action of convection flow in the liquid core of the Earth, crystallization processes and solar heating devices. The

first significant attempt to explain thermal convection appears to have been made by Thomson [3]. However, the phenomenon of convection in a horizontal fluid layer heated from below was first investigated experimentally by Rayleigh [1], who also provided the theoretical framework underpinning the now common approaches for the solution of the resulting equations. He developed the linear stability theory for the flow instabilities using the Oberbeck-Boussinesq approximation. His results showed that instability would occur only when the adverse temperature gradient is very large, that is, when the Rayleigh number defined by

$$Ra = \frac{\alpha\beta g h^4}{\kappa\nu},$$

exceeds a certain critical value. Here, α is the thermal expansion coefficient, β is the temperature difference between top and bottom layer, g is the acceleration due to gravity, h is the depth of the layer of fluid, κ is the thermal diffusivity and ν is the kinematic viscosity. When this critical value is exceeded, fluid motion takes place only on a large horizontal scale. Finding the value of the Rayleigh number requires solving an eigenvalue problem for thermal instability in a horizontal fluid layer. The onset of the convection occurs at the critical Rayleigh number, which is independent of the material properties of the convection fluid. A sketch of the neutral curve of the convective instability in the (Ra, a)-plane is shown in Figure 1.1, where a denotes the wavenumber. The fluid layer is convectively unstable if the Rayleigh number Ra is greater than the critical Rayleigh number Ra^c and stable if it is less than the critical value. The case $Ra = Ra^c$ corresponds to neutral or marginal stability. When the Rayleigh number increases, the gravitational forces become more dominant and at the critical Rayleigh number instability sets in and convection cells appear.

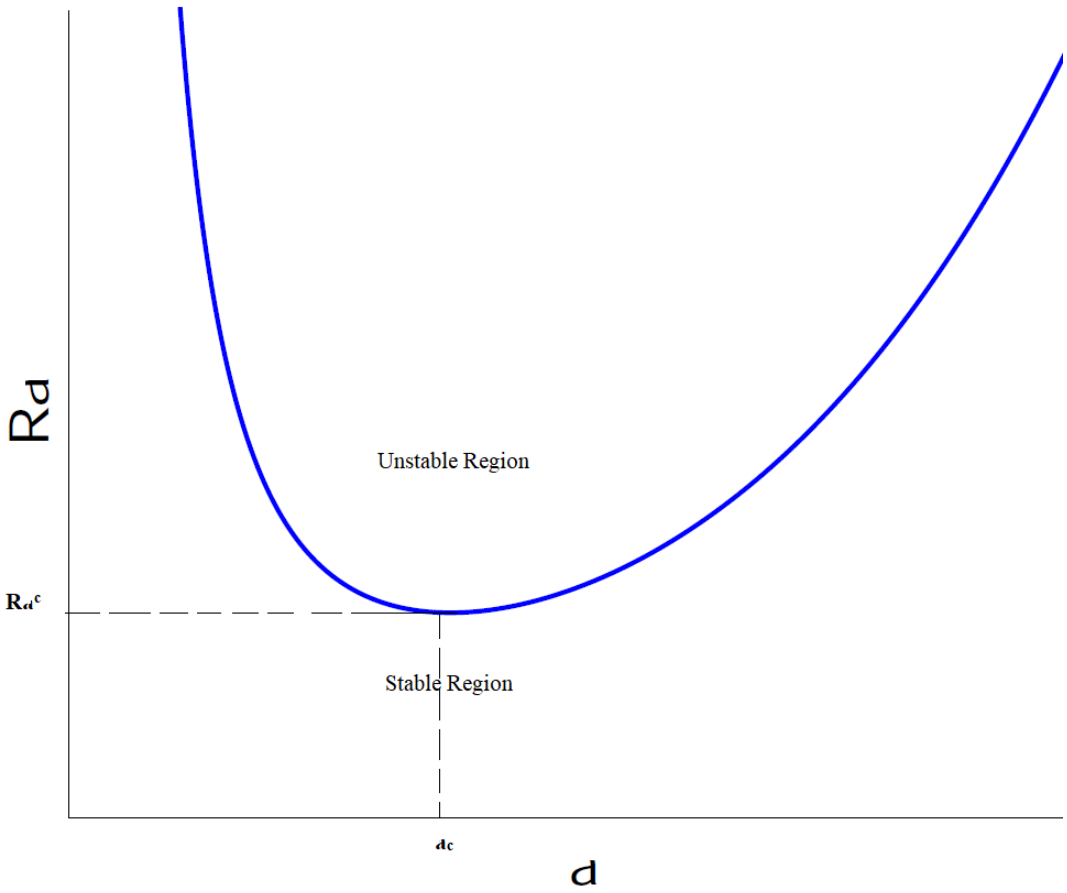

Figure 1.1: The neutral curve of the convective instability and the critical Rayleigh number, Ra^c.

Rayleigh-Bénard convection differs from the Bénard-Marangoni mechanism in certain important ways. In Bénard-Marangoni convection the temperature fluctuation at the surface induces tangential stresses that can be amplified by the hot fluid from the inside. In this study our attention is focussed only on the Rayleigh-Bénard convection, which is a model for many natural flows including those undergoing a rotation, radiation and phase changes. The theory of hydrodynamic stability adequately explains the physics of the motion of a fluid in a horizontal layer, in which top and bottom boundaries are held at fixed temperatures.

A comprehensive study of thermal convective instability in a horizontal layer is given by Chandrasekhar [2] for a linearized problem. The problem of Rayleigh-Bénard convection was extended to include the effects of rotation and a magnetic field. The derivation of hydrodynamic equations and an analysis of flow instabilities can also be found in the book by Drazin and Reid [4]. A study of the structure and dynamics of Rayleigh-Bénard convection has also been reported by Getling [5] and Koschmieder [6]. In all these studies it was shown that if the Rayleigh number is less than or equal to its critical value, all disturbance modes are stable, and when the Rayleigh number assumes a super-critical value, at least one of the disturbance modes is unstable.

Over the last few decades the onset of thermal convective instability in a horizontal layer heated from below has become an increasingly popular topic for researchers. Among these, Chapman and Proctor [7] studied thermal convection instability in horizontal layer of fluid heated from below with the assumption that the heat flux at the boundaries was unaffected by the fluid motion. They used an expansion method to seek a time independent solution for the two dimensional problem. At fixed temperature the basic state is unstable if the Rayleigh number is sufficiently large. Their results showed that when the Rayleigh number is above the critical value for the onset of convection, the motion in the horizontal layer is much greater than it is at depth. When the Rayleigh number, on the one hand, exceeded the critical value the heat transport by convection reduces the potential for instability in the flow. On the other hand, thermal diffusion and viscous friction increases due to the horizontal gradient imposed by the modulation. In addition to the Rayleigh number the stability of a fluid in a horizontal layer depends on the wave number of the convection

cells and the Prandtl number, the later defined as

$$Pr = \frac{\nu}{\kappa},$$

where ν and κ are as previously defined. A review of Rayleigh-Bénard convection problem in nonlinear dynamics and the transition to turbulence is given in Busse [8] where the impact of the Rayleigh number and Prandtl number on the stability of convection cells was studied. Kelly and Hu [9] investigated thermal convection in nonplanar oscillatory flow. Linear stability analysis was used to explore the onset of thermal convection in non-planar oscillatory flow. Their results showed that increasing the Prandtl number destabilizes the system.

Many of the earlier studies were on unsteady fluid motions. Chana and Daniels [10] studied the onset of thermal convection in an infinite horizontal rectangular channel. The hydrodynamic flow was assumed to be in steady linear motion and the equations were simplified using the Oberbeck-Boussinesq approximation. They used a two-dimensional Galerkin method to predict the onset of the thermal convection instability. The influence of the aspect ratio of the channel on critical Rayleigh and wave numbers was investigated. Their results showed that values of the critical Rayleigh number and wave number were in a good agreement with the asymptotic solution for small and large aspect ratios.

A numerical study of Rayleigh-Bénard convection for a boundary layer turbulent flow was studied by Shi et al. [11]. They considered a cylindrical cell with aspect ratio of unity for a high Rayleigh number and Prandtl number $Pr = 0.7$ representing air at room temperature. Their boundary layer analysis shows that the near wall dynamics of the flow combine elements of forced Blasius type and natural convection. A similar study was considered by Scheel et al. [12]. They found that the mean velocity boundary layer profiles collapsed well for a Rayleigh number above 10^6, on the other hand the thermal boundary layer profiles did not collapse for that value of the Rayleigh number. Although the analysis was similar to Shi et al. [11], but the issue of the collapse of the boundary layer profiles is not discussed. Hirata et al. [13] adopted linear stability analysis to investigated viscoelastic fluid flow with a horizontal throughflow and a vertical temperature gradient. A one-mode Galerkin expansion method and shooting technique was used to solve the boundary value

problem and predict the onset of thermal instability convection in a viscoelastic fluid. Their results showed that longitudinal rolls were the most unstable modes at the onset of convection instability. Further, as the fluid elasticity increases a throughflow stabilization of transverse rolls in weakly regime was found. Related studies on numerical investigations of Rayleigh-Bénard convection in viscoelastic/viscoplastic fluids were presented by Park [14], Aghighi et al. [15]. Recently, Wesfreid [16] gave a detailed historical review of Rayleigh-Bénard studies on thermal convection and vortex shedding.

Rayleigh-Bénard convection with a zero Prandtl number was investigated by Thual [17] for both no slip and free-slip boundary conditions. His numerical results suggested that the stationary and oscillatory instabilities interact closely for a zero Prandtl number. Later, the same problem was extended to low Prandtl numbers for the bifurcation structure near the onset of convection by Nandukumar and Pal [18]. They used direct numerical simulation to predict the instabilities and chaos in the Rayleigh-Bénard convection at low Prandtl numbers. They suggested that the results for very low Prandtl numbers were similar to those for the zero Prandtl numbers case. However, the bifurcation structure on the the onset of convective for a zero and low Prandtl numbers fluid including wavy rolls and stationary cross rolls has been considered in study by Nandukumar and Pal [18], but this has not been considered in study by Thual [17].

There are many experimental and theoretical investigations of the onset of thermal convection in a horizontal fluid layer heated from below. Among many others, Chillà and Schumacher [19], Xia [20], Lowman and Jarvis [21] investigated the experimental aspects of the Rayleigh-Bénard convection. These studies suggested that investigation of an extension of the Rayleigh-Bénard convection to nonclassical Rayleigh-Bénard convection is an important direction for future research. Recently, Wang et al. [22] studied experimentally thermal convection with mixed thermal boundary conditions. They found that upwelling of hot fluid always occurs beneath lids while on the other hand downwelling of cold fluid occurs beneath the conducting walls.

1.2 Convection in a porous layer

A porous medium consists of a solid matrix with interconnected voids that allow the fluid to pass through the material. Typical examples of porous media include sand, sandstone, wood, limestone and bread. Studies of convection in a horizontal layer of porous medium heated from below were reported by Horton and Rogers [23] and Lapwood [24]. The convection in a porous medium differs from the standard Rayleigh-Bénard convection in a horizontal layer heated from below, although the onset of thermal convection instabilities of flows is similar. Cheng [25] studied thermal convective heat transport in porous media with high permeability. He used the integral method to solve the equations that model free and mixed convection in the medium. The convective heat and mass transport in a porous medium have very important applications in engineering and geophysics, such as in thermo-solutal convection in geothermal fields.

The onset of thermal instability in boundary layer flow in a porous medium was investigated by Wooding [26] who used linear stability to analyse the fluid motion. He calculated critical values of the Rayleigh and wave numbers. His results showed that the layer is stable at the critical value and that the wave number of the critical growth disturbance is finite. For convection in a porous medium, the primary flow is very slow and thermal diffusion from the boundary layer into the porous medium becomes important and a thermal boundary layer appears. The vertical component of the flow may be assumed to be constant and the steady state flow density is distributed exponentially. In convection in a porous medium, the system is highly nonlinear due to heat transport. The boundary conditions of convection in a porous medium are also important for the instability to occur. Elder [27] investigated, both experimentally and numerically, steady convection in a layer of homogeneous horizontal porous medium heated from below. He used the steady Darcy model subject to impermeable and semi-impermeable boundary conditions. His results showed that above the critical Rayleigh number, the heat transfer across the layer is proportional to the square of the temperature difference across the layer but is independent of the thermal conductivity of the porous medium or the depth of the layer. Elder's results near the critical Rayleigh number were in

good agreement with those from studies by Horton and Rogers [23] and Lapwood [24]. A similar analysis, with similar agreement for the critical wave number and corresponding Rayleigh number was shown by Palm et al. [28] of the onset of convection in a porous medium using the expansion method up to sixth order of approximation.

A comprehensive study of convection in fluids in saturated porous media is documented in the book by Nield and Bejan [29]. The onset of convection in a horizontal porous medium layer heated from below under thermal non-equilibrium conditions was investigated by Rees [30] analytically and numerically using a multi-dimensional Newton-Raphson iteration scheme. The critical Rayleigh and wave numbers were modified for the non-equilibrium model. Rees showed that the inter-phase heat transfer and porosity conductivity ratio have significant effects on modified Rayleigh and wave numbers. Analytic and numerical study of convective instability in a porous media layer subject to a temperature gradient inclined with respect to gravitation was investigated by Barletta and Nield [31]. They used linear stability theory to investigate the transverse and longitudinal rolls. Their results showed that flow is more unstable for the longitudinal rolls than for the transverse rolls. Convection in a porous medium has been a topic of interest to many researchers. Among others, Baytas and Pop [32], Rees [33] and, Chen and Chen [34] investigated convection in a porous medium cavity. An analytic investigation of the onset of convection in a horizontal fluid layer overlying a porous layer was carried out by Nield [35]. He considered the steady motion of a fluid layer subject to constant heat flux boundary conditions. He studied the linear stability using the Galerkin expansion method. His results suggested that the effect of the surface tension parameter may be determined from the deflection of upper free surface quantity. Hewitt et al. [36] investigated convection in a porous medium at high Rayleigh numbers, for which results suggested that the flow is well described by a steady heat exchange solution.

1.2.1 Double-diffusive convection

Many of the above studies considered pure heat transfer from natural convection in a porous medium. There are, however, many situations where convection leads to both heat and mass transfer. These convection processes are driven by buoyancy forces. This type of convection in a porous medium is usually known as thermohaline, thermosolutal or double-diffusive convection. Double-diffusion convection is found in engineering applications and geophysical flow, such as found in seawater flow and the mantle in Earth's crust. In double-diffusion convection, the density depends linearly on both the temperature field T and solute concentration field C and takes the form

$$\rho = \rho_0 \left(1 - \beta_T (T - T_0) - \beta_C (C - C_0)\right), \tag{1.2.1}$$

where β_T and β_C are the volumetric thermal expansion coefficient and the solute concentration expansion coefficient. The subscript zero refers to the reference state.

Considerable attention is given to the onset of double-diffusive convection in a porous medium layer in books by Nield and Bejan [29] and, Vafai [37]. In addition, combined heat and mass transfer driven by buoyancy forces in a fluid-saturated porous medium was considered by Trevisan and Bejan [38], who reviewed and summarized the essential elements of linear stability analysis for natural convection with buoyancy forces in porous media. They assumed all fluid quantities vanished at the boundary. The onset of convective instability induced by buoyancy due to a vertical temperature gradient was first considered by Jeffreys [39] for a horizontal layer of viscous fluid. Nield [40] later extended the idea to double-diffusive convection in a horizontal layer of a viscous fluid. He applied linear stability analysis to double-diffusive convection using Fourier series. He found approximate solutions to eigenvalue equations that predict the occurrence of both oscillatory and monotonic convective instability. For the stability of double-diffusive convection in a regular viscous fluid the eigenvalue is a linear combination of thermal and solutal Rayleigh numbers. The solutal Rayleigh number Ra_S is defined by

$$Ra_S = \frac{\beta_C \Delta C g h^3}{D\nu},$$

where D is the solutal diffusivity and ΔC is the solute concentration difference between the top and bottom of the layer.

The onset of thermal instability in double-diffusion convection is dependent on the many dimensionless parameters embedded in the flow equations. The mechanisms of double-diffusion convection are complicated due to the interaction between the porous matrix and the fluid particles. For a porous media flow heated from the side, attention has been given to double-diffusion convection instability near a vertical wall immersed in a saturated porous layer. For instance, Mojtabi and Charrier-Mojta [41] studied the linear flow with double-diffusion convection in a situation where the thermal and solutal buoyancy forces are equal and opposing. The effects of embedded parameters for the porous medium layer were investigated. They observed that when the thermal and solutal buoyancy effects opposed each other the flow pattern differed from that for Rayleigh-Bénard convection. Experimental studies of double-diffusion convection in a porous medium were reported by Murray and Chen [42]. They observed that the onset of convection in porous media is marked by a change in the slope of the heat flux. The onset of thermal instability in double-diffusive convection in a rectangular porous cavity was studied by Mamou et al. [43], who used Galerkin and finite element methods to predict supercriticality and overstability for the onset of convection. The influence of parameters values, such as the Lewis number, normalized porosity and enclosure aspect ratio on the onset of convection, was determined. The Lewis number is an important parameter for diffusive convection and is defined by

$$Le = \frac{\alpha}{D},$$

where α and D are the thermal diffusivity of the fluid and mass diffusivity, respectively.

The diffusion of mass due to the temperature gradient is known as the Soret or thermodiffusion effect while the energy flux due to mass solute concentration gradient is called the Dufour effect. Bahloul et al. [44] studied the Soret effect induced by convection in a shallow horizontal porous

layer. They used normal mode analysis to predict the occurrence of supercritical and subcritical convection due to the Soret parameter. In many studies on double-diffusive convection in a porous medium, the effects of Soret and Dufour are generally assumed to be negligible. However, these effects could be significant when a density difference exists in the flow regime. The effects of Soret and Dufour parameters on double-diffusive free convection in a fluid saturated porous medium using the Darcy model were studied by Murthy et al. [45]. They used a finite difference scheme based on the Keller-Box method to solve the equations. The influence the Dufour and, Soret parameters and Lewis numbers was analyzed for their impact on the average Nusselt and Sherwood numbers. Studies on double-diffusive convection in a porous medium where the flows are induced by buoyancy forces include those by Benzeghiba et al. [46], Da Costa et al. [47], Huppert and Moore [48] and Radko and Smith [49]. Numerical studies of convection in a porous cavity have been made by Rees [33] and Mondal and Sibanda [50].

The case of a two-component horizontal layer of fluid in a saturated porous medium subjected to temperature and solute concentration gradients is often encountered in geophysical flows, such as saline geothermal fields and groundwater storage. For convection in a two-component fluid, the temperature diffusivity is usually higher than the diffusivity of the solute concentration. We note substantial research interest on linear and nonlinear stability analysis of double diffusion-convection in porous media. Rudraiah and Malashetty [51] studied the effect of molecular diffusion on double-diffusive convection in a horizontal layer of fluid in a saturated porous medium. They used linear and nonlinear analysis to study the occurrence of finger and diffusive instabilities. Their results showed that these flow instabilities could never occur together. A similar analysis is given by Rudraiah and Siddheshwar [52] for the effect of cross diffusion on double-diffusive convection in a horizontal layer of fluid in a saturated porous medium. Their study included the nonlinear stability analysis of the flow. The Fourier series expansion was used to obtain the evolution equations for finite amplitude convection of the flow. Similar results were obtained for finger and diffusive instabilities. Quere et al. [53] studied thermally driven laminar flow in rectangular cross-section cavities. They used the finite difference method to solve the flow equations and then investigated the effect of the parameters on local heat transfer. Chamkha and Al-Naser [54] investigated the

laminar double-diffusive convective flow of a binary gas mixture in an inclined rectangular porous enclosure using the finite difference method. The influence of the buoyancy ratio on the average Nusselt and Sherwood numbers was analyzed. It was noted that the effect of increasing the enclosure inclination angle was to reduce both the average Nusselt and Sherwood numbers. Wang et al. [55] analyzed the natural convection and heat transfer in an inclined porous cavity with time periodic boundary conditions. The influence of the inclination angle and oscillating frequency on hydrodynamic stability and heat transfer were investigated. Numerical studies on double-diffusive convection in an electrically conducting fluid layer in inclined cavities were also studied by Polat and Bilgen [56] and Khanafer and Chamkha [57].

The double-diffusive convection problem is a fascinating nonlinear phenomenon with possible density reversal. The influence of boundary conditions defines heat and mass transport processes and the dynamics of the flow. The effect of heterogeneity and the thermal non-equilibrium on the onset of thermal convection in horizontal layer saturated porous medium was considered by Nield and Kuznetsov [58] using hydrodynamic boundary conditions. They presented a linear stability analysis and solution of the system of equations using the Galerkin expansion method. It was noted that the major impact on the onset of convection came from the heterogeneity of the fluid and its conductivity. The problem was extended by Nield et al. [59] to study the local thermal non-equilibrium on the onset of double-diffusive convection in a porous medium. A similar analysis using the Galerkin expansion method was performed, where it was also noted that the major impact on the onset of convection is due to the heterogeneity of the medium.

1.2.2 Nanofluid flow in a porous medium

Recent studies show that the suspension of solid nanoparticles in a fluid can substantially improve the fluid's thermophysical properties, including thermal conductivity, Choi and Eastman [60]. The term "nanofluid" describes a liquid containing a suspension of nanometer-sized solid particle, of the order 1 to 100nm . Examples of commonly used nanoparticles include metallic particles such as

aluminium, copper and silver and oxides such as aluminium oxide and cupric oxide. The common base fluids include water, ethylene-glycol or oil. The enhancement of thermal conductivity and viscosity of a nanofluid was reported by Masuda et al. [61]. For the analysis of convective transport in nanofluid flow, two models have been proposed; the homogeneous flow and dispersion models. In the homogeneous model, the transport equation for a pure fluid may be directly extended to a nanofluid flow, so that heat transfer is due to the higher thermconductivity of nanofluid flow. For the dispersion model, heat transfer is due to two mechanisms; a higher thermal conductivity and the dispersion of nanoparticles. However, it has been shown that results from the homogeneous flow model not agree with experimental findings. This conflict was resolved by Buongiorno [62]. He considered nanoparticle dispersion in convective transport of nanofluids and studied the effects of seven slip mechanisms; namely, inertia, Brownian diffusion, thermophoresis, diffusiophoresis,the Magnus effect, fluid drainage and gravity. It has been shown that, in the absence of turbulence, the most significant of these seven mechanisms are the Brownian diffusion and thermophoresis. Tzou [63] investigated thermal instability in nanofluid flow with natural convection using the method of eigenfunction expansions and weight residual. It was ascertained that the Brownian diffusion and thermophoresis both have a significant effect on the onset of convection. His results showed that the critical Rayleigh number for the onset of instabilities in a nanofluid flow is smaller in magnitude that of a regular fluid.

Extensive studies on convection in nanofluid flow through a saturated porous medium using linear stability have been made by the pair of researchers, Kuznetsov and Nield [64, 65, 66, 67] and Nield and Kuznetsov [68, 69]. In these studies, these researchers analyzed nanofluid flow in a horizontal layer porous medium using linear stability theory. They used a model that incorporates the effects of Brownian motion and thermophoresis, as proposed by Buongiorno [62] for a Darcy model with imposed vertical temperature and concentration gradients. It was shown that the critical Rayleigh number can be reduced or increased depending on whether the basic nanoparticle distribution is top heavy or bottom heavy. In addition, one of the key parameters for determining the onset of

convection in nanofluid flows is the Darcy parameter, which is defined by

$$Da = \frac{\hat{\mu}K}{\mu h^2},$$

where $\hat{\mu}$ and K are the effective viscosity and permeability respectively, while μ and h are as previously defined. Most previous studies of convection in porous media have used the Darcy model for the flow equations. The magnitude of the Darcy number has an important influence on the critical Rayleigh number and corresponding critical wave number. The transition to convection instability when Darcy models are used differs from the case obtained when using the full Naiver-Stokes equations to model the flow. It is thus important to consider the effect of the Darcy number on the onset of convection in a porous medium. It has been observed that for large Lewis numbers the structure of a nanofluid flow is strongly influenced by both buoyancy and the contribution of nanoparticles to the thermal energy. The effect of cross-diffusion in nanofluid flow was investigated by Kuznetsov and Nield [70] and Nield and Kuznetsov [71, 72]. Their studies considered a horizontal layer of nanofluid in a saturated porous medium. In addition, they used models that incorporated the effect of Brownian motion and thermophoresis. The linear stability of the flow was investigated using a one-term Galerkin expansion method. The influence of parameters such as the Prandtl number and nanoparticle Lewis number on the onset of stationary and oscillatory convection was analyzed. Also, the effects of the Soret and Dufour parameters on the onset of convection were investigated. It was noted that the onset of oscillatory instability depends on buoyancy forces acting in opposite directions. When the effects of the Soret and Dufour parameters was neglected, nonoscillatory modes of convection are expected to occur.

The study by Siddheshwar and Titus [73] focussed on the investigation of stability in Rayleigh-Bénard convection in a Newtonian liquid. They obtained the Ginzburg-Landau equation describing the Rayleigh-Bénard convection from three low order modes in a double Fourier expansion. They showed that three order modes in the double Fourier expansion are sufficient for the weakly nonlinear stability regime. Recently, Siddheshwar et al. [74] studied Rayleigh-Bénard convection in nanofluid flow using a two-phase model. Weakly nonlinear stability theory was used to analyze the heat transfer for different base fluids such as water, ethylene-glycol and engine oil. It was observed

that the convection is much stronger in the center of cells for ethylene-lycol silver nanofluids compared with the other nanofluids. This suggests that this nanofluid may be the best suited, so far, for heat transfer. Furthermore, it was observed that thermophoresis has the effect of delaying the onset of convection. Double-diffusive convection in a nanofluid flow also occurs in the case of binary fluid mixtures. The study by Yadav et al. [75] focussed on the stability of a horizontal layer for a binary nanofluid flow in a saturated porous medium heated and salted from below. They used linear theory to analyze three different boundary conditions namely, stress-free, rigid-rigid and rigid-free boundary conditions. The influence of parameters such as the Dufour and Soret parameters on the onset of stationary convection was analyzed. It was noted that the Dufour and Soret parameters both had a stabilization effect on the onset of stationary convection. Double-diffusive convection in the binary viscoelastic fluid in a horizontal layer was investigated by Narayana et al. [76], by application of linear and weakly nonlinear stability analysis to study the onset of convection in a binary viscoelastic fluid. It was noted that finger and diffusive instabilities did not occur simultaneously. The influence of Soret and Dufour parameters on heat and mass transport was also analyzed. The study by Agarwal et al. [77] focussed on convection in a nanofluid flow along a horizontal layer heated from below using a thermal non-equilibrium model. The effects of increasing the parameters on the onset of thermal convective instability and heat transfer were analyzed. It was shown that increasing the parameters have a stabilizing effect on the onset of convection. In addition, it was noted from the study that convection sets is earlier for local thermal non-equilibrium than for local thermal equilibrium. Related studies of thermal convection in a horizontal layer of nanofluid include those by Nield and Kuznetsov [78], Umavathi and Kumar [79], Narayana et al. [80] and Rees et al. [81]. Recently, Siddheshwar [82] studied the effect of local thermal non-equilibrium on the onset of Brinkman-Rayleigh-Bénard convection with isothermal boundary conditions. They used the linear stability theory and an asymptotic expansion for a small value of the inter-phase heat transfer coefficient. Here the stability was studied using a Fourier series expansion method. It was observed that the onset of convection was delayed for the rigid-rigid isothermal boundary condition compared to the case of free-free isothermal boundary conditions. Studies on the instability of Darcy-Bénard convection in an inclined layer were reported by Rees and Bassom [83]. They

used a numerical scheme based on the eigenvalue matrix to examine the linear stability. It was observed that the inclination angle of 31.49° is the maximum angle of inclination for transverse modes to become unstable. They noted that the convective instability could arise only when the inclination angle is less than or equal to 31.30°.

Studies on double-diffusive magneto-convection have received considerable attention because they have applications in oceanography, geophysics, astrophysics and engineering. Turner [84] studied the buoyancy effect on fluid flow. Rudraiah [85] applied linear and nonlinear stability theories to study double-diffusive magneto-convection, in which the effects of cross diffusion, rotation and chemical reaction on double-diffusive magneto-convection were analyzed. Comprehensive studies on hydromagnetic convection in a conducting fluid in an inclined cavity are given by Bian et al. [86], Revnic et al. [87] and Mansour et al. [88]. In these studies, the Darcy model for a porous medium was used for the fluid flow. The effect of inclination angle, Rayleigh number and heat generation were examined using streamline patterns in the numerical experiment.

1.3 The effect of rotation and a magnetic field

The onset of convection in a horizontal layer heated from below is a classical problem in hydrodynamic stability. The problem of the onset of convection in a horizontal layer of an electrically conducting fluid subjected to a magnetic field is often referred to as hydromagnetic stability. For this problem, the critical Rayleigh number depends on the Chandrasekhar number or the magnetic field parameter, [2]. This is defined by

$$Q = \frac{\sigma \mu_m^2 H_0^2 h^2}{\rho \nu},$$

where σ is the electrical conductivity, μ_m is the magnetic permeability and H_0 is the strength of the uniform magnetic field, the other parameters are as previously defined. Magneto-convection occurs in many natural processes in astrophysics and hydrology and in material processing technologies; thus generating an interest in studying its effects. Chandrasekhar [2] focussed on hydromagnetic

stability in a horizontal layer of a Newtonian fluid. The study showed that the magnetic field parameter plays the same role as does the Taylor number when applied in a rotating layer of fluid. In the outer layers of the sun and other stars, thermal convection is affected by the magnetic field. The phenomenon of magneto-convection was studied by Proctor and Weiss [89]. Recently, Narayana et al. [90] investigated the effect of the magnetic field on heat and mass transport in double-diffusive convection for a viscoelastic fluid layer heated from below using linear and nonlinear stability theories. Their results showed that the magnetic field parameter has a stabilizing effect on the onset of convection in a viscoelastic fluid. Investigation were reported by Yadav et al. [91] and Gupta et al. [92] on the effect of a vertical magnetic field with free-free, rigid-rigid and rigid-free boundary conditions for an electrically conducting nanofluid layer. The influence of parameters such as the magnetic field parameter on the onset of convection was analyzed. They found that increasing values of the magnetic field parameter has the effect of making the system more stable by delaying transition to chaotic flow. Further, they observed that the system is more stable for the rigid-rigid boundary condition than for the free-free or free-rigid boundary conditions. In the study by Yadav et al. [91] the effects of Brownian motion and thermophoresis were neglected whereas Gupta et al. [92] considered these effects. It was observed that an increasing magnetic field parameter increases the critical Rayleigh number.

The effect of rotation on thermal convection instability in a fluid layer heated from below was considered by Chandrasekhar [2]. In studying thermal convective instability in a rotating horizontal layer, the Taylor number plays an important role in the onset of convection. This dimensionless parameter is defined by

$$Ta = \frac{4\Omega^2 h^4}{\nu^2},$$

where Ω is a constant angular velocity, an h and ν are as previously defined. It has been shown that increasing the Taylor number has a stabilizing effect on the onset of convection. Studies by Van et al. [93], Hunter and Riahi [94] and Cox and Matthews [95] focussed on theoretical and experimental investigations of the convective instability in a horizontal fluid layer rotating about vertical axes. Hunter and Riahi [94] studied the nonlinear convection regime and showed that when the Taylor number exceeds a certain value the rate of heat transfer decreases. Hence increasing the

Taylor number reduces the rate of heat transfer and the layer becomes stable.

The Darcy model has been extended to the Darcy-Brinkman and Darcy-Forchheimer models in recent studies. Many researchers have used these model to study convective instability in a horizontal layer of a nanofluid in a porous medium subjected to rotation or an external magnetic or other fields. Agarwal et al. [96] investigated convective instability in a rotating nanofluid in a horizontal layer using the Darcy model with Brownian motion and thermophoresis effects. They applied the linear stability theory to study the onset of stationary and oscillatory convection. They showed that increasing the Taylor number had the effect of delaying the onset of convection. The same problem was extended by Chand and Rana [97] to study the effect of rotation on thermal convective instability in a nanofluid in a porous medium, but they used the Darcy-Brinkman model. They showed that increasing the Darcy number may be both stabilizing and destabilizing depending on the Taylor number.

The recent study by Yadav et al. [98] focussed on investigating rotation in double-diffusive convection assuming zero nanoparticle flux at the boundaries. They applied linear stability theory using the Galerkin expansion method. A numerical study of the boundary layer convection in a rotating fluid layer was investigated by Liao et al. [99]. They showed that the basic structure of the boundary layer convection does not change in the strongly nonlinear regime. The combined effect of rotation and introduction of a magnetic field on the onset of convection in an electrically conducting fluid heated from below has been an attractive topic to many researchers. Among these researchers, Chand and Rana [100], Gupta et al. [101] and Soward [102] and Sanchez-Alvarez et al. [103] investigated the combined effects of rotation and a magnetic field on the onset of convection in horizontal fluid layer. The onset of steady two-dimensional convection, subject to a magnetic field and rotation, was investigated by Cox and Matthews [104]. They noted that the convective instabilities are dependent on the boundary conditions; for a rotating layer, the convective instabilities required stress-free boundary conditions, whereas the magnetoconvection instabilities required Neumann boundary conditions. However, most experimental studies used the rigid-rigid boundary as the most appropriate boundary condition for studying the onset of convective flow. Recently,

Yadav et al. [105] studied magneto-convection instability in a rotating horizontal layer of an electrically conducting nanofluid. They used the linear stability theory and three different boundary conditions. They investigated the onset of convection analytically for stress-free boundary condition and numerically for rigid-rigid boundary conditions. It was ascertained that the critical value for the onset of magnetoconvection is lower than the critical value for the onset of convection in a regular fluid.

The study by Yadav et al. [106] focussed on an numerical investigation of the onset of convection in a rotating nanofluid layer. They used a six-term Galerkin approximation expansion method to obtain the eigenvalue equations, which they then solved numerically. The effect of parameters including the Taylor number on the onset of convection was analyzed. Recently, Duba et al. [107] used linear and weakly nonlinear stability theories to study double-diffusive convection in a rotating fluid including Soret and Dufour effects. They used a minimal double Fourier series for the weakly nonlinear stability. The influence of parameters such as the Taylor number, Soret and Dufour parameters on the onset of convection was investigated. Thermal instability in a nanofluid subjected to a vertical magnetic field was studied by Gupta et al. [101]. They used a model that incorporated the effects of Brownian motion and thermophoresis with free-free boundary conditions. Here, they observed that the instability occurs due to fluid buoyancy coupled and the effect of nanoparticles. They also noted that the instability set in as oscillatory convection rather than stationary convection. The impact of increasing the magnetic field parameter was to delay the onset of convection. A similar problem was considered by Yadav et al. [108] where they studied the flow with nanoparticle flux at the boundaries.

1.4 Temperature modulation

Thermal instability in a horizontal layer of fluid in a saturated porous medium with a steady temperature gradient has been considered in many earlier studies. There are many situations where the temperature gradient and gravity are functions of both space and time. This non-uniform tempera-

ture gradient is known as temperature modulation or a time-periodic temperature boundary. In the investigation of Rayleigh-Bénard convection, the amplitude and the frequency of modulation are used as effective mechanisms to control the onset of convection. In such a case, the temperature at the lower wall may be defined by

$$T = T_0 + \frac{\Delta T}{2}\left(1 + \varepsilon \cos(\omega t)\right),$$

and at the upper wall by

$$T = T_0 - \frac{\Delta T}{2}\left(1 - \varepsilon \cos(\omega t + \phi)\right),$$

where T_0 is the reference temperature, ε is a small amplitude, ω is the modulation frequency and ϕ is the phase angle. These temperature boundary conditions with a free-free surface boundary condition were used in an earlier study by Venezian [109] in which linear stability was assumed and a perturbation method used. The shift in the critical Rayleigh number was calculated. It was observed that a large frequency modulation and amplitudes had a small effect on the onset of convection. A similar study, also with a free-free boundary condition, was reported by Roppo et al. [110] using the weakly nonlinear stability theory and temperature modulation at the walls. They showed that temperature modulation led to stable hexagonal rolls at the critical Rayleigh number. In addition, it was found that the system destabilized at lower modulation frequencies and stabilized at higher modulation frequencies. The authors, however, did not give an analysis of the heat transport.

Recently, the study by Bhadauria et al. [111] used the weakly nonlinear stability theory to investigate the effect of temperature and gravity modulation on thermal instability in a rotating viscous fluid layer. They derived the Ginzburg-Landau equation for the stationary mode of convection. The effect of modulation on heat transport was also investigated. In general there are three types of temperature modulation; namely, in-phase modulation when the phase angle $\phi = 0$, out-of-phase modulation when $\phi = \pi$, and lower boundary modulation when $\phi = -i\infty$. They confined their analysis to limited values of the Prandtl number and Rossby number. Based on their findings, they suggested that the temperature and gravity modulation could be used as external means to increase or reduce the heat transport in a rotating viscous fluid layer. The study by Kiran and Bhadauria

[112] focussed on the weakly nonlinear oscillatory mode of convection in a rotating fluid layer, subjected to temperature modulation. They gave some analysis of the bifurcation of the solutions of the complex Ginzburg-Landau equation and showed the existence of supercritical bifurcation. They further observed that increasing the Prandtl number has the effect of enhancing heat transport for in-phase, out-of-phase and lower boundary modulations.

In general, there are many natural phenomena, or applications, where flows are significantly influenced by the existence and the magnitude of buoyancy forces, temperature modulation, rotation and a magnetic field. There are thus sound reasons to study changes in a fluid rotating about horizontal or vertical axes or with a vertical magnetic field or temperature modulation. These types of problems are relevant in astrophysical and geophysical phenomena, including oceanic convection. Bhadauria [113] investigated Rayleigh-Bénard convection subject to a magnetic field in a saturated porous medium with temperature modulation. It was found that temperature modulation may have the effect of either stabilizing or destabilizing the system. They also found that increasing the magnetic field parameter could delay the onset of convection. Two studies by Bhadauria [114, 115] considered Rayleigh-Bénard convection with rotation, magnetic field and temperature modulation using Flouquet theory. As in related previous studies, they observed that temperature modulation may either stabilize or destabilize the system. Bhadauria and Kiran [116] studied the effect of temperature modulation in a binary viscoelastic fluid-saturated porous medium. Using nonlinear stability theory, they derived a Lorenz type system of nonlinear ordinary differential equations that described the amplitude of convection in the viscoelastic fluid. They observed a transition between regular and chaotic behaviours for various values of the modulation frequency and amplitude of temperature modulation. Siddheshwar et al. [117] studied double-diffusive convection in a viscous fluid in a saturated porous medium subjected to temperature and gravity modulations. It was noted that increasing the Darcy number reduced the heat transfer for in-phase modulation, while it increased heat transfer for both out-of-phase modulation and modulation at the lower boundary. In addition, it was observed that the heat transfer for out-of-phase modulation is much more than at in-phase modulation and modulation at the lower boundary. Other relevant studies on thermal convective instability in a horizontal fluid layer with temperature modulation include those by Suthar

et al. [118], Bhadauria and Kiran [119], Siddheshwar et al. [120] and Siddheshwar and Abraham [121].

1.5 Ferrofluid convection

Ferromagnetic fluids are magnetic colloids consisting of nanometer-sized magnetic particles suspended in a fluid carrier. The first synthesis of ferromagnetic fluids was reported in the pioneering work by Stephen [122]. The theory of ferrohydrodynamics deals with the mechanics of fluid motion influenced by strong forces of magnetic polarization. In this respect, there are important differences between the theories of magnetohydrodynamics and ferrohydrodynamics. In the magnetohydrodynamic theory, the fluid force is the Lorentz force that arises when an electric current flows at an angle to the direction of an imposed magnetic field whereas in ferrohydrodynamics the fluid force is due to the polarization force. In general, the magnetization of a ferromagnetic fluid is dependent on the temperature, magnetic field, and density of the fluid. The magnetic force and the thermal state of the fluid may give rise to convection currents in magnetic fluids. An authoritative introduction to convective instability in magnetic fluids was given by Rosensweig [123]. The study by Finlayson [124] focussed on the convective instability in a ferromagnetic fluid. He considered free-free and rigid-rigid boundary conditions for his study, which used the linear stability theory. The critical Rayleigh number for the onset of convection with both magnetic and buoyancy forces was predicted.

There are many studies of heat transfer in a horizontal layer of ferromagnetic fluids. These have technological applications in the sealing of rotating shafts, ink and electronic cooling. Schwab et al. [125] presented an experimental study of the problem that had been proposed by Finlayson [124] in the case of a strong magnetic field. The onset of convection was determined by plotting the Nusselt number against the Rayleigh number and findings were in good agreement with the results that had been obtained by Finlayson [124]. Stiles and Kagan [126] extended the experimental study to the case of a strong magnetic field. A weakly nonlinear stability study was presented by

Russell et al. [127] for a horizontal layer of magnetized ferrofluids heated from above. The control parameter for the onset of convection was the Rayleigh number and the magnetic Rayleigh number. They showed that heat transfer depends on the nonlinearity in the temperature difference. More recently, Shivakumara et al. [128] investigated the thermogravitational convection in a horizontal layer where viscosity depended exponentially on the temperature. They showed that the onset of convection depends strongly on the viscosity and magnetic parameters. The effect of rotation on ferrofluids, subject to stress-free, rigid-rigid paramagnetic and rigid-rigid ferromagnetic effects, was studied by Venkatasubramanian and Kaloni [129]. They showed that rotation delayed the onset of the convective instability. Further, they showed that the stabilization of the system depended on the chosen boundary conditions.

Convection in a horizontal ferromagnetic fluid layer heated from above with magnetic modulation was considered by Aniss et al. [130]. They used both the Galerkin method and the Floquet theory in this study where they noted that the occurrence of harmonic and subharmonic modes of convection depended on the ratio between the magnetic and the gravitation forces. Nanjundappa and Shivakumara [131] studied the effect of velocity and temperature boundary condition on the onset of ferromagnetic convection. It was observed that suitable values for the ratio of magnetic to buoyancy forces and the Biot number stabilized the system. Further, they ascertained that nonlinearity of fluid magnetization has no effect on the onset of convective instability in ferromagnetic fluids. Studies by Sharma et al. [132] and, Mittal and Rana [133] focussed on the investigation of double-diffusive convection in a micropolar ferromagnetic fluid layer heated from below. They determined the critical value of Rayleigh number for influencing of the ratio of magnetic to buoyancy forces.

In this study we give analytical and numerical solutions of the convective instability in different flow configurations. It is now well understood that linear stability analysis provides neither sufficient information about the amplitude of convection nor the rate of heat and mass transfer in Rayleigh-Bénard convection problems. We thus use the nonlinear stability theory to study the evolution of the convection amplitudes and the heat and mass transport. Vadasz [134] and, Vadasz and Olek [135] presented investigations of centrifugally driven free convection in a rotating porous

layer. They used a truncated Galerkin approximation method to derive a nonlinear system of differential equations to describe the amplitude of convection. These equations were solved numerically using Adomain decomposition techniques. Their results showed that there is a transition from steady convection to non-periodic convection via a Hopf bifurcation and from chaos to periodic convection for different Rayleigh numbers. Following these earlier studies, we use linear and nonlinear stability theories to study Rayleigh-Bénard convection in diverse flows such as a nanofluid flow through a horizontal porous medium heated from below and cooled from above, double-diffusive natural convection in an inclined open cavity with an inclined magnetic field and ferromagnetic fluids in a rotating horizontal layer with temperature modulation at the boundaries.

1.6 Method of Solution

In this section, we describe the method that will be used in thesis to solve the nonlinear initial value problems that describe the amplitude of convection instabilities. We use the multidomain spectral collocation method which is a powerful technique for solving differential equations when the physical domain is smooth. Motsa et al. [136] have shown that it has higher accuracy than some other common numerical methods such as finite differences and the finite element method. This multidomain spectral collocation technique uses the Chebyshev differentiation matrix, for which details can found in Canuto et al. [137] and Trefethen [138].

To describe the multidomain spectral collocation method, consider the system of nonlinear initial value problems, defined by

$$\frac{dy_n}{dt} + a_{n,n}y_n + \sum_{k=1}^{M} a_{n,k}y_k(1-\delta_{nk}) + f_n\left(y_1,\cdots,y_{n-1},y_{n+1},\cdots,y_M\right) = g_n, \tag{1.6.1}$$

subject to the initial condition

$$y_n(0) = \alpha_n^0, \tag{1.6.2}$$

where $a_{n,n}$ and g_n are known constants but in general can be functions of t, y_n are unknown variables, f_n are the nonlinear term in the n^{th} equation, α_n^0 are the initial condition in the n^{th} equation

and $t \in [0,T]$ is time. Here $n,k = 1,2,3,\cdots,M$ and the Kronecker delta function is defined as

$$\delta_{nk} = \begin{cases} 1 & \text{if } n = k, \\ 0 & \text{if } n \neq k. \end{cases} \tag{1.6.3}$$

For simplicity we consider the case when $M = 3$ and following the iteration scheme proposed by [136], we introduce the following:

$$\frac{dy_{1,r+1}}{dt} + a_{1,1}y_{1,r+1} + a_{1,2}y_{2,r} + a_{1,3}y_{3,r} + f_1\left(y_{2,r}, y_{3,r}\right) = g_1, \tag{1.6.4}$$

$$\frac{dy_{2,r+1}}{dt} + a_{2,1}y_{1,r+1} + a_{2,2}y_{2,r+1} + a_{2,3}y_{3,r} + f_2\left(y_{1,r+1}, y_{3,r}\right) = g_2, \tag{1.6.5}$$

$$\frac{dy_{3,r+1}}{dt} + a_{3,1}y_{1,r+1} + a_{3,2}y_{2,r+1} + a_{3,3}y_{3,r+1} + f_3\left(y_{1,r+1}, y_{2,r+1}\right) = g_3, \tag{1.6.6}$$

subject to the initial condition

$$y_{n,r+1}(0) = \alpha^0_{n,r+1},\ n = 1,2,3. \tag{1.6.7}$$

The multidomain method assumes that the interval $\Omega = [0,T]$ can be decomposed into p non-overlapping subintervals. To this end, we let $t \in \Omega$ so that each subinterval Ω_i is defined as

$$\Omega_i = [t_{i-1}, t_i],\ \ i = 1,2,3,\cdots,p, \tag{1.6.8}$$

with

$$0 = t_0 < t_1 < t_2 <, \cdots, < t_p = T.$$

Thus equations (1.6.4)-(1.6.7) can be written in the form

$$\frac{dy^i_{1,r+1}}{dt} + a_{1,1}y^i_{1,r+1} + a_{1,2}y^i_{2,r} + a_{1,3}y^i_{3,r} + f_1\left(y^i_{2,r}, y^i_{3,r}\right) = g_1, \tag{1.6.9}$$

$$\frac{dy^i_{2,r+1}}{dt} + a_{2,1}y^i_{1,r+1} + a_{2,2}y^i_{2,r+1} + a_{2,3}y^i_{3,r} + f_2\left(y^i_{1,r+1}, y^i_{3,r}\right) = g_2, \tag{1.6.10}$$

$$\frac{dy^i_{3,r+1}}{dt} + a_{3,1}y^i_{1,r+1} + a_{3,2}y^i_{2,r+1} + a_{3,3}y^i_{3,r+1} + f_3\left(y^i_{1,r+1}, y^i_{2,r+1}\right) = g_3, \tag{1.6.11}$$

subject to the initial condition

$$y^{i-1}_{n,r+1}(t_{i-1}) = \alpha^i_{n,r+1},\ n = 1,2,3. \tag{1.6.12}$$

To apply the spectral collocation method, we need to transform each subinterval Ω_i into $[-1,1]$ using the transformation

$$t = \frac{t_i - t_{i-1}}{2}\tau + \frac{t_i + t_{i-1}}{2}. \tag{1.6.13}$$

Each subinterval is discretized using Chebyshev-Gauss-Lobatto collocation points, as defined in Motsa et al. [136], Trefethen [138] and Canuto et al. [137],

$$\tau_j = \cos(\frac{\pi j}{N}),\ j = 0,1,2,\cdots,N. \tag{1.6.14}$$

The Lagrange basis polynomials are given by

$$l_k(t) = \prod_{\substack{k=0 \\ j\neq k}}^{N} \frac{t - t_j}{t_k - t_j}, \tag{1.6.15}$$

and

$$l_k(t_j) = \delta_{kj} = \begin{cases} 1 & \text{if } j = k, \\ 0 & \text{if } j \neq k, \end{cases} \tag{1.6.16}$$

where δ_{kj} is the Kronecker delta function. The solution in each subinterval is approximated by the Lagrange interpolation polynomial of the form

$$y^i_{n,r+1}(t)|_{t=\tau_j} \approx \sum_{k=0}^{N} y^i_{n,r+1}(\tau_k) l_k(\tau_j). \tag{1.6.17}$$

Thus, the derivatives at the collocation points are approximated by

$$\begin{aligned} \frac{dy^i_{n,r+1}}{dt}|_{t=\tau_j} &= \frac{2}{\Delta t_i} \sum_{k=0}^{N} y^i_{n,r+1}(\tau_k) \frac{dl_k(\tau_j)}{dt} \\ &= \sum_{k=0}^{N} D_{jk} y^i_{n,r+1}(\tau_k) \\ &= \sum_{k=0}^{N} \mathbf{D}_{jk} y^i_{n,r+1}(\tau_k), \end{aligned} \tag{1.6.18}$$

where $\Delta t_i = t_i - t_{i-1}$, $\mathbf{D}_{jk} = \frac{2}{\Delta t_i} D_{jk}$ and $D_{jk} = \frac{dl_k(\tau_j)}{dt}$ is the Chebyshev differentiation matrix of size $(N+1)\times(N+1)$, as given in Motsa et al. [136], Trefethen [138] and Canuto et al. [137].

Now, substituting equations (1.6.17) and, (1.6.18) into equations (1.6.9) to (1.6.12) and applying the initial condition, we obtained

$$\sum_{k=0}^{N-1} \mathbf{D}_{jk} y^i_{1,r+1}(\tau_k) + a_{1,1} y^i_{1,r+1}(\tau_j) = g_1 - \mathbf{D}_{jN} y^i_{1,r+1}(\tau_N) - a_{1,2} y^i_{2,r}(\tau_j) - a_{1,3} y^i_{3,r}(\tau_j) - f_1\left(y^i_{2,r}(\tau_j), y^i_{3,r}(\tau_j)\right), \tag{1.6.19}$$

$$\sum_{k=0}^{N-1} \mathbf{D}_{jk} y^i_{2,r+1}(\tau_k) + a_{2,2} y^i_{2,r+1}(\tau_j) = g_2 - \mathbf{D}_{jN} y^i_{2,r+1}(\tau_N) - a_{2,1} y^i_{1,r+1}(\tau_j) - a_{1,3} y^i_{3,r}(\tau_j) - f_1\left(y^i_{1,r+1}(\tau_j), y^i_{3,r}(\tau_j)\right), \tag{1.6.20}$$

$$\sum_{k=0}^{N-1} \mathbf{D}_{jk} y^i_{3,r+1}(\tau_k) + a_{3,3} y^i_{3,r+1}(\tau_j) = g_3 - \mathbf{D}_{jN} y^i_{3,r+1}(\tau_N) - a_{3,1} y^i_{1,r+1}(\tau_j) - a_{3,2} y^i_{2,r+1}(\tau_j) - f_1\left(y^i_{1,r+1}(\tau_j), y^i_{2,r+1}(\tau_j)\right), \tag{1.6.21}$$

Equations (1.6.19)–(1.6.21) can be expressed in the matrix form as follows:

$$\mathbf{A}_n \mathbf{Y}^i_{n,r+1} = \mathbf{R}^i_n, \tag{1.6.22}$$

where

$$\mathbf{A}_n = \mathbf{D} + a_{n,n}\mathbf{I},\ \mathbf{Y}^i_{n,r+1} = \left(y^i_{n,r+1}(\tau_0), y^i_{n,r+1}(\tau_1), \cdots, y^i_{n,r+1}(\tau_{N-1})\right)^T,$$

and

$$\mathbf{R}^i_n = \left(R^i_n(\tau_0), R^i_n(\tau_1), \cdots, R^i_n(\tau_{N-1})\right),$$

with

$$R^i_1(\tau_j) = g_1 - \left(\mathbf{D}_{jN}\alpha^i_{1,r+1} + a_{1,2} y^i_{2,r}(\tau_j) + a_{1,3} y^i_{3,r}(\tau_j) + f_1\left(y^i_{2,r}(\tau_j), y^i_{3,r}(\tau_j)\right)\right), \tag{1.6.23}$$

$$R^i_2(\tau_j) = g_2 - \left(\mathbf{D}_{jN}\alpha^i_{2,r+1} + a_{2,1} y^i_{1,r+1}(\tau_j) + a_{2,3} y^i_{3,r}(\tau_j) + f_2\left(y^i_{1,r+1}(\tau_j), y^i_{3,r}(\tau_j)\right)\right), \tag{1.6.24}$$

$$R^i_3(\tau_j) = g_3 - \left(\mathbf{D}_{jN}\alpha^i_{3,r+1} + a_{3,1} y^i_{1,r+1}(\tau_j) + a_{3,2} y^i_{2,r+1}(\tau_j) + f_3\left(y^i_{1,r+1}(\tau_j), y^i_{2,r+1}(\tau_j)\right)\right). \tag{1.6.25}$$

The identity matrix $\mathbf{I}$ has size $N \times N$. Thus starting from the initial condition in equation (1.6.12) the approximate solutions are obtained by solving equation (1.6.22). Although we consider the case of three nonlinear differential equations, this procedure is valid for any number of nonlinear ordinary differential equations.

1.7 Thesis Objectives

The main objective of this study is to investigate the development of convective instabilities in various fluid flows, such as in a rotating horizontal layer and flow through an inclined open cavity. We investigate the influence of dimensionless parameters on fluid convection using both the linear and weakly nonlinear stability theories. The specific problems addressed, and for which solutions are determined in this thesis include

- The effect of a magnetic field and Darcy numbers on cross-diffusive convection in a nanofluid flow in a horizontal layer in a porous medium.
- The effect of Soret and Dufour parameters on finite amplitude convection in a nanofluid flow subjected to cross-diffusion.
- The effect of magnetic field in double-diffusive convection in an inclined open square cavity with an inclined magnetic field.
- The effect of rotation on convective ferromagnetic fluid flow in a rotating horizontal layer with temperature modulation at the walls.
- The influence of fluid parameters on the rate of heat and mass transfer in a horizontal ferromagnetic fluid layer and an inclined magnetic field.

We solve the evolution equations for the amplitude of convection of fluid using the multidomain spectral collocation technique.

1.8 The structure of the thesis

This thesis consists of six chapters with Chapters 1 and 6 being the introduction and conclusion of the study, respectively. Chapters 2 to 5 consists of research papers that form the main body of the study.

Chapters 2 and 3 deal with the analysis of a nanofluid flow in a horizontal layer in a saturated porous medium. Studies of this nature are important in engineering and science due to their wide range of applications in many physical settings. In Chapter 2 we model the flow of a nanofluid in a horizontal layer subjected to an applied magnetic field. We use the linear stability theory to analyze the flow and determine the effect of the magnetic field parameter and Darcy number on the onset of convection in the nanofluid flow in Part I of Chapter 2 and the effect of all, other parameters on the onset of convection were given in Part II of Chapter 2 . In Chapter 3 we extend the problem presented in Chapter 2 to nanofluid flow in horizontal layer, and there use the weakly nonlinear stability theory to study the evolution of small disturbances. A truncated Fourier series is used to transform the flow equations to a Lorenz type system of nonlinear initial value problems that describe the amplitude of convection in the nanofluid. These equations were solved numerically using a multidomain spectral collocation technique. The influence of parameters on the rate of heat and mass transfer is analyzed.

In Chapter 4 we study double-diffusive convection in an inclined open square cavity subjected to an inclined magnetic field. We adopt both linear and nonlinear stability theories for the flow analysis using the Galerkin expansion method. The influence of dimensionless parameters on double-diffusive convection in an inclined cavity and the onset of convection were investigated. The rate of heat and mass transport is studied.

Chapter 5 focuses on the convective instability in a ferromagnetic fluid flow in a rotating horizontal layer subject to a time-periodic temperature at the walls. A weakly nonlinear stability analysis is given. The influence of dimensionless parameters, such as the Taylor number and magnetization

parameter on flow behaviour and structure were investigated. The Ginzburg-Landau equation is derived and the heat transfer analyzed for in-phase and out-of-phase modulation. In Chapter 6, we give our overall conclusion and suggest ideas for possible future work.

Chapter 2

Onset of instability in a horizontal porous layer in a cross diffusive nanofluid flow

In this chapter, we study the stability and cross-diffusion in nanofluid flow through a horizontal layer of a saturated porous medium subjected to a magnetic field. The Galerkin method is used to solve the equations derived from a linear stability analysis. The chapter is in two parts. In Part I we study the effect of the magnetic field parameter and the Darcy number on the stability of the flow. In Part II we extend the study to consider the effects of parameters such as the Dufour and Soret parameters, and the Lewis and Prandtl numbers for a nanofluid. The momentum equations have been modified using the Darcy model and the Galerkin method is used to solve the equations derived from a linear stability analysis.

Part I: Onset of instability in a horizontal porous layer: Effect of the magnetic field and the Darcy number

International Conference Numerical Heat Transfer and Fluid Flow
NIT Warangal, India – Jan 19-21,2018
Paper No. XXX (The number assigned when the papaer is accepted)

Onset of instability in a horizontal porous layer of a cross diffusive nanofluid flow

O.A.I. Noreldin [a], S. Mondal [b,*], P. Sibanda [a]

[a]*School of Mathematics, Statistics and Computer Science, University of KwaZulu-Natal*

Pietermaritzburg, Private Bag X01 Scottsville 3209, South Africa

[b]*Department of Mathematics, Amity University, Kolkata*

Newtown-700135, West Bengal, India

**Corresponding author Email:sabya.mondal.2007@gmail.com*

Received: Date? Accepted: Date?

The instability in a horizontal porous layer of infinite extent of a cross diffusive nanofluid with magnetic field subject to stress free and revised nanopraticle boundary conditions is studied here. A Galerkin-type method is used in linear stability. The influence of the important parameters such as Chandrasekher number (Q) and Darcy number (Da) on both stationary Rayleigh number is to stabilize the system.

Keywords: Instability; Nanofluid flow; Porous medium, Galerkin method.

1. Introduction

The enhancement of the thermal conductivity of a fluid is a matter of great interest to engineers due to the important applications of nanofluids in heat and mass transfer processes. Kuznetsov and Nield [1] investigated the thermal instability in a porous layer saturated with a nanofluid using a Brinkman model. They investigated the onset of instability in a horizontal porous layer using a model for the nanofluid that incorporated particle Brownian motion and thermophoresis. In recent decades many researchers have investigated thermal instability in a horizontal nanofluid layer subject to an applied magnetic field under different assumptions. Chandrasekher [2] was among the first to study thermal instability in a Newtonian fluid under various assumptions. The effects of a magnetic field on convection and the onset of instability has important applications in varies problems such as in cooling systems, pumps, magnetohydrodynamic generators, etc. The onset of Darcy-convection in fluid saturated porous medium in the presence of a magnetic field and subject to temperature modulation at the boundaries was investigated by Bhadauria et al. [3]. They examined the effect of the Darcy-Chandrasekhar number in stabilizing the system. Gupta et al. [4] studied Rayleigh-Benard convection of nanofluid with magnetic field and permeability effects. The influence of study parameters such as the Darcy number, magnetic field parameter etc. on both stationary and oscillatory Rayleigh number are analyzed.

2. Mathematical Formulation

Consider viscous incompressible MHD nanofluid in an infinitely extended horizontal porous layer, confined between two boundaries at z = 0 and z = h, which is heated from below and cooled from above. A Cartesian frame of reference has been chosen in which the z-axis is vertically upwards. The boundaries are perfectly conducting. The temperature at the lower and upper walls is taken to be T_c and T_h respectively with $T_h<T_c$. The Oberbeck - Boussinesq approximation and the Darcy law are assumed to be applicable. The continuity equation, momentum equation, energy equation, concentration equation and volumetric fraction nanoparticle equation describing the above configuration are given as

$$\nabla^* \cdot V^* = 0, \tag{1}$$

$$\frac{\rho_f}{\varepsilon}\frac{\partial V^*}{\partial t} = -\nabla^* P^* + \tilde{\mu}\nabla^{*2}V^* - \frac{\mu}{K}V^* + \Big\{\phi^*\rho_p + (1-\phi^*)\{\rho_f(1-\beta_1(T^*-T_c^*)) - \beta_2(C^*-C_c^*)\}\Big\}\mathbf{g} + \delta\mathbf{B}_0^2 V^*\hat{e}_z, \tag{2}$$

$$(\rho c)_m\frac{\partial T^*}{\partial t} + (\rho c)_f(V^*\cdot\nabla^* T^*) = \kappa_m\nabla^{*2}T^* + \varepsilon(\rho c)_p\Big\{D_B\nabla^*\phi^*\cdot\nabla^*T^* + \frac{D_T}{T_c^*}\nabla^*T^*\cdot\nabla^*T^*\Big\} + (\rho c)_m D_{TC}\nabla^{*2}C^*, \tag{3}$$

$$\frac{\partial C^*}{\partial t} + (V^*\cdot\nabla^*C^*) = D_S\nabla^{*2}C^* + D_{CT}\nabla^{*2}T^*, \tag{4}$$

$$\frac{\partial \phi^*}{\partial t} + \frac{1}{\varepsilon}(V^*\cdot\nabla^*\phi^*) = D_B\nabla^{*2}\phi^* + \frac{D_T}{T_c}\nabla^{*2}T^*, \tag{5}$$

where V^* is the fluid velocity, $T^*$is the temperature field, C^* is the solutal concentration and $\phi\phi^*$ is the volumetric fraction of nanoparticle. While ρ_f, ρ_p, μ, β_1, β_2, κ_m, δ, ε and K are the fluid density, nanoparticle density, effective viscosity of porous medium, thermal volumetric expansion coefficient of the fluid, solutal volumetric expansion coefficient, the thermal conductivity of porous medium, the electrical conductivity, the porosity, and permeability of porous medium respectively. The gravitational acceleration vector is denoted by g and D_B is the Brownian diffusion coefficient, D_T is the thermophoresis diffusion coefficient, D_S is the solutal diffusion coefficient, D_{TC} is the Dufour parameter and D_{CT} is the Soret parameter. The heat capacity of the fluid is $(\rho c)_f$, $(\rho c)_p$ is the effective heat capacity of the nanoparticle, $(\rho c)_m$ is the effective heat capacity of the porous medium and B_0 is the uniform magnetic field strength. We assume that the temperature and concentration are constant at the boundaries. The volumetric fraction of nanoparticle flux is vanishes at the boundaries. Then the boundary conditions are given as

$$V^* = 0,\ T^* = T_h^*,\ C^* = C_h^*\quad D_B\frac{\partial\phi^*}{\partial z^*} + \frac{D_T}{T_c}\frac{\partial T^*}{\partial z^*} = 0 \text{ at } z^* = 0, \tag{6}$$

$$V^* = 0,\ T^* = T_c^*,\ C^* = C_c^*\quad D_B\frac{\partial\phi^*}{\partial z^*} + \frac{D_T}{T_c}\frac{\partial T^*}{\partial z^*} = 0 \text{ at } z^* = h. \tag{7}$$

We define dimensionless variables as follows,

$$(x,y,z)=(x^*,y^*,z^*)/h,\ \ t=\frac{t^*\alpha_m}{\sigma h^2},\ \ V=\frac{V^*h}{\alpha_m},\ \ \alpha_m=\frac{\kappa_m}{(\rho c)_f},\quad \sigma=\frac{(\rho c)_m}{(\rho c)_f}$$
$$P=\frac{P^*K}{\mu\alpha_m},\ \ T=\frac{T^*-T_c^*}{T_h^*-T_c^*},\ \ C=\frac{C^*-C_c^*}{C_h^*-C_c^*},\ \ \phi=\frac{\phi^*-\phi_0^*}{\phi_1^*-\phi_0^*}.$$

Substituting the dimensionless variables in equations (1)-(7) and neglecting the products of ϕ and T, we have,

$$\nabla\cdot V=0, \tag{8}$$
$$\frac{Da}{Pr}\frac{\partial V}{\partial t}=-\nabla P+Da\nabla^2V-V+QV\hat{e}_z-Rm\hat{e}_z+RaT\hat{e}_z+RsC\hat{e}_z-Rn\phi\hat{e}_z, \tag{9}$$
$$\frac{\partial T}{\partial t}+V\cdot\nabla T=\nabla^2T+\frac{N_B}{Les}\nabla\phi\cdot\nabla T+\frac{N_AN_B}{Les}\nabla T\cdot\nabla T+Du\nabla^2C, \tag{10}$$
$$\frac{\partial C}{\partial t}+V\cdot\nabla C=\frac{1}{Le}\nabla^2C+Sr\nabla^2T, \tag{11}$$
$$\frac{1}{\sigma}\frac{\partial\phi}{\partial t}+\frac{1}{\varepsilon}V\cdot\nabla\phi=\frac{1}{Les}\nabla^2\phi+\frac{N_A}{Les}\nabla^2T, \tag{12}$$

subject to boundary conditions,

$$V=0,\ \ T=1,\ \ C=1\quad \frac{\partial\phi}{\partial z}+N_A\frac{\partial T}{\partial z}=0\ \text{ at }\ z=0, \tag{13}$$
$$V=0,\ \ T=0,\ \ C=0\quad \frac{\partial\phi}{\partial z}+N_A\frac{\partial T}{\partial z}=0\ \text{ at }\ z=1, \tag{14}$$

where Da is the Darcy number modified by the viscosity ratio, Pr is the Prandtl number, Q is the Hartmann-Darcy number, Ra is the thermal Rayleigh-Darcy number, Rn is the nanoparticle Rayleigh number and Rm is the basic density Rayleigh number. The parameter N_A is a modified diffusivity ratio, Le is the Lewis number, Rs is solutal Rayleigh number, N_B is a modified nanoparticle density increment and Du is a modified Dufour parameter. The parameter Les is the thermo-nanofluid Lewis number, ν is the kinematic viscosity and Sr is a modified Soret parameter.

3. The Basic State

The basic state is time independent solution of the equations (8) – (14) which depends on z only. To determine the linear stability of the nanofluid flow, we superimpose perturbations on the basic state defining the nanofluid quantities as

$$V = V',\ P = P_b + P',\ T = T_b + T',\ C = C_b + C\ \ \phi = \phi_b + \phi'. \tag{15}$$

We reduce the number of unknowns by taking the curl, twice of equation (9). Then equations (8) – (14), after neglecting the nonlinear terms reduce to

$$
\begin{aligned}
\frac{Da}{Pr}\frac{\partial \nabla^2 W'}{\partial t} &= Da\nabla^4 W' - \nabla^2 W' - Q\nabla_L^2 W' + Ra\nabla_L^2 T' + Rs\nabla_L^2 C' - Rn\nabla_L^2 \phi', \\
\frac{\partial T'}{\partial t} - W' &= \nabla^2 T' + \frac{N_B}{Les}\left(\frac{\partial T'}{\partial z} - \frac{\partial \phi'}{\partial z}\right) - \frac{2N_A N_B}{Les}\frac{\partial T'}{\partial z} + Du\nabla^2 C' - \nabla V' \cdot \nabla T', \\
\frac{\partial C'}{\partial t} - W' &= \frac{1}{Le}\nabla^2 C' + Sr\nabla^2 T' - \nabla V' \cdot \nabla C', \\
\frac{1}{\sigma}\frac{\partial \phi'}{\partial t} + \frac{N_A}{\varepsilon}W' &= \frac{1}{Les}\nabla^2 \phi' + \frac{N_A}{Le}\nabla^2 T' - \nabla V' \cdot \nabla \phi',
\end{aligned}
\tag{16}
$$

subject to boundary conditions,

$$
W' = \frac{\partial^2 W'}{\partial z^2} = 0, \;\; T' = 0, \;\; C' = 0, \;\; \frac{\partial \phi'}{\partial z} + N_A \frac{\partial T'}{\partial z} = 0 \;\; \text{at} \;\; z = 0, 1.
$$

where

$$
\nabla_L^2 = \frac{\partial^2}{\partial x^2} + \frac{\partial^2}{\partial y^2}.
\tag{17}
$$

4. Linear Stability Analysis

To study the linear stability of the flow, we linearized equations (16) which we get from the basic state section by neglecting the nonlinear terms. Thus, employing the normal modes defined the perturbation quantities in the form

$$
(W', T', C', \phi') = (W(z), \Theta(z), F(z), \Phi(z)) \exp[st + i(lx + my)]. \tag{19}
$$

$$
\begin{aligned}
&\left\{Da(D^2 - \alpha^2)^2 - (1 + \frac{sDa}{Pr})(D^2 - \alpha^2) + Q\alpha^2\right\}W - \alpha^2 Ra\Theta - \alpha^2 RsF + \alpha^2 Rn\Phi = 0 \\
&W + \left\{D^2 + \frac{N_B}{Les}D - \frac{2N_A N_B}{Les}D - \alpha^2 - s\right\}\Theta + Du(D^2 - \alpha^2)F - \frac{N_B}{Les}D\Phi = 0, \\
&W + Sr(D^2 - \alpha^2)\Theta + \left\{\frac{1}{Le}D^2 - \frac{\alpha^2}{Les} - s\right\}F = 0, \\
&-\frac{N_A}{\varepsilon}W + (\frac{N_A}{Les}D^2 - \frac{N_A\alpha^2}{Les})\Theta + \left\{\frac{1}{Les}D^2 - \frac{\alpha^2}{Les} - \frac{s}{\sigma}\right\}\Phi = 0.
\end{aligned}
$$

These equations are to be solved subject to the free-free boundary conditions

$$
W = D^2 W = 0, \;\; \Theta = 0, \;\; F = 0, \;\; D\Phi + N_A D\Theta = 0 \;\; \text{at } z = 0 \text{ and } z = 1,
$$

where D = d/dz. A related analysis for rigid-rigid, and rigid-free boundary conditions is given in [1]. Here we present results for free-free boundary conditions. Here, the dimensionless horizontal wave number is denoted by α and s is denoted the complex quantity. To apply Galerkin approximation the flow quantities are defined as follows:

$$W = \sum_{n=1}^{M} A_n W_n, \quad \Theta = \sum_{n=1}^{M} B_n \Theta_n, \quad F = \sum_{n=1}^{M} C_n F_n, \quad \Phi = \sum_{n=1}^{M} D_n \Phi_n,$$

and chose the trial functions

$$W_n = \Theta_n = F_n = \sin n\pi z, \ \Phi_n = -N_A \sin n\pi z.$$

Apply the orthogonality of trial functions from these previous equations in this section to introduce the Rayleigh number (Ra) as eigenvalue of the system in terms of the other parameters.

5. Stationary convection

In this case we assume s = 0 and for the first approximate we take M = 1. From the linear stability equations, we obtain,

$$\mathbf{Ra}^{\alpha} = \frac{\gamma^3 Da + \gamma^2 + \gamma\alpha^2 Q}{\alpha^2}\lambda_1 + Rs\lambda_2 + RnN_A\lambda_3,$$

where

$$\lambda_1 = \frac{DuSr - 1}{Du - 1}, \lambda_2 = \frac{Sr - 1}{Du - 1} \quad \text{and} \quad \lambda_3 = \frac{\varepsilon(DuLe - 1) + Les(DuSrLe - 1)}{\varepsilon Le(Du - 1)}.$$

Here Ra^{α} is the stationary Rayleigh number for marginal instability convection. In the case of Rs = 0; Du = 0 and Sr = 0 with absence of magnetic field has been discussed in details in [1]. The corresponding critical Rayleigh number equations depend on Da and Q. When Da $\rightarrow\infty$, the critical wave number will be $\alpha = \frac{\pi}{\sqrt{2}}$ and the corresponding critical Rayleigh number will be $R\alpha = \frac{27}{4}\pi^4 = 657.5$. This result agrees with the literature such as [1] and [2].

6. Results and Discussion

In this paper, we have studied the linear stability of nanofluid flow in a horizontal layer in the case of stress-free and revised nanoparticles boundary conditions. The critical Rayleigh number for stationary convection has been determined in the linear stability regime. The parameter values for simulations are chosen from the literature on nanofluid flow. Furthermore, the instability of nanofliud was demonstrated by [1]. Figure 1, presents the neutral stability curves for stationary Rayleigh number (Ra^{α}) versus wave number α for the influence of different parameters. It is interesting to note that the value of stationary Rayleigh number starts from a higher note, then falls rapidly with increasing wave number and then increases steadily. Figure 1(a) shows that increasing the Chandrasekhar number (Q) increases the stationary Rayleigh number leading to a stabilization of the nanofluid convection. Also, it is observed that the effect of magnetic field

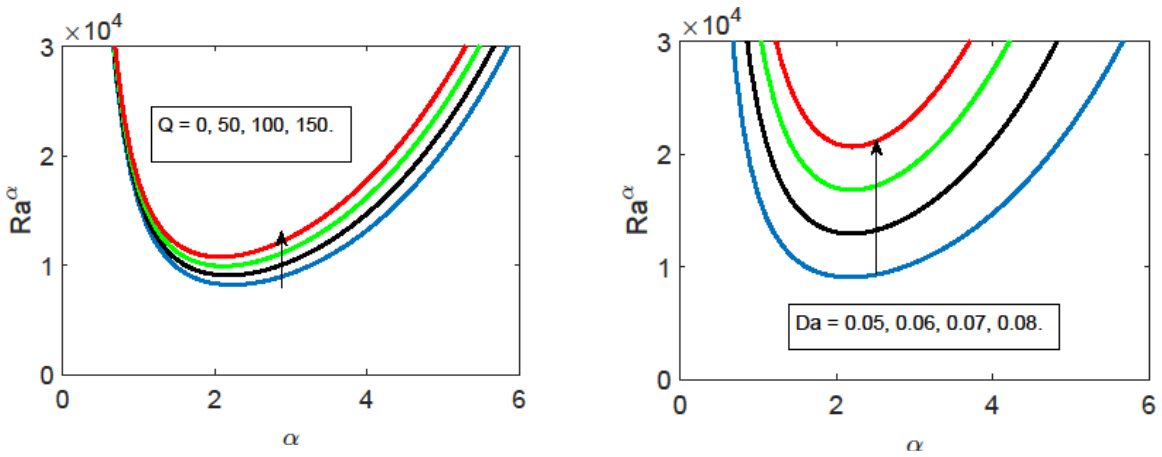

Fig 1. The effect of (a) the Chandrasekhar number (Q), (b) the Darcy number (Da), on the stationary Rayleigh number.

parameter on stationary Rayleigh number is very small, so we can deny that magnetic field effect on nanofluid flow. The effect of increasing the Darcy number (Da) in Figure 1(b) is to increase the stationary Rayleigh number, thus delaying the onset of stationary instability. This may be explained by the observation that increasing the Darcy number increases the effective viscosity which has the tendency to retard the nanofluid flow, hence more heating is required for the onset of convection.

7. Conclusion

In this work, the results illustrate the onset of instability in a horizontal porous layer of infinite extent in a cross diffusive nanofluid flow with magnetic field. The effects of the Darcy number (Da) and Chandrasekhar number (Q) on the onset of stationary instability have been studied. An increase in the Darcy number (Da) increases the critical Rayleigh number for the onset of instability. The effect of the Darcy number is thus to delay the onset of instability in the nanofluid in the porous medium. Also the Chandrasekher number (Q) stabilizes the instability of nanofluid convection.

References

[1] A.V. Kuznetsov, D. A. Nield, Transp. Porous Med. 81, 409 (2010)

[2] S. Chandrasekhar, Oxford University Press, Oxford (1961)

[3] B. S. Bhadauria, Phys. Scr. 73, 296 (2006)

[4] U. Gutpa, J. Ahuja, R. K. Wanchoo, Procedia Eng. 127, 325 (2015)

Part II: Onset of instability in a horizontal porous layer: Effect of the Soret and Dufour parameters

In this section, we investigate the influence of the Dufour and Soret parameters, nanofluid Lewis and Prandtl numbers on the onset of stationary and oscillatory convection.

For the case of stationary convection we have $\mathbf{Ra}^{\alpha}$ the stationary Rayleigh number for marginal instability convection, given by

$$\mathbf{Ra}^{\alpha} = \frac{\gamma^3 Da + \gamma^2 + \gamma\alpha^2 Q}{\alpha^2}\lambda_1 + Rs\lambda_2 + RnN_A\lambda_3, \tag{2.0.1}$$

where

$$\lambda_1 = \frac{DuSr-1}{Du-1}, \lambda_2 = \frac{Sr-1}{Du-1} \quad \text{and} \quad \lambda_3 = \frac{\varepsilon(DuLe-1)+Les(DuSrLe-1)}{\varepsilon Le(Du-1)}.$$

The condition of oscillatory convection occurs when the real part of s is zero. Hence $s = i\omega$ where the ω denotes dimensionless oscillations frequency. We have

$$\omega^2 = \frac{\sigma N_A\lambda_5 + LePr\lambda_4}{DaLe} + \frac{\alpha^2 Rs(\sigma N_A - (1-Sr)Les)}{Da\gamma} - \frac{\alpha^2\sigma N_A^2(\varepsilon + (1+Le)Les)}{\varepsilon Da\gamma}, \tag{2.0.2}$$

where $\lambda_4 = Da\gamma^2 + \gamma + \alpha^2 Q$ and $\lambda_5 = Da(1+Pr) + Pr(\gamma + \alpha^2 Q)$. For the oscillatory Rayleigh number, we obtain

$$\begin{aligned} Ra^{osc} = {} & \frac{\sigma N_A\gamma(Da\gamma^2\omega^2\lambda_6 + Pr\lambda_4\lambda_7) + PrLe\gamma\omega^2\lambda_4 + DaLes\gamma\omega^2\lambda_8}{\alpha^2(LeLes\omega^2 + \sigma N_A\gamma^2\lambda_9)} \\ & + \frac{\sigma RnN_A^2(LeLes(DuSr\gamma^2+\omega^2) - \gamma^2(Le^2Les+\sigma) - \sigma DuLe\gamma^2)}{LeLes\omega^2 + \sigma N_A\gamma^2\lambda_9} - \\ & - \frac{RsLe(\sigma N_A\gamma(Sr-1) + Les\omega^2)}{LeLes\omega^2 + \sigma N_A\gamma^2\lambda_9}, \end{aligned} \tag{2.0.3}$$

where

$$\begin{aligned} \lambda_6 &= (1+Le), \quad \lambda_7 = DuSrLe\gamma^2 - \gamma^2 + Le\omega^2, \quad \lambda_8 = \gamma^2 - SrLe\gamma - Le\omega^2 \\ \text{and} \quad \lambda_9 &= DuLe - 1. \end{aligned}$$

Results and discussion

We studied the stability of nanofluid flow in a horizontal layer in the case of stress-free boundary conditions. The critical Rayleigh numbers for stationary and oscillatory convection have been determined. For simulations, the parameter values are chosen from the literature on nanofluid flow, such as in Tzou [63] and Yadav et al. [91].

The influence of the parameters on the onset of convection is presented in Figures 2.1 to 2.4. Here the neutral stability curves for stationary and oscillatory Rayleigh numbers Ra^{α} are plotted against the wave number α. Figure 2.4(a), shows that the effect of increasing the value of the Dufour parameter *Du* is to increase the critical value of the stationary Rayleigh number. Hence the influence of the Dufour parameter is to stabilize the system by delaying the onset of convection. Figure 2.4(b) shows that the Soret parameter *Sr* reduces the critical stationary Rayleigh number at which instabilities set in.

In Figure 2.1(a) it can be seen that increasing the porosity ε causes a slight decrease in the critical stationary Rayleigh number, thus the effect of increasing porosity is to reduce the critical stationary Rayleigh number. This has a destabilizing effect on the onset of stationary convection. Figure 2.1(b) shows the effect of the nanofluid Lewis number *Le* on the stationary Rayleigh number. Increasing the nanofluid Lewis number reduces the critical stationary Rayleigh number. This destabilized the nanofluid flow. Figure 2.2 and 2.3 show the effect of the thermo-nanofluid Lewis number *Les*, nanoparticle density increment N_A and the nanoparticle Rayleigh number *Rn* on the stationary Rayleigh number. Increasing each of these parameters increases the critical value of the stationary Rayleigh number. Hence these parameters have the effect of stabilizing the system by delaying the onset of convection instabilities.

Figure 2.5 to 2.9 show the neutral stability curves for oscillatory convection. In the set of figures, for most of parameters, increasing their values has the effect of increasing the critical oscillatory Rayleigh number, which delays the onset of oscillatory convection. However, increasing porosity reduces the critical oscillatory Rayleigh number; hence it has a destabilization effect.

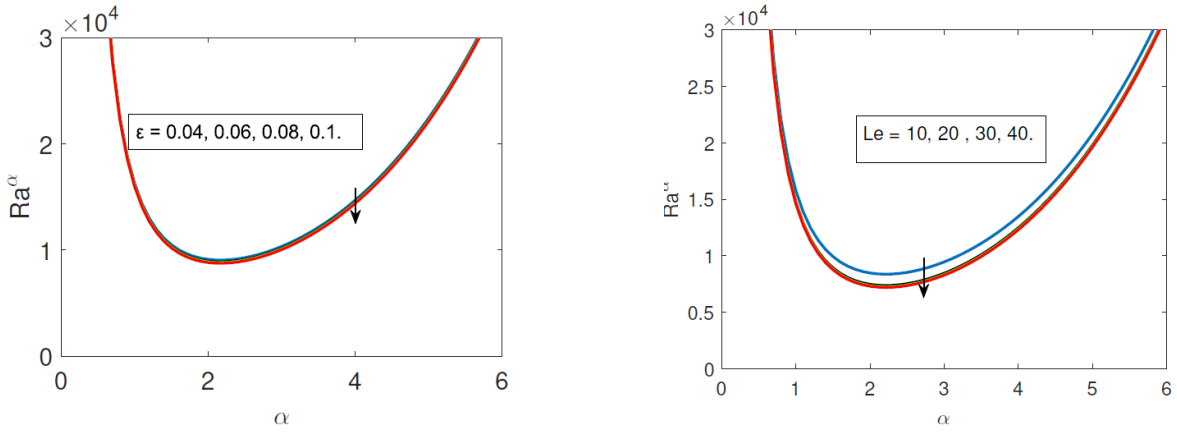

(a) (b)

Figure 2.1: The effect of (a) the porosity and (b) the Lewis number on the onset of stationary convection. Here $Q = 50, \sigma = 0.05, Da = 0.05, Du = 0.2, Sr = 0.3$.

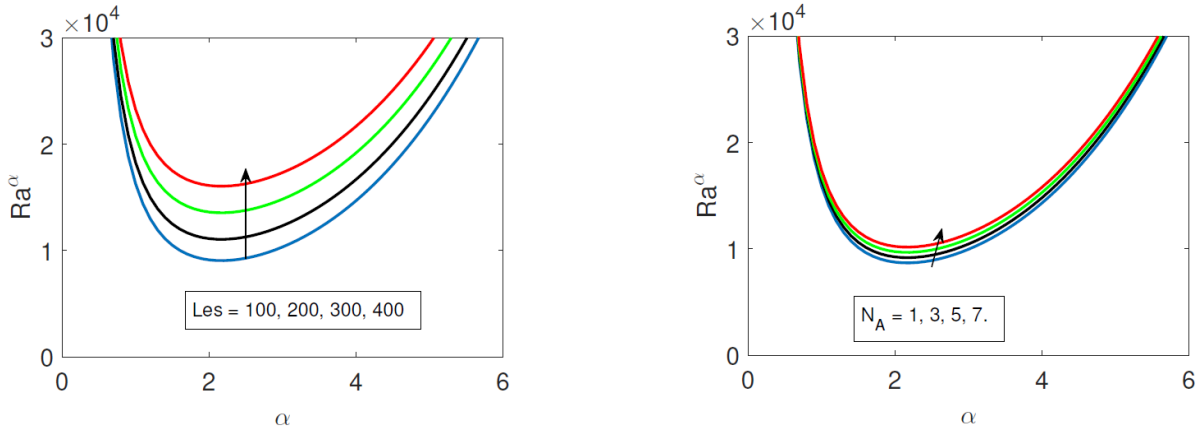

(a) (b)

Figure 2.2: The effect of (a) the nanofluid Lewis number and (b) the nanoparticle density increment parameter on the onset of stationary convection. Here $Q = 50, \sigma = 0.05, Da = 0.05, Du = 0.2, Sr = 0.3$.

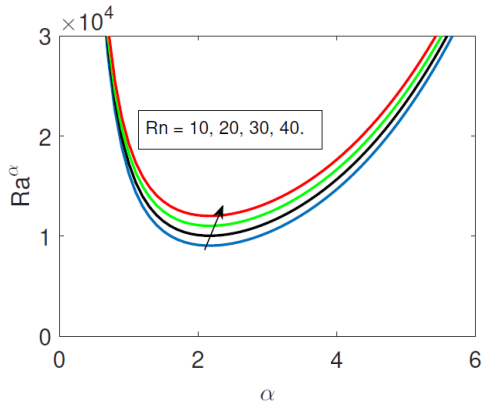

Figure 2.3: The effect of the nanoparticle Rayleigh number on the onset of stationary convection. Here $Q = 50, \sigma = 0.05, Da = 0.05, Du = 0.2, Sr = 0.3$.

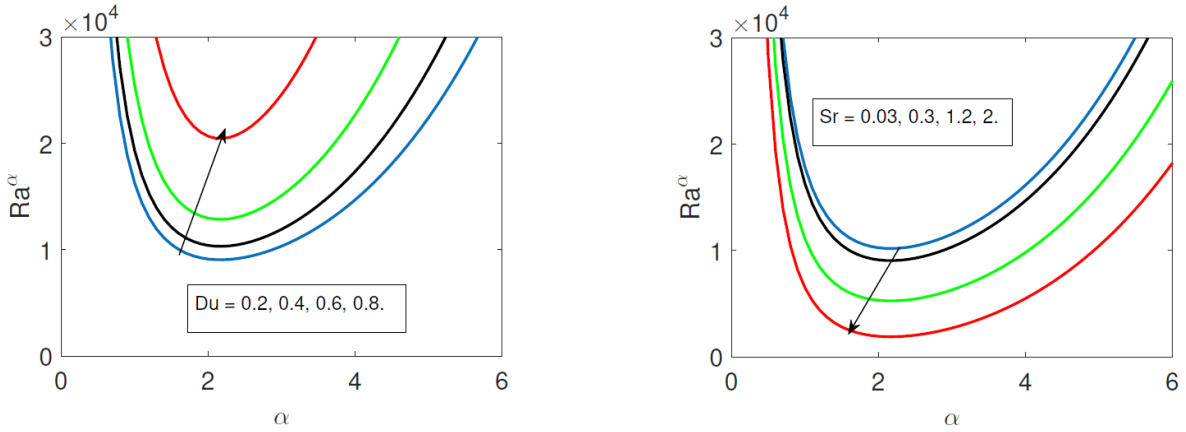

(a) (b)

Figure 2.4: The effect of (a) the Dufour parameter Du, and (b) the Soret parameter Sr on the onset of stationary convection. Here $Le = 10, \varepsilon = 0.04, Les = 100, \sigma = 0.05, N_A = 4, Rn = 10$.

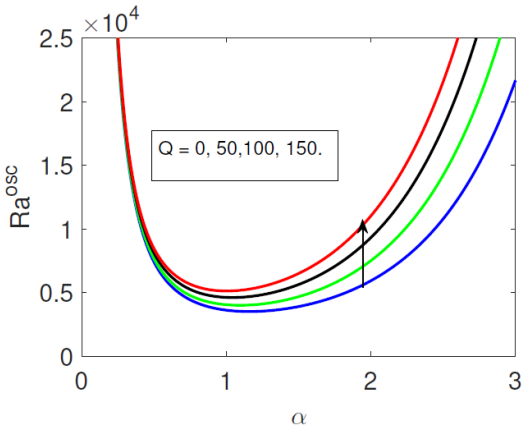

(a)

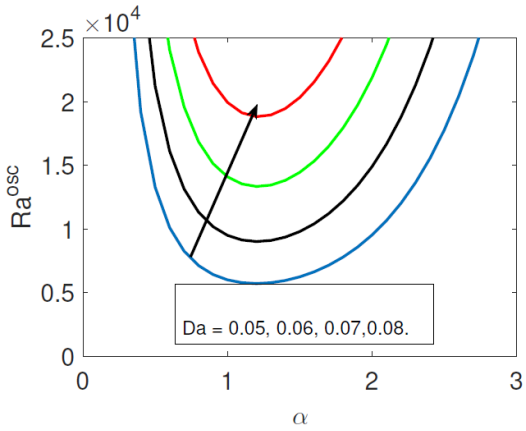

(b)

Figure 2.5: The effect of (a) the Chandrasekhar number and (b) the Darcy number on the onset of oscillatory convection. Here $Le = 10, \varepsilon = 0.04, Les = 100, \sigma = 0.05, N_A = 4, Rn = 10$.

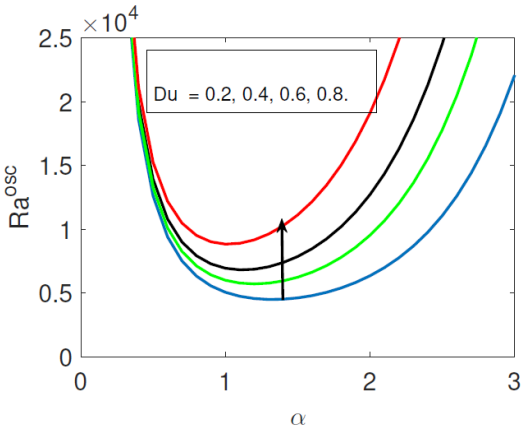

(a)

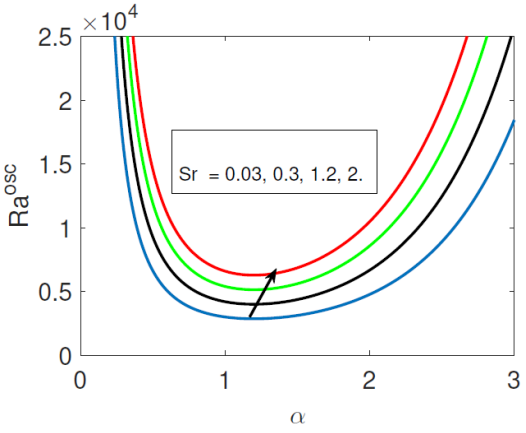

(b)

Figure 2.6: The effect of (a) the Dufour parameter and (b) the Soret parameter on the onset of oscillatory convection. Here $Le = 10, \varepsilon = 0.04, Les = 100, \sigma = 0.05, N_A = 4, Rn = 10$.

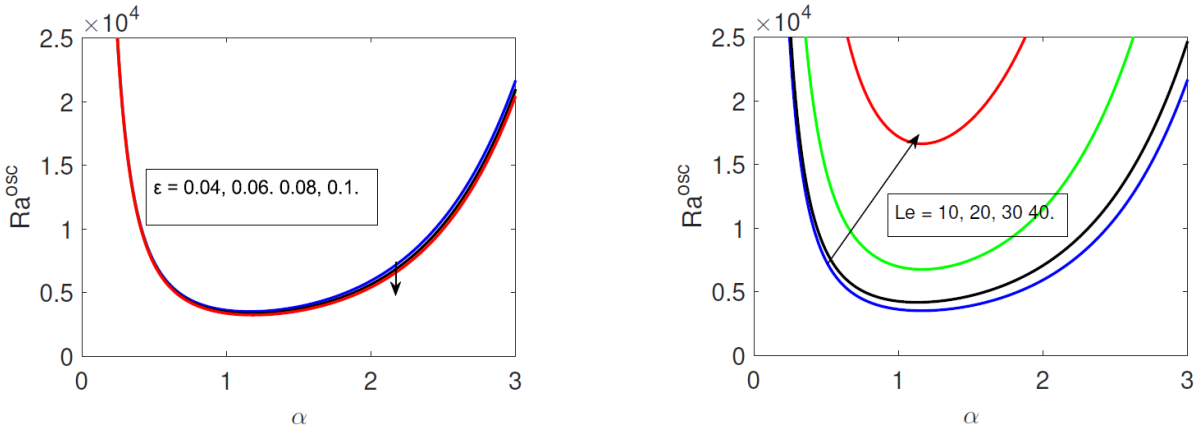

(a) (b)

Figure 2.7: The effect of (a) the porosity and (b) the Lewis number on the onset of oscillatory convection. Here $Q = 50, \sigma = 0.05, Da = 0.05, Du = 0.2, Sr = 0.3$.

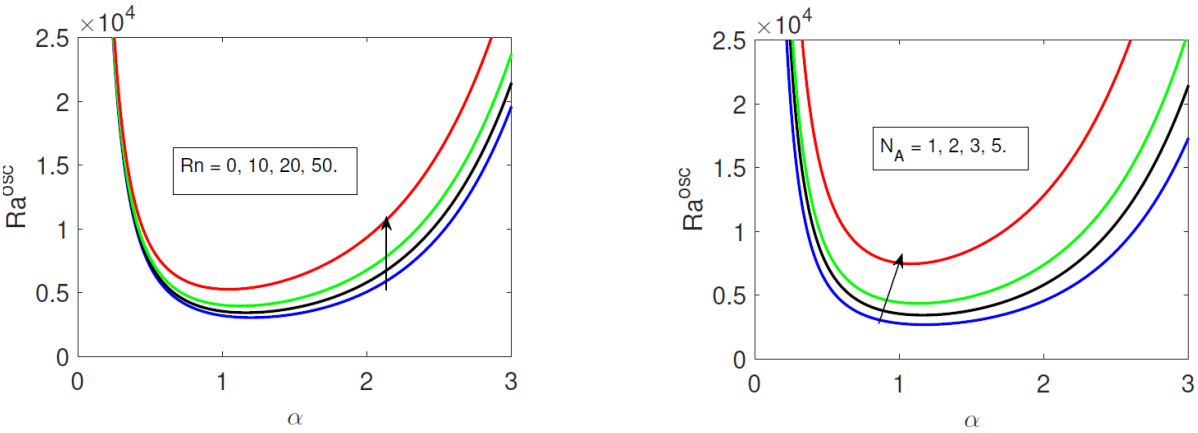

(a) (b)

Figure 2.8: The effect of(a) the nanoparticle Rayleigh number and (b) the nanoparticle density increment parameter on the onset of oscillatory convection. Here $Q = 50, \sigma = 0.05, Da = 0.05, Du = 0.2, Sr = 0.3$.

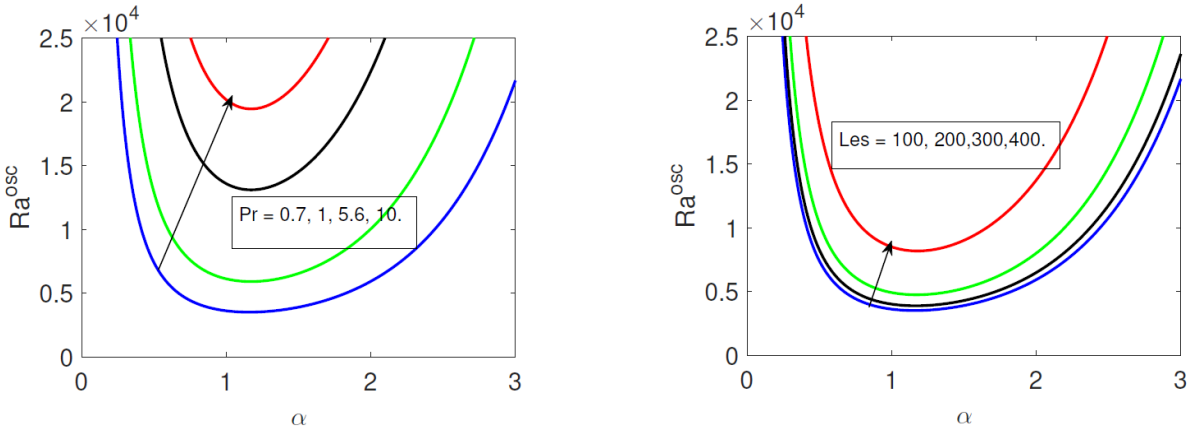

(a) (b)

Figure 2.9: The effect of (a) the Prandtl number and (b)the nanofluid Lewis number on the onset of oscillatory convection. Here $Q = 50, \sigma = 0.05, Da = 0.05, Du = 0.2, Sr = 0.3$.

Summary

In this chapter we have used the linear theory to analyze the stability of a horizontal layer of a nanofluid flow in a porous medium. The results show how certain parameters influence the onset of convection in the cross-diffusive nanofluid flow. The focus of the study has been on stress-free boundary conditions with zero nanoparticle flux at the boundary.

The following conclusions can be drawn from the study;

1- An increase in the value of the nanofluid Lewis number *Les* increases both the stationary and oscillatory Rayleigh numbers. This has the effect of increasing the value of the Rayleigh number at the turning point of the neutral stability curve, which in turn has a stabilizing effect on the system.

2 - The Soret and Dufour parameters, have the effect of reducing and increasing the critical Rayleigh number, respectively.

3- The critical stationary and oscillatory Rayleigh numbers are both independent of modified nanoparticle density increment.

Chapter 3

Weakly Nonlinear Stability Analysis of a Nanofluid in a Horizontal Porous Layer Using a Multidomain Spectral Collocation Method

In this chapter, we used weakly nonlinear stability theory to analyze the onset of instabilities in a nanofluid flow in a porous medium with zero nanoparticle flux at the walls. A truncated Fourier series is used to derive the evolution equations that describe the amplitudes of convection. A multidomain spectral collocation method is used to solve the evolution equations. The influence of parameters on the heat and mass transfer characteristics is determined. A limited phase space analysis is presented.

Chapter 9

Weakly Nonlinear Stability Analysis of a Nanofluid in a Horizontal Porous Layer Using a Multidomain Spectral Collocation Method

Osman A.I. Noreldin, Precious Sibanda and Sabyasachi Mondal

Additional information is available at the end of the chapter

http://dx.doi.org/10.5772/intechopen.71066

Abstract

In this chapter, we present a weakly nonlinear stability analysis of the flow of a nanofluid in a porous medium with stress-free boundary conditions. Some previous studies have investigated cross-diffusion in a nanofluid layer although in most cases these studies mostly deal with linear stability analysis. It is important to study the nonlinear stability in flows subject to cross-diffusion due to the wide range of applications where such flows arise such as in hydrothermal growth, compact heat exchanges, the solidification of binary mixtures, geophysical systems, solar pond, etc. Here we consider flow between parallel plates with an applied magnetic field and zero nanoparticle flux at the boundaries. A truncated Fourier series is introduced reducing the flow equations to a Lorenz-type system of nonlinear evolution equations. The multidomain spectral method is used to solve the equations that describe the growth of the convection amplitudes. The solutions are obtained as sets of trajectories in the phase space. Some interesting spiral trajectories and their sensitivity to the Rayleigh number are given.

Keywords: nonlinear instability, nanofluid flow, porous medium, multidomain spectral collocation method

1. Introduction

The enhancement of thermal conductivity of a fluid is a matter of supreme interest to engineers due to the important applications of fluids in heat transfer processes. Natural and forced convection plays an important role in heat transfer processes due to continuous molecular movements in fluid. Recent studies show that the suspension of solid nanoparticles in a fluid can substantially improve the fluid's thermophysical properties, including thermal conductivity.

The term nanofluid describes a liquid containing a suspension of nanometer sized 1–100 nm solid particles [1]. Examples of commonly used nanoparticles include metallic particles such as Al, Cu and Ag, and oxides such as Al_2O_3 and CuO. The base fluid is often a common liquid such as water, ethylene, glycol, or oil. The enhancement of thermochemical properties of a fluid due to the addition of nanoparticles has been observed in experimental studies such as in [2, 3]. Researchers have investigated the influence of seven slip mechanisms, namely, inertia, Brownian diffusion, thermophoresis, diffusiophoresis, magnus effect, fluid drainage, and gravity in nanofluids. It has been shown that, in the absence of turbulence, the most significant among these mechanisms are the Brownian diffusion and thermophoresis.

The classical Rayleigh-Benard convection problem in a heated horizontal layer has been extensively studied in the literature. Among recent studies on nanofluids, Tzou [4] studied the thermal instability and natural convection in nanofluid flow using an eigenfunction expansion method. Narayana et al. [5, 6] studied convection and the stability of a Maxwell fluid in a porous medium. Yadav et al. [7] investigated thermal instability of a rotating nanofluid layer. The studies by Kuznetsov and Nield [8–11] focused on thermal instability in a porous layer saturated with a nanofluid. They investigated the onset of instability in a horizontal porous layer using a model for the nanofluid that incorporated particle Brownian motion and thermophoresis. Related studies with various assumptions on the geometry and flow structure have been made by [12–15]. In the last few decades, researchers have also investigated thermal instability in a horizontal nanofluid layer subject to an applied magnetic field [16, 17]. The effects of a magnetic field on convection and the onset of instability have important applications in problems such as in cooling systems, pumps, magnetohydrodynamics and generators. The experimental study by Heris et al. [18] showed that thermal efficiency could be achieved by subjecting the flow to a magnetic field. The studies by Ghasemi et al. [19] and Hamad et al. [20] focused on the flow behavior and heat transfer in an electrically conducting nanofluid under the influence of a magnetic field and subject to Brownian diffusion and thermophoresis. They used a water-based nanofluid containing different types of nanoparticles such as copper, alumina and silver in their numerical simulations. Related studies of interest include [21–24]. Rana et al. [25] studied thermal convection in a Walters (Model B) fluid in a porous medium. They showed that a magnetic field may introduce oscillatory instability modes and acts to stabilize the system.

In this chapter, we give a weakly nonlinear stability analysis of a nanofluid layer with an applied magnetic field, stress free boundary conditions and under the assumption of zero nanoparticle flux at the boundary. The studies by Kuznetsov and Nield [9] and Nield and Kuznetsov [10, 11] investigated cross-diffusion in a nanofluid layer. However, these studies mostly presented a linear stability analysis. It is important to study the nonlinear regime for a nanofluid flow subject to cross-diffusion due to the wide range of applications where such flows may arise. Typical examples may be found in hydrothermal growth, compact heat exchanges, solidification of binary mixtures, geophysical systems, and so on. Hence, with this in mind, we studied the finite amplitude convection in a nanofluid flows subject to cross-diffusion. By introducing a truncated Fourier series, a Lorenz-type system of seven nonlinear differential equations is obtained. The recent multidomain spectral method is used to solve the nonlinear equations. This method is accurate and very easy to implement compared to older methods such as finite difference methods. An analysis of heat and mass transfer for different parameters such as the Prandtl number, the Dufour and thermophoresis is presented.

http://dx.doi.org/10.5772/intechopen.71066

2. Mathematical formulation

Consider viscous incompressible MHD nanofluid flow in an infinitely extended horizontal porous layer, confined between two boundaries at $z = 0$ and $z = h$. The layer is heated from below and cooled from above, see **Figure 1**. A Cartesian frame of reference is chosen in which the z-axis is vertically upward. The boundaries are perfectly conducting. The temperature at the lower and upper walls is T_c and T_h, respectively with $T_h > T_c$. The Oberbeck-Boussinesq approximation and the Darcy law are assumed to be applicable. The continuity equation, momentum equation, energy equation, concentration equation and volumetric fraction nanoparticle equation, which describe the above configuration in dimensionless form, are given as

$$\nabla \cdot V = 0, \tag{1}$$

$$\frac{Da}{\mathrm{Pr}}\frac{\partial V}{\partial t} = -\nabla P + Da\nabla^2 V - V + QV\widehat{e}_z - Rm\widehat{e}_z + RaT\widehat{e}_z + RsC\widehat{e}_z - Rn\phi\widehat{e}_z, \tag{2}$$

$$\frac{\partial T}{\partial t} + V \cdot \nabla T = \nabla^2 T + \frac{N_B}{Les}\nabla\phi \cdot \nabla T + \frac{N_A N_B}{Les}\nabla T \cdot \nabla T + Du\nabla^2 C, \tag{3}$$

$$\frac{\partial C}{\partial t} + V \cdot \nabla C = \frac{1}{Le}\nabla^2 C + Sr\nabla^2 T, \tag{4}$$

$$\frac{1}{\sigma}\frac{\partial \phi}{\partial t} + \frac{1}{\varepsilon}V \cdot \nabla\phi = \frac{1}{Les}\nabla^2\phi + \frac{N_A}{Les}\nabla^2 T, \tag{5}$$

subject to the boundary conditions

$$V = 0, T = 1, C = 1\frac{\partial \phi}{\partial z} + N_A\frac{\partial T}{\partial z} = 0 \ \text{ at } z = 0, \tag{6}$$

$$V = 0, \quad T = 0, \quad C = 0 \qquad \frac{\partial \phi}{\partial z} + N_A\frac{\partial T}{\partial z} = 0 \quad \text{at} \quad z = 1, \tag{7}$$

where V is the fluid velocity, T is the temperature, C is the solute concentration and ϕ is the volumetric fraction of nanoparticles. The dimensionless parameters are the Darcy number (modified by the viscosity ratio) Da, Prandtl number Pr, Hartmann-Darcy number Q, thermal Rayleigh-Darcy number Ra, nanoparticle Rayleigh number Rn and the basic density Rayleigh number Rm. The parameter N_A is a modified diffusivity ratio, Le is the Lewis number, Rs is solutal Rayleigh number, N_B is a modified nanoparticle density increment and Du is a modified Dufour parameter. The parameter Les is the thermo-nanofluid Lewis number, ν is the kinematic viscosity and Sr is a modified Soret parameter. These parameters have the form

$$Da = \frac{\tilde{\mu}K}{\mu h^2}, \quad \mathrm{Pr} = \frac{\mu}{\rho_f \alpha_m}, \quad Q = \frac{\delta \mathbf{B}_0^2 K}{\mu}, \quad Ra = \frac{\rho_f \beta K h g\left(T_h^* - T_c^*\right)}{\mu\alpha_m}, \quad Les = \frac{\alpha_m}{D_B}, \tag{8}$$

$$Rn = \frac{\left(\rho_p - \rho_f\right)\left(\phi_1^* - \phi_0^*\right)gKh}{\mu\alpha_m}, \quad Rm = \frac{\rho_p\phi_0^* + \left(1 - \phi_0^*\right)\rho_f gKh}{\mu\alpha_m}, \quad Le = \frac{\alpha_m}{D_S}, \tag{9}$$

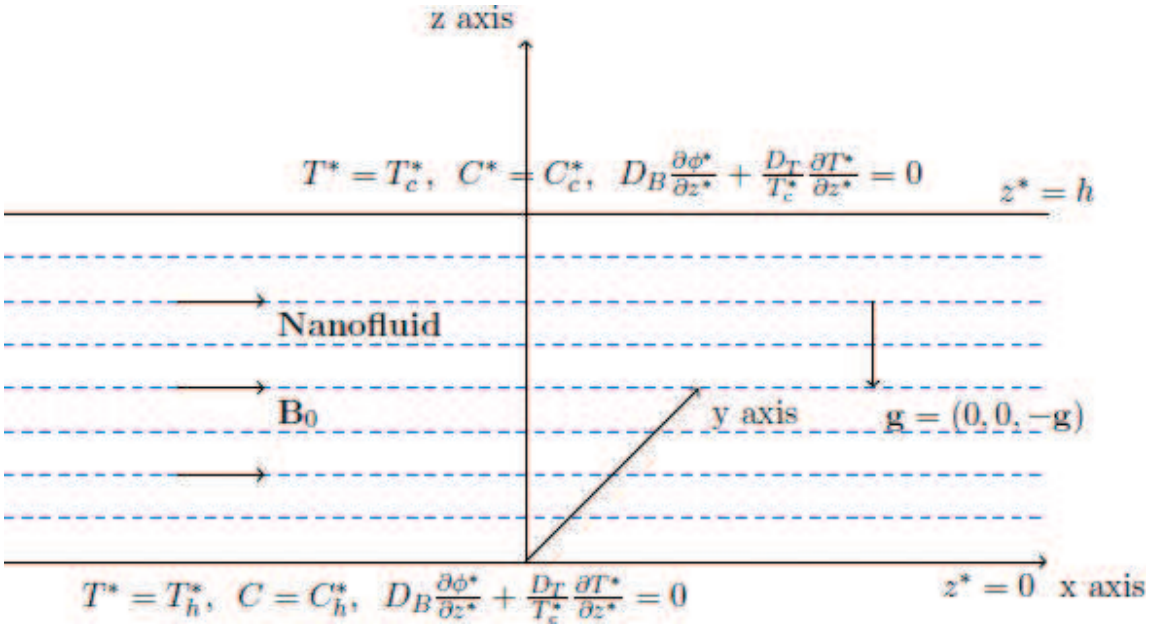

Figure 1. A schematic diagram of the problem.

$$N_B = \frac{\varepsilon(\rho c)_p}{(\rho c)_f}\left(\phi_1^* - \phi_0^*\right), \quad N_A = \frac{D_T\left(T_h^* - T_c^*\right)}{D_B T_c^*\left(\phi_1^* - \phi_0^*\right)}, \quad Rs = \frac{\rho_f \beta K h g\left(C_h^* - C_c^*\right)}{\mu \alpha_m}, \tag{10}$$

$$Du = \frac{\sigma D_{TC}\left(C_h^* - C_c^*\right)}{\alpha_m\left(T_h^* - T_c^*\right)}, \quad Sr = \frac{\sigma D_{CT}\left(T_h^* - T_c^*\right)}{\alpha_m\left(C_h^* - C_c^*\right)}, \tag{11}$$

where ρ_f, ρ_p, $\tilde{\mu}$, β_1, β_2, κ_m, δ, ε and K are the fluid density, nanoparticle density, effective viscosity of porous medium, thermal volumetric expansion coefficient of the fluid, solutal volumetric expansion coefficient, the thermal conductivity of porous medium, the electrical conductivity, the porosity, and permeability of porous medium, respectively. The gravitational acceleration is denoted by g and D_B is the Brownian diffusion coefficient, D_T is the thermophoresis diffusion coefficient, D_S is the solutal diffusion coefficient, D_{TC} is the Dufour parameter and D_{CT} is the Soret parameter. The heat capacity of the fluid is $(\rho c)_f$, $(\rho c)_p$ is the effective heat capacity of the nanoparticle, $(\rho c)_m$ is the effective heat capacity of the porous medium and $\mathbf{B}_0$ is the uniform magnetic field strength.

The basic state is the time independent solution of Eqs. (1)–(5). Solving these equations with boundary conditions, we obtain

$$T_b = 1 - z, \quad C_b = 1 - z, \quad \phi_b = \phi_0 + N_A z. \tag{12}$$

3. Weakly nonlinear stability analysis

In this section, we restrict the analysis to the case of two-dimensional disturbances. We define the stream function Ψ by the equations

$$u = \frac{\partial \Psi}{\partial z}, \quad w = -\frac{\partial \Psi}{\partial x}.$$

Eqs. (1)–(5) may now be simplified by introducing the truncated Fourier series

$$\Psi' = A_{11} \sin \alpha x \sin \pi z, \quad T' = B_{11} \cos \alpha x \sin \pi z + B_{02} \sin 2\pi z, \tag{13}$$

$$C' = C_{11} \cos \alpha x \sin \pi z + C_{02} \sin 2\pi z, \quad \phi' = -N_A(D_{11} \cos \alpha x \sin \pi z + D_{02} \sin 2\pi z), \tag{14}$$

where A_{11}, B_{11}, B_{02}, C_{11}, C_{02}, D_{11} and D_{02} are amplitudes that depend on time. This leads to the Lorenz-type system of nonlinear ordinary differential equations

$$\dot{Y}_1 = \frac{\mathrm{Pr}}{Da}\left\{-BY_1 - N(Y_2 + Y_4) + \frac{N_A Rn}{R} Y_6\right\} \tag{15}$$

$$\dot{Y}_2 = RY_1 - Y_2 - DuY_4 - Y_1Y_3 \tag{16}$$

$$\dot{Y}_3 = \frac{1}{2} Y_1Y_2 - G(Y_3 + DuY_5) \tag{17}$$

$$\dot{Y}_4 = RY_1 - \frac{1}{Les} Y_4 - SrY_2 - Y_1Y_5 \tag{18}$$

$$\dot{Y}_5 = \frac{1}{2} Y_1Y_2 - G\left(\frac{1}{Les} Y_5 + SrY_3\right) \tag{19}$$

$$\dot{Y}_6 = \frac{\sigma R}{\varepsilon} Y_1 - \frac{\sigma}{Le}(Y_6 - Y_2) - \frac{N_A \sigma}{\varepsilon} Y_1Y_7 \tag{20}$$

$$\dot{Y}_7 = \frac{N_A \sigma}{2\varepsilon} Y_1Y_7 - \frac{G}{Le}(Y_7 - Y_3) \tag{21}$$

subject to $Y_n(0) = Y_n^0$ for $n = 1, 2, \cdots, 7$. The following variables have been introduced in the equations above:

$$Y_1 = \frac{\alpha\pi}{\gamma} A_{11}, \quad Y_2 = -\pi R B_{11}, \quad Y_3 = -\pi R B_{02}, \quad Y_4 = -\pi R C_{11}, \quad Y_5 = -\pi R C_{20},$$

$$Y_6 = -\pi R D_{11}, \quad Y_7 = -\pi R D_{20}, \quad t^* = \gamma t, \quad R = \frac{\alpha^2}{\gamma^3} Ra, \quad G = \frac{4\pi^2}{\gamma} \quad \text{and} \quad N = \frac{Rs}{Ra},$$

$$B = \frac{Da\gamma^2 + \gamma - \alpha^2 Q}{\gamma^2}.$$

Eqs. (15)–(21) give an approximate description of the full dimensional nonlinear system. An analytical solution of the system of nonlinear ordinary differential Eqs. (15)–(21) is not possible for the general time variable t. However, it is possible to discuss the stability of the nonlinear system of equations. The system of equations is uniformly bounded in time and dissipative in the phase space. We can easily show that

$$\sum_{i=1}^{7}\frac{\partial \dot{Y}_i}{\partial Y_i} = -\left[\frac{DaB}{\Pr} + 1 + G + Les^{-1} + GLes^{-1} + \sigma Le^{-1} + GLe^{-1}\right]. \tag{22}$$

This is always true if $B \geq 0$. As has been shown in previous studies, the trajectories may be attracted to a fixed point, limit cycle or other attractor. For a set of initial points in the phase space occupying a region $V(0)$ at time $t = 0$, after a time $t > 0$, the end point of the corresponding trajectories fills a volume

$$V(t) = V(0)\exp\left\{-\left[\frac{DaB}{\Pr} + 1 + G + Les^{-1} + GLes^{-1} + \sigma Le^{-1} + GLe^{-1}\right]t\right\}. \tag{23}$$

Eq. (23) shows that the volume decays exponentially with time. Further, it can be noted that the system of Eqs. (15)–(21) are invariant under the transformation

$$S(Y_1, Y_2, Y_3, Y_4, Y_5, Y_6, Y_7) \rightarrow -S(Y_1, Y_2, Y_3, Y_4, Y_5, Y_6, Y_7). \tag{24}$$

We obtain the possible stationary points of the nonlinear system of equations by setting $\dot{Y}_i = 0$ for $i = 1, 2, \cdots, 7$. One of these stationary points is $Y_i = 0$ and by linearizing about this point, we obtain the Jacobian matrix

$$A = \begin{pmatrix} -\frac{PrB}{Da} & -\frac{\Pr}{Da} & 0 & \frac{PrN}{Da} & 0 & \frac{PrN_ARn}{DaR} & 0 \\ R & -1 & 0 & -Du & 0 & 0 & 0 \\ 0 & 0 & -G & 0 & -GDu & 0 & 0 \\ R & -Sr & 0 & -Les^{-1} & 0 & 0 & 0 \\ 0 & 0 & -GSr & 0 & -GLes^{-1} & 0 & 0 \\ \frac{\sigma R}{\varepsilon} & \sigma Le^{-1} & 0 & 0 & 0 & -\sigma Le^{-1} & 0 \\ 0 & 0 & GLe^{-1} & 0 & 0 & 0 & -GLe^{-1} \end{pmatrix}. \tag{25}$$

The eigenvalues of the above matrix depend on the various parameters. For the specific parameters $R = 10^3$, $Da = 20$, $\Pr = 10$, $N = 25$, $Du = 0.2$, $Sr = 3$, $Les = 10$, $Le = 5$, $\sigma = 0.05$, $G = 3$ and $\varepsilon = 0.04$, the characteristic polynomial is

$$P(\lambda) = \lambda^7 + 21.41\lambda^6 + 651.5\lambda^5 + 5391.7\lambda^4 + 12772.232\lambda^3 - 370.962\lambda^2 - 2996.712\lambda + 545.8$$

with eigenvalues

$$\lambda_1 = 0.2955056985,\ \lambda_2 = 0.2402382976,\ \lambda_3 = -0.6139990637,\ \lambda_4 = -4.886000936,$$
$$\lambda_5 = -5,\ \lambda_6 = -5.7228719981 - 21.9033954659i,\ \lambda_7 = -5.7228719981 + 21.9033954659i.$$

This stationary point is a saddle point. Nonetheless, because the eigenvalues depend on various parameters, we cannot make general conclusions as to the stability of the system. We note, however, that if we denote the trace of the matrix A by T and the determinant d, then

$$T = -\left(\frac{DaB}{\Pr} + 1 + G + Les^{-1} + GLes^{-1} + \sigma Le^{-1} + GLe^{-1}\right), \tag{26}$$

and

$$d = \frac{\sigma \Pr G^3}{DaLeLes}\left(-\frac{DuNRSr}{Le} - \frac{DuNRSr}{\varepsilon} + \frac{BDuSr}{Le} + \frac{DuRSr}{Le} + \frac{NR}{LeLes} + \frac{NR}{Les\varepsilon} - \frac{B}{LeLes} - \frac{R}{LeLes}\right). \tag{27}$$

The trace is always negative, but the sign of determinant depends on the parameter values. If $d < 0$ then

$$(1-N)\varepsilon DuSrRLes + (\varepsilon B - NRLe)DuSrLes + (\varepsilon + Le)NLe < (B+R)\varepsilon, \tag{28}$$

suggesting a saddle point.

4. Method of solution

To study the influence of various physical parameters on the average Nusselt and Sherwood numbers, we solved the nonlinear system of Eqs. (15)–(21) numerically using the multidomain spectral collocation method. This is a novel technique for solving nonlinear initial value problems and parabolic equations with large time domains. It has been suggested in the literature that the method gives better accuracy compared to other methods such as finite difference and Runge-Kutta methods [26]. To apply the multidomain spectral collocation to the nonlinear system of equations, we first divide the interval $[0, T]$ into subintervals $\Omega_i = [t_{i-1}, t_i]$ for $i = 1, 2, \cdots, p$. The transformation

$$t = \frac{t_i - t_{i-1}}{2}\tau + \frac{t_i + t_{i-1}}{2} \tag{29}$$

is used to transform each subinterval Ω_i into the interval $[-1, 1]$. The system of Eqs. (15)–(21) can be written in the form

$$\frac{dY_1^i}{dt} = \frac{\Pr}{Da}\left\{-BY_1^i - N\left(Y_2^i + Y_4\right) + \frac{N_A Rn}{Ra}Y_6^i\right\}, \tag{30}$$

$$\frac{dY_2^i}{dt} = RY_1^i - Y_2^i - DuY_4^i - Y_1^i Y_{3,}^i \tag{31}$$

$$\frac{dY_3^i}{dt} = \frac{1}{2}Y_1^i Y_2^i - G\left(Y_3^i + DuY_5^i\right), \tag{32}$$

$$\frac{dY_4^i}{dt} = RY_1^i - \frac{1}{Les}Y_4^i - SrY_2^i - Y_1^i Y_{5,}^i \tag{33}$$

$$\frac{dY_5^i}{dt} = \frac{1}{2}Y_1^i Y_2^i - G\left(\frac{1}{Les}Y_5^i + SrY_3^i\right), \tag{34}$$

$$\frac{dY_6^i}{dt} = \frac{\sigma R}{\varepsilon} Y_1^i - \frac{\sigma}{Le}\left(Y_6^i - Y_2^i\right) - \frac{N_A \sigma}{\varepsilon} Y_1^i Y_7^i, \tag{35}$$

$$\frac{dY_7^i}{dt} = \frac{N_A \sigma}{2\varepsilon} Y_1^i Y_7^i - \frac{G}{Le}\left(Y_7^i - Y_3^i\right), \tag{36}$$

subject to

$$Y_n^i(t_{i-1}) = Y_n^{i-1}(t_{i-1}) \quad \text{for} \quad n = 1, 2, \cdots, 7. \tag{37}$$

The first step in using the multidomain spectral collocation method (MDSCM) concerns the quasilinearization of Eqs. (30)–(36) leading to a system of equations in the form

$$\sum_{n=1}^{7} a_{(j,n)r}^i Y_{n,r+1}^i - \frac{dY_{j,r+1}^i}{dt} = R_{jr}^i, \tag{38}$$

subject to

$$Y_{n,r+1}^i(t_{i-1}) = Y_{n,r+1}^{i-1}(t_{i-1}) \quad \text{for} \quad n = 1, 2, \cdots, 7. \tag{39}$$

where $a_{(j,n)r}^i$ and R_{jr}^i for $j = 1, 2, \ldots, 7$ are given in the Appendix. Having linearized the equations, the second step is to integrate Eqs. (30)–(36). To this end, we use the Gauss-Lobatto nodes

$$\tau_j^i = \cos\frac{\pi j}{Nc}, \quad \text{for } j = 0, 1, \cdots, Nc. \tag{40}$$

We approximate the derivatives of the unknown functions $Y_{n,r+1}^i(t)$ at the collocation points by

$$\frac{dY_{n,r+1}^i}{dt}\left(\tau_j^i\right) = \sum_{k=0}^{Nc} \mathbf{D}_{jk} Y_{n,r+1}^i\left(\tau_j^j\right) = \left[\mathbf{D}\mathbf{U}_{n,r+1}^i\right]_j, \tag{41}$$

where $\mathbf{D} = 2D/(t_i - t_{i-1})$, D is the Chebyshev differentiation matrix and

$$\mathbf{U}_{n,r+1}^i = \left(Y_{n,r+1}^i(\tau_0^i), \cdots Y_{n,r+1}^i(\tau_{Nc}^i)\right)^T,$$

is a vector of the unknown functions at the collocation points. Substituting Eq. (41) into Eqs. (38) and reducing the result into matrix form, we obtain

$$\begin{aligned} \mathbf{A}\mathbf{U}_{n,r+1}^i &= \mathbf{R}_n^i, \\ \mathbf{U}_{n,r+1}^i\left(\tau_{N_c}^{i-1}\right) &= \mathbf{U}_n^i\left(\tau_{N_c}^{i-1}\right), \quad n = 1, 2, \cdots, 7. \end{aligned} \tag{42}$$

where the matrices $\mathbf{A} = \left[A_{ij}\right]$ and $\mathbf{R}_n^i$ are given in the Appendix.

5. Heat and mass transfer

The study of heat and mass transfer in a horizontal nanofluid layer heated from below and cooled from above has important engineering applications. We define the rate of heat transfer by the average Nusselt number $Nu(t)$ where

$$Nu(t) = 1 + \left[\frac{\frac{\alpha}{2\pi}\int_0^{\frac{2\pi}{\alpha}} \frac{\partial T}{\partial z} dx}{\frac{\alpha}{2\pi}\int_0^{\frac{2\pi}{\alpha}} \frac{\partial T_b}{\partial z} dx}\right]_{z=0} + Du\left\{1 + \left[\frac{\frac{\alpha}{2\pi}\int_0^{\frac{2\pi}{\alpha}} \frac{\partial C}{\partial z} dx}{\frac{\alpha}{2\pi}\int_0^{\frac{2\pi}{\alpha}} \frac{\partial C_b}{\partial z} dx}\right]_{z=0}\right\}. \tag{43}$$

Substituting Eqs. (12) and (13) into Eq. (43), we obtain

$$Nu(t) = 1 + \frac{2}{R} Y_3 + Du\left(1 + \frac{2}{R} Y_5\right). \tag{44}$$

Similarly, the rate of mass transfer stated in terms of the average Sherwood number is

$$Sh(t) = 1 + \frac{2}{R} Y_5 + Sr\left(1 + \frac{2}{R} Y_3\right) \tag{45}$$

6. Results and discussion

We have studied the weakly nonlinear instability of nanofluid flow in a horizontal layer with stress free boundary conditions. For numerical simulations, the parameter values were chosen from the literature on nanofluid flow such as [4, 7]. In the literature, the critical Rayleigh number is found when the Darcy number is very large. In this study, we investigated the critical Rayleigh number for low Darcy numbers.

The method of solution described in Section 4 was used to solve Eqs. (15)–(21). All computations are carried out up to a value of maximum time $t_{max} = 1$, and solutions are obtained using initial conditions selected in the neighborhood of stationary points. Periodic solution sets were obtained for the system of nonlinear equations. We determined the rate of heat and mass transfer as functions of time for different parameter values. The results are shown in **Figures 2–4**. **Figure 2** shows the effect of the Dufour and Soret parameters on the Nusselt and Sherwood numbers with time t. **Figure 2(a)** shows how the heat transfer coefficient changes with both the Dufour parameter and time. The heat transfer coefficient increases with the Dufour parameter but eventually settles to a steady value with time. In **Figure 2(b)**, the Soret parameter is similarly shown to enhance the mass transfer coefficient. We investigated the effect of the Prandtl and Lewis numbers (see **Figures 3** and **4**). An increase in the Lewis number enhances both heat and mass transfer in a nanofluid layer heated from below. However, **Figure 3** shows that increasing the Prandtl number reduces the amplitude of oscillatory heat and mass transfer. The Prandtl number can lead to both positive and negative contributions to the Nusselt and Sherwood numbers. It is interesting to note that our investigation shows that the magnetic field parameter has very little effect on the heat and mass transfer for this type of flow.

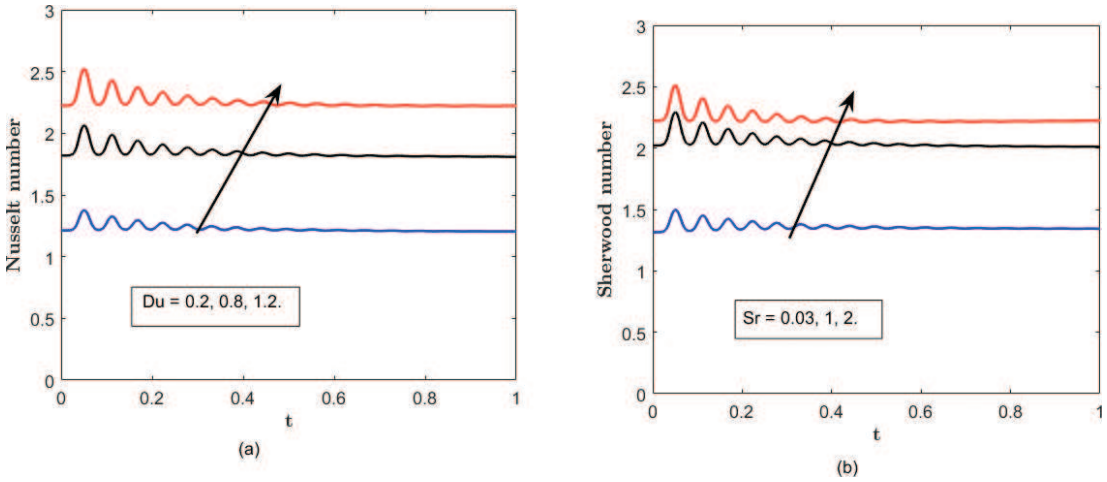

Figure 2. The effect of cross-diffusive parameters on (a) the Nusselt number Nu and (b) the Sherwood number Sh for $Da = 0.05$, $Le = 2$, $Du = 0.2$, $\varepsilon = 0.04$, $\sigma = 0.05$, $Les = 100$, $Rn = 5$, $Ra = 1000$ and various values of the Dufour and Soret parameters.

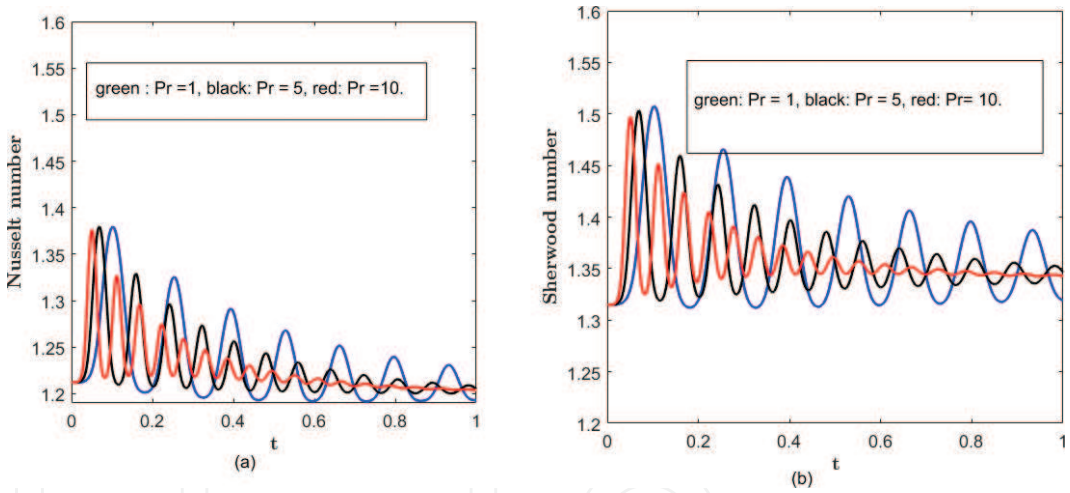

Figure 3. The effect of Prandtl number Pr on (a) the Nusselt number Nu and (b) the Sherwood number Sh when $Da = 0.05$, $Le = 2$, $Du = 0.2$, $\varepsilon = 0.04$, $\sigma = 0.05$, $Les = 100$, $Rn = 5$ and $Ra = 1000$.

Figures 5–11 show the effect of the Rayleigh number on the trajectories projected onto the (Y_i, Y_j) phase planes. The solution sets provide a visual representation of the system's behavior with every phase point on the phase space representing the physical state of the system. The convective solution sets for different values of R have been presented with the trajectories projected onto the (Y_i, Y_j) phase planes. These trajectories spiral toward the fixed point for Rayleigh numbers from 10^2 to 10^4. The solution sets give spiral phase portraits as R increases and for the high Rayleigh numbers, the trajectories spiral many times before they reach a fixed point.

Figures 5–8 show the phase portraits projected onto the (Y_i, Y_j)- plane correspond to a simple spiral for $R = 100$. As R is increased to 10^4, the complexity of the trajectories

http://dx.doi.org/10.5772/intechopen.71066

increases leading to certain chaotic forms. **Figures 8–11** show the trajectories in the three-dimensional phase space. Here, we observe similar solution sets as in the two-dimensional phase portraits.

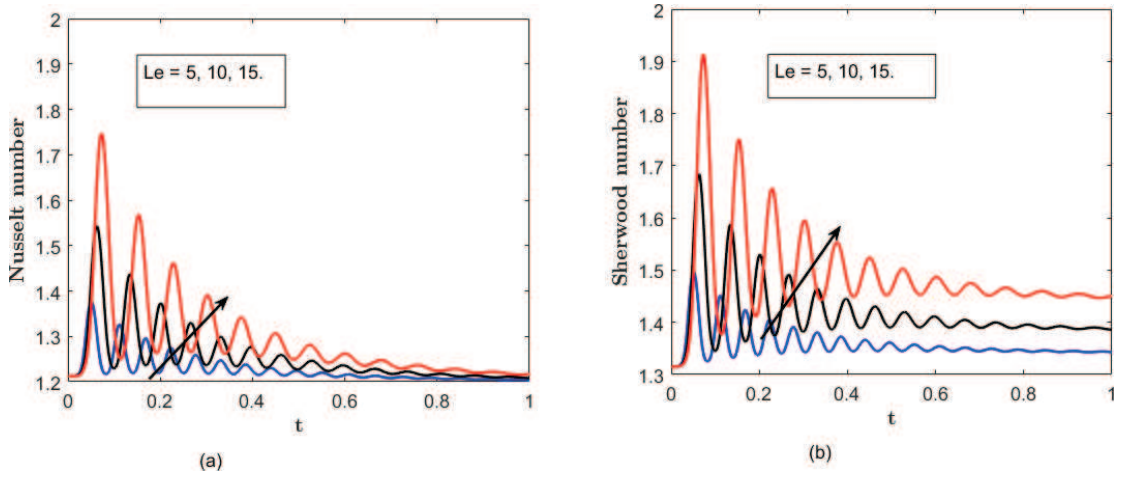

Figure 4. The effect of Lewis number on (a) the Nusselt number Nu and (b) the Sherwood number Sh when $Da = 0.05$, $Du = 0.2$, $\varepsilon = 0.04$, $\sigma = 0.05$, $Les = 100$, $Rn = 5$ and $Ra = 1000$.

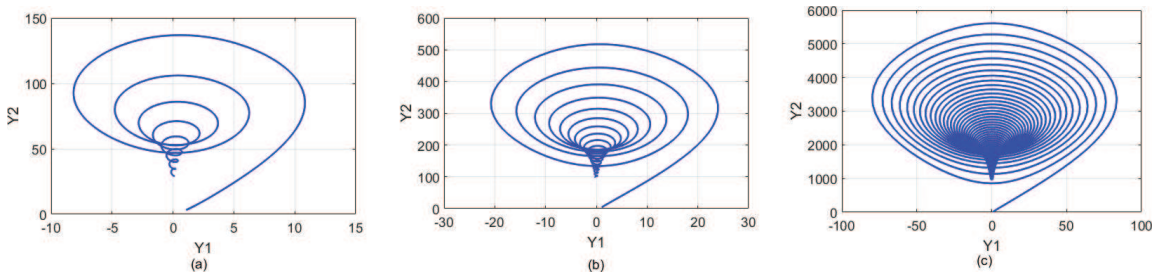

Figure 5. The trajectories of the system of nonlinear equations projected on the Y_1, Y_2-plane when revised Rayleigh number (a) $R = 10^2$, (b) $R = 10^3$ and (c) $R = 10^4$ when $Da = 0.05$, $Les = 100$, $\sigma = 0.05$, $\varepsilon = 0.04$, $Q = 10$, $Du = 0.2$, $Sr = 0.3$, $Le = 2$, $N = 25$ and $Rn = 5$.

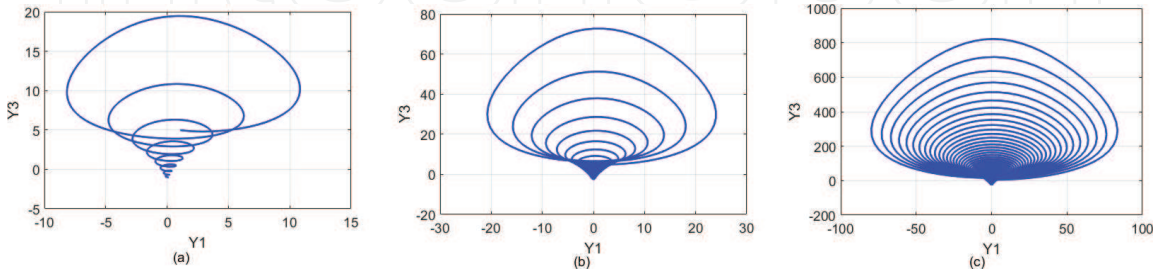

Figure 6. Trajectories of the system of nonlinear equations projected on the (Y_1, Y_3) plane when the revised Rayleigh number (a) $R = 10^2$, (b) $R = 10^3$ and (c) $R = 10^4$ when $Da = 0.05$, $Les = 100$, $\sigma = 0.05$, $\varepsilon = 0.04$, $Q = 10$, $Du = 0.2$, $Sr = 0.3$, $Le = 2$, $N = 25$ and $Rn = 5$.

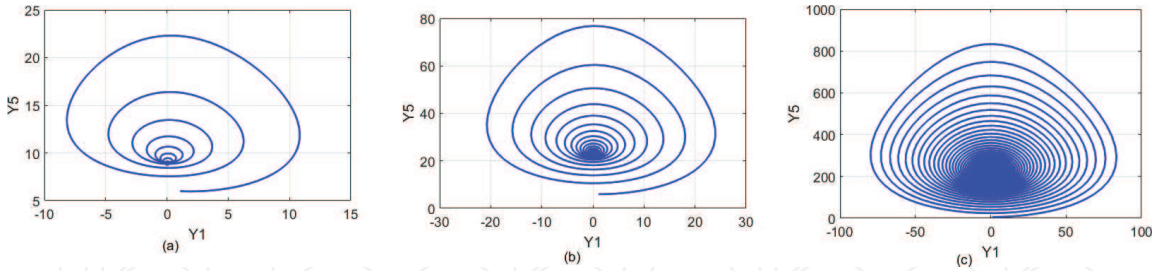

Figure 7. Trajectories of the system of nonlinear equations projected on the (Y_1, Y_5)-plane showing the sensitive dependence of the trajectories on the revised Rayleigh number for (a) $R = 10^2$, (b) $R = 10^3$ and (c) $R = 10^4$ when $Da = 0.05$, $Les = 100$, $\sigma = 0.05$, $\varepsilon = 0.04$, $Q = 10$, $Du = 0.2$, $Sr = 0.3$, $Le = 2$, $N = 25$ and $Rn = 5$.

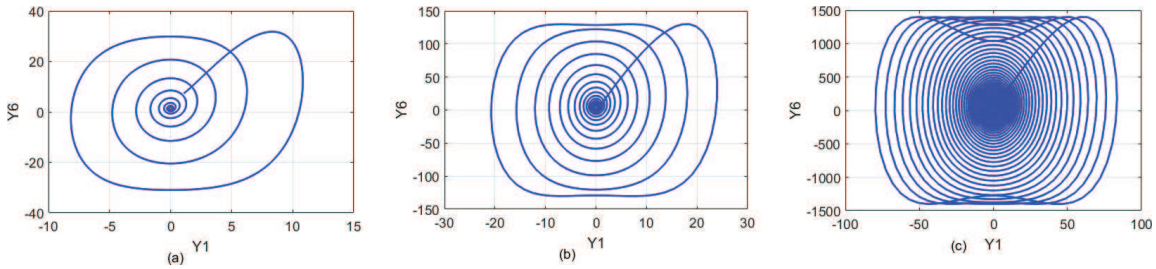

Figure 8. Trajectories of the system of nonlinear equations projected on the (Y_1, Y_6)-plane showing the sensitive dependence of the trajectories on the revised Rayleigh number for (a) $R = 10^2$, (b) $R = 10^3$ and (c) $R = 10^4$ when $Da = 0.05$, $Les = 100$, $\sigma = 0.05$, $\varepsilon = 0.04$, $Q = 10$, $Du = 0.2$, $Sr = 0.3$, $Le = 2$, $N = 25$ and $Rn = 5$.

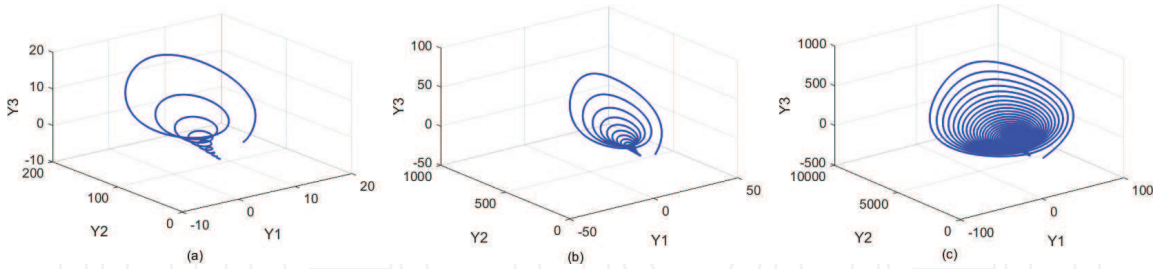

Figure 9. The bifurcations in the three-dimension solution space (Y_1, Y_2, Y_3) for (a) $R = 10^2$, (b) $R = 10^3$ and (c) $R = 10^4$ when $Da = 0.05$, $Les = 100$, $\sigma = 0.05$, $\varepsilon = 0.04$, $Q = 10$, $Du = 0.2$, $Sr = 0.3$, $Le = 2$, $N = 25$ and $Rn = 5$.

Figures 12 and **13** show the streamline, isotherm and isoconcentration contours in the nanofluid flow for different values of the Darcy number and buoyancy ratio. **Figure 12** displays the streamlines for various values of the buoyancy ratio term. Two different eddies are observed. The clockwise and anticlockwise flows are shown via negative and positive stream function values, respectively. The anticlockwise rotating flow occupies the largest area of the nanofluid layer.

For low buoyancy ratio parameters, the flow structure is significantly influenced by the buoyancy within the whole enclosure. Increasing the buoyancy ratio causes the boundary layer thickness to

http://dx.doi.org/10.5772/intechopen.71066

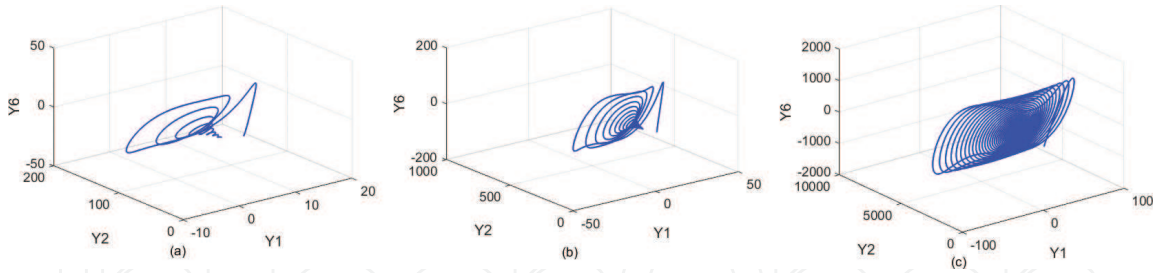

Figure 10. Flow trajectories and bifurcations in the three-dimensional space (Y_1, Y_2, Y_6) for Rayleigh numbers (a) $R = 10^2$, (b) $R = 10^3$ and (c) $R = 10^4$.

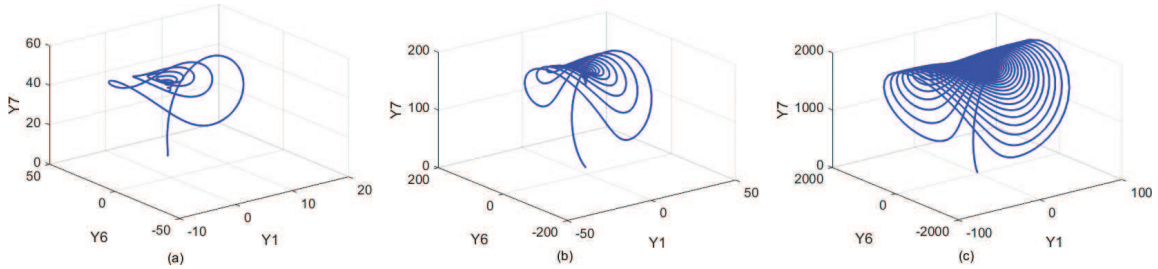

Figure 11. Flow trajectories and bifurcations in the three-dimensional space (Y_1, Y_6, Y_7) for Rayleigh numbers (a) $R = 10^2$, (b) $R = 10^3$ and (c) $R = 10^4$.

become thinner. Also, a high buoyancy ratio changes the flow structure, and this impacts significantly on the concentration field, which builds up a vertical stratification in the enclosure. It is interesting to note that for $N = -25$, the effect of the solutal buoyancy force is in the opposite direction of the thermal buoyancy force. The isothermal and isoconcentration profiles are situated toward the left wall, while for $N = 1$, the thermal and solutal buoyancy forces are equal. For $N = 25$, the effect of solutal buoyancy force is in the same direction as the thermal buoyancy force. In such cases, the isothermal and isoconcentration contours are mostly toward the right wall.

We observe that when $N = -25$, the stream function values in the central eddies increase because the thickness of the boundary layer increases with the buoyancy ratio. The streamlines and the flow behavior are affected by the change in the buoyancy ratio, but the flow pattern remains unaltered. As N decreases from 1 to -25, the streamlines become very dense to the left side of nanofluid layer while when N increases from 1 to 25, the streamlines are less so. The buoyancy forces that drive the nanofluid motion are mainly due to the temperature gradient.

Three different types of eddies are observed for the isoconcentration contours when $N = 25$. Of these, two have a clockwise rotation and one is anticlockwise. It is seen that the small eddy at the right bottom edge is diminished as N decreases from 1 to -25. Here, the concentration boundary layer decreases due to increasing N values, hence the buoyancy ratio has a significant influence on the concentration gradient. As the buoyancy ratio N increases from 1 to 25 the isoconcentrations become very dense at the bottom of nanofluid layer.

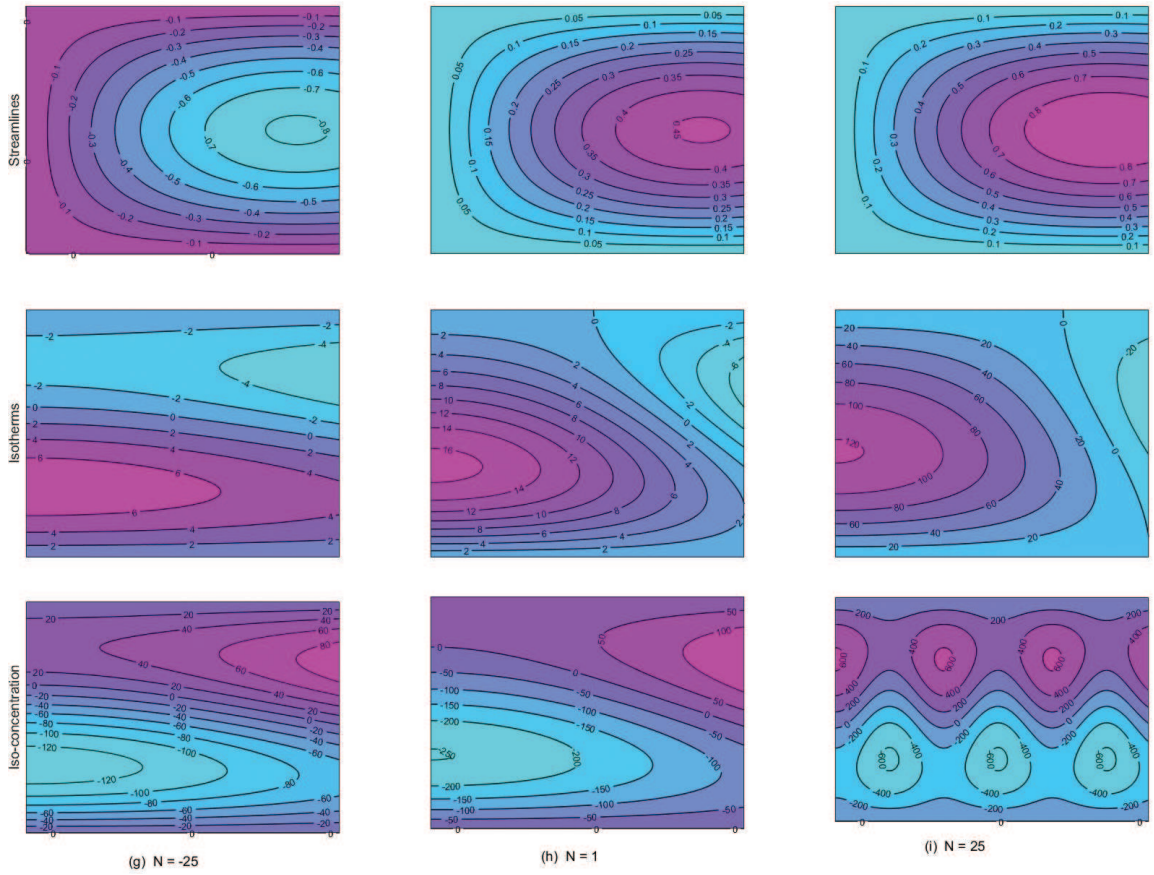

Figure 12. The pattern of streamlines (top), isotherms (middle) and isoconcentration (bottom) for different values of the buoyancy ratio *N*.

The effect of the Darcy number on the nanofluid flow in the porous medium is shown in detail in **Figure 13**. The streamline patterns are similar to those depicted in **Figure 12**. However, as *Da* increases from 0.05 to 0.07, the rotation of the streamlines changes. Similarly, the isotherm patterns change with increasing Darcy numbers. The value of the center eddies increases with increasing *Da*. Increasing *Da* has the effect of increasing the effective fluid viscosity and reducing the thermal and solutal boundary layers.

7. Conclusion

We have investigated the onset of thermal instability in a horizontal porous layer of infinite extent in a cross-diffusive nanofluid flow. The focus of the study has been on stress free boundary conditions with zero nanoparticle flux at the wall. A multidomain spectral collocation method was used to solve the system of nonlinear evolution equations. As the Rayleigh

http://dx.doi.org/10.5772/intechopen.71066

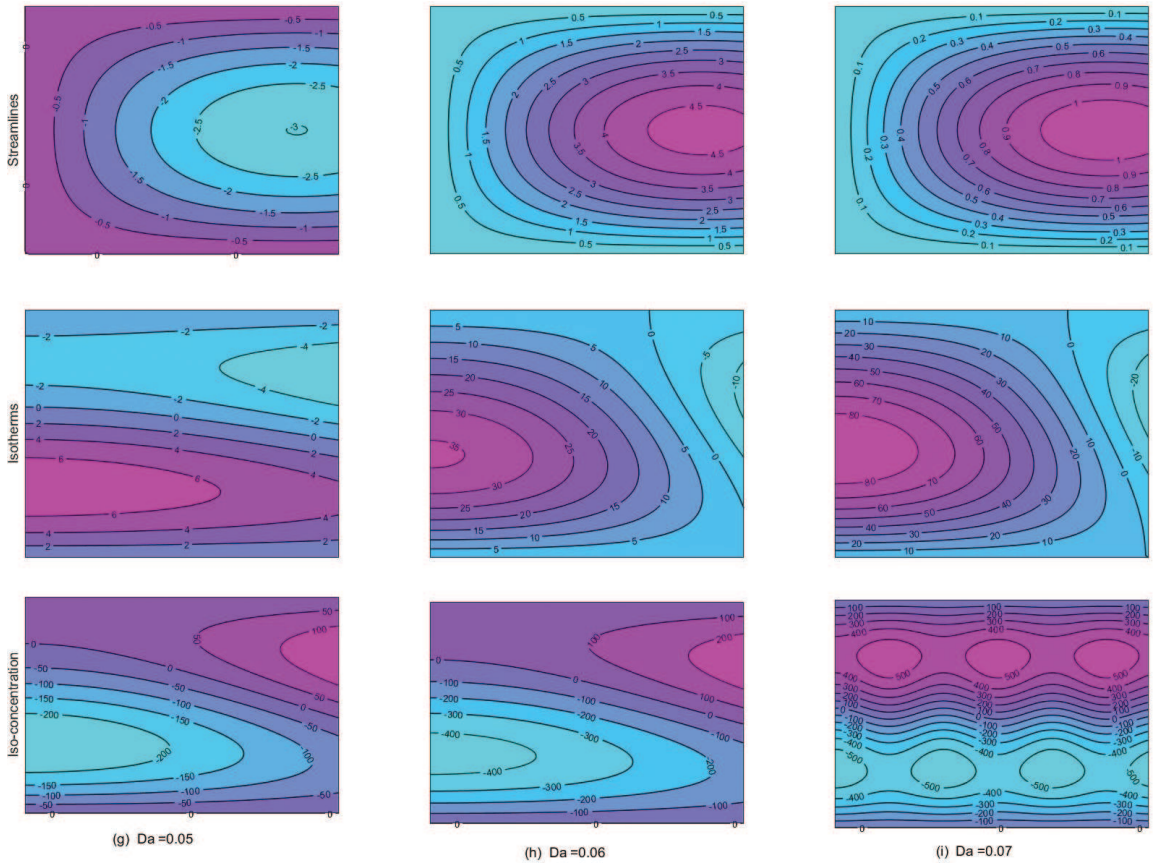

Figure 13. The streamlines (top), isotherms (middle) and isoconcentration (bottom) for different values of the Darcy number *Da*.

number increases to 10^4, the trajectories spiral many times before reaching a fixed point. The nanofluid convection regime is complex for Rayleigh numbers higher than $R = 10^4$, and the flow pattern presents difficulties in interpreting correctly.

Additionally, a change in system parameters, such as an increase in the flow Lewis number, improves the rate of heat and mass transfer in the nanofluid saturated porous media. The Dufour parameter has the effect of increasing heat transfer, while increasing the Soret parameter increases the rate of mass transfer.

Acknowledgements

The authors are grateful to the University of KwaZulu-Natal and the Claude Leon Foundation, South Africa for financial support.

A. Appendix

The terms $a^i_{(j,n)r}$ and R^i_{jr} for $j = 1, 2, \ldots, 7$ in Eq. (38) are given by

$$
\begin{aligned}
a^i_{(1,1)r} &= -\gamma_3 B,\ a^i_{(1,2)r} = -\gamma_3,\ a^i_{(1,4)r} = -\gamma_3 N,\ a^i_{(1,6)r} = \frac{\gamma_3 N_A R n}{Ra},\\
a^i_{(1,3)r} &= a^i_{(1,5)r} = a^i_{(1,7)r} = 0,\ a^i_{(2,1)r} = R - Y^i_{3,r},\ a^i_{(2,2)r} = -1,\ a^i_{(2,3)r} = -Y^i_{1,r},\\
a^i_{(2,4)r} &= -Du,\ a^i_{(2,5)r} = a^i_{(2,6)r} = a^i_{(2,7)r} = 0 a^i_{(3,1)r} = -\frac{\alpha\pi}{2} u^i_{2,r},\ a^i_{(3,2)r} = \frac{1}{2} Y^i_{1,r},\\
a^i_{(3,3)r} &= -G,\ a^i_{(3,5)r} = -GDu a^i_{(3,4)r} = a^i_{(3,6)r} = a^i_{(3,7)r} = 0, a^i_{(4,1)r} = R - Y^i_{5,r},\\
a^i_{(4,2)r} &= -Sr,\ a^i_{(5,3)r} = -GSr\\
a^i_{(4,4)r} &= -\frac{1}{Les}, a^i_{(4,5)r} = -Y^i_{1,r},\ a^i_{(4,3)r} = a^i_{(4,6)r} = a^i_{(4,7)r} = 0,\ a^i_{(5,1)r} = \frac{1}{2} Y^i_{4,r},\\
a^i_{(5,4)r} &= \frac{1}{2} Y^i_{1,r}, a^i_{(5,5)r} = -\frac{G}{Les}, a^i_{(5,2)r} = a^i_{(5,6)r} = a^i_{(5,7)r} = 0, a^i_{(6,1)r} = \gamma_1 - \gamma_2 Y^i_{7,r},\\
a^i_{(6,2)r} &= \frac{\sigma}{Le}, a^i_{(6,6)r} = -\frac{\sigma}{Le},\ a^i_{(6,7)r} = -\gamma_2 Y^i_{1,r},\ a^i_{(6,3)r} = a^i_{(6,4)r} = a^i_{(6,5)r} = 0,\\
a^i_{(7,1)r} &= \frac{\gamma_2}{2} Y^i_{6,r}, a^i_{(7,3)r} = \frac{G}{Le}, a^i_{(7,6)r} = \frac{\gamma_2}{2} Y^i_{1,r},\ a^i_{(7,7)r} = -\frac{G}{Le},\\
a^i_{(7,2)r} &= a^i_{(7,4)r} = a^i_{(7,5)r} = 0,\\
R^i_{1r} &= 0, R^i_{2r} = -Y^i_{1,r} Y^i_{3,r} R^i_{3r} = \frac{1}{2} Y^i_{1,r} Y^i_{2,r},\ R^i_{4r} = -Y^i_{1,r} Y^i_{5,r},\ R^i_{5r} = \frac{1}{2} Y^i_{1,r} Y^i_{4,r},\\
R^i_{6r} &= -\frac{\sigma N_A}{\varepsilon} Y^i_{1,r} Y^i_{7,r},\ R^i_{7r} = \frac{\sigma N_A}{2\varepsilon} Y^i_{1,r} Y^i_{6,r},
\end{aligned}
$$

where $\gamma_1 = \frac{\sigma R}{\varepsilon}$, $\gamma_2 = \frac{N_A \sigma}{\varepsilon}$ and $\gamma_3 = \frac{\mathrm{Pr}}{Da}$.

B. Appendix

The matrices A_{ij} in Eq. (42) are given by

$$
\begin{aligned}
&A_{nn} = \mathbf{diag}\,(a_{n,n}) r^i) - \mathbf{D},\ A_{12} = \mathbf{diag}\left(a^i_{(1,2)r}\right),\ A_{16} = \mathbf{diag}\left(a^i_{(1,6)r}\right),\\
&A_{13} = A_{14} = A_{15} = A_{17} = \mathbf{O},\\
&A_{21} = \mathbf{diag}\left(a^i_{(2,1)r}\right),\quad A_{23} = \mathbf{diag}\left(a^i_{(2,3)r}\right),\quad A_{24} = \mathbf{diag}\left(a^i_{(2,4)r}\right),\quad A_{25} = A_{26} = A_{27} = \mathbf{O},\\
&A_{31} = \mathbf{diag}\left(a^i_{(3,1)r}\right),\quad A_{32} = \mathbf{diag}\left(a^i_{(3,2)r}\right),\quad A_{35} = \mathbf{diag}\left(a^i_{(3,5)r}\right),\quad A_{34} = A_{36} = A_{37} = \mathbf{O},\\
&A_{41} = \mathbf{diag}\left(a^i_{(4,1)r}\right),\quad A_{42} = \mathbf{diag}\left(a^i_{(4,2)r}\right),\quad A_{45} = \mathbf{diag}\left(a^i_{(4,5)r}\right),\quad A_{43} = A_{46} = A_{47} = \mathbf{O},\\
&A_{51} = \mathbf{diag}\left(a^i_{(5,1)r}\right),\quad A_{53} = \mathbf{diag}\left(a^i_{(5,3)r}\right),\quad A_{54} = \mathbf{diag}\left(a^i_{(5,4)r}\right),\quad A_{52} = A_{56} = A_{57} = \mathbf{O},\\
&A_{61} = \mathbf{diag}\left(a^i_{(6,1)r}\right),\quad A_{62} = \mathbf{diag}\left(a^i_{(6,2)r}\right),\quad A_{67} = \mathbf{diag}\left(a^i_{(6,7)r}\right),\quad A_{63} = A_{64} = A_{65} = \mathbf{O},
\end{aligned}
$$

$$A_{71} = \mathbf{diag}\left(a^i_{(7,1)r}\right), \quad A_{73} = \mathbf{diag}\left(a^i_{(7,3)r}\right), \quad A_{76} = \mathbf{diag}\left(a^i_{(7,6)r}\right), \quad A_{72} = A_{74} = A_{75} = \mathbf{O},$$

where $\mathbf{O}$ is an $(N+1) \times (N+1)$ matrix of zeros and **diag** is an $(N+1) \times (N+1)$ diagonal matrix.

Author details

Osman A.I. Noreldin[1], Precious Sibanda[1]* and Sabyasachi Mondal[2]

*Address all correspondence to: sibandap@ukzn.ac.za

1 School of Mathematical Sciences, University of KwaZulu-Natal, South Africa

2 Department of Mathematics, Amity University, Kolkata, West Bengal, India

References

[1] Choi SU, Eastman JA. Enhancing Thermal Conductivity of Fluids with Nanoparticles, Technical Report. IL, United States: Argonne National Lab; 1995

[2] Buongiorno J. Convective transport in nanofluids. Journal of Heat Transfer. 2006;**128**(3): 240-250

[3] Masuda H, Ebata A, Teramae K. Alteration of thermal conductivity and viscosity of liquid by dispersing ultra-fine particles. Netsu Bussei. 1993;**4**:227-233

[4] Tzou D. Thermal instability of nanofluids in natural convection. International Journal of Heat and Mass Transfer. 2008;**51**(11):2967-2979

[5] Narayana M, Sibanda P, Motsa S, Lakshmi-Narayana P. Linear and nonlinear stability analysis of binary maxwell fluid convection in a porous medium. Heat and Mass Transfer. 2012;**48**(5):863-874

[6] Narayana M, Sibanda P, Siddheshwar PG, Jayalatha G. Linear and nonlinear stability analysis of binary viscoelastic fluid convection. Applied Mathematical Modelling. 2013;**37**(16): 8162-8178

[7] Yadav D, Bhargava R, Agrawal G. Numerical solution of a thermal instability problem in a rotating nanofluid layer. International Journal of Heat and Mass Transfer. 2013;**63**:313-322

[8] Kuznetsov A, Nield D. Effect of local thermal non-equilibrium on the onset of convection in a porous medium layer saturated by a nanofluid. Transport in Porous Media. 2010;**83**(2): 425-436

[9] Kuznetsov A, Nield D. Thermal instability in a porous medium layer saturated by a nanofluid: Brinkman model. Transport in Porous Media. 2010;**81**(3):409-422

[10] Nield D, Kuznetsov A. The onset of double-diffusive convection in a nanofluid layer. International Journal of Heat and Fluid Flow. 2011;**32**(4):771-776

[11] Nield D, Kuznetsov A. Thermal instability in a porous medium layer saturated by a nanofluid: A revised model. International Journal of Heat and Mass Transfer. 2014;**68**:211-214

[12] Bhadauria B. Double diffusive convection in a porous medium with modulated temperature on the boundaries. Transport in Porous Media. 2007;**70**(2):191-211

[13] Bhadauria B, Siddheshwar P, Kumar J, Suthar OP. Weakly nonlinear stability analysis of temperature/gravity-modulated stationary rayleigh–bénard convection in a rotating porous medium. Transport in Porous Media. 2012;**92**(3):633-647

[14] Gresho P, Sani R. The effects of gravity modulation on the stability of a heated fluid layer. Journal of Fluid Mechanics. 1970;**40**(4):783-806

[15] Kiran P, Bhadauria B. Chaotic convection in a porous medium under temperature modulation. Transport in Porous Media. 2015;**107**(3):745-763

[16] Chandrasekhar S. Hydrodynamic and Hydromagnetic Stability. Oxford University Press; 1961

[17] Thompson W. Cxliii. Thermal convection in a magnetic field. The London, Edinburgh, and Dublin Philosophical Magazine and Journal of Science. 1951;**42**(335):1417-1432

[18] Heris SZ, Salehi H, Noie S. The effect of magnetic field and nanofluid on thermal performance of two-phase closed thermosyphon (tpct). International Journal of Physical Sciences. 2012;**7**(4):534-543

[19] Ghasemi B, Aminossadati S, Raisi A. Magnetic field effect on natural convection in a nanofluid-filled square enclosure. International Journal of Thermal Sciences. 2011;**50**(9): 1748-1756

[20] Hamad M, Pop I, Ismail AM. Magnetic field effects on free convection flow of a nanofluid past a vertical semi-infinite flat plate. Nonlinear Analysis: Real World Applications. 2011;**12**(3):1338-1346

[21] Bergman MI, Fearn DR. Chimneys on the earth's inner-outer core boundary? Geophysical Research Letters. 1994;**21**(6):477-480

[22] Furmanski P, Banaszek J. Modelling of the mushy zone permeability for solidification of binary alloys. Materials Science Forum. Trans Tech Publ. 2006;**508**:411-418

[23] Gupta U, Ahuja J, Wanchoo R. Rayleigh-bénard convection of nanofluids with magnetic field and permeability effects. Procedia Engineering. 2015;**127**:325-332

[24] Imomnazarov KK. Modified darcy laws for conducting porous media. Mathematical and Computer Modelling. 2004;**40**(1–2):5-10

[25] Rana G, Kango S, Chadha K. Magneto-thermal convection in Walters' (model b') elastico-viscous fluid saturated by a Darcy-Brinkman porous medium. Engineering Mechanics. 2014;**21**:425-435

[26] Motsa S, Dlamini P, Khumalo M. A new multistage spectral relaxation method for solving chaotic initial value systems. Nonlinear Dynamics. 2013;**72**(1–2):265-283

IntechOpen

Chapter 4

Thermal instability in double-diffusive natural convection in an inclined open square cavity

In this chapter, we present a study of thermal instability in double-diffusive convection in an inclined open cavity subjected to an inclined magnetic field. The evolution equations that describe the amplitude of convection are obtained. These equations are solved numerically using a multidomain spectral collocation method. A trapping region for the solutions is obtained. In addition, streamlines and heat transfer coefficients for different Rayleigh numbers and inclination angles are presented.

Acta Technica *63* No. 3/2018, 385–406

Thermal instability of double-diffusive natural convection in an inclined open square cavity[1]

O. A. I. Noreldin[2], S. Mondal[3,4], P. Sibanda[2]

Abstract. The thermal instability of fluid layer is investigated in an inclined open square cavity with an inclined magnetic field. A Galerkin-type method is used to solve the equations in the case of linear stability, and in the nonlinear case a truncated Fourier series is used to obtain a system of five general Lorenz type equations. A multi-domain spectral collocation method was used to solve the differential equations that describe the evolution of the disturbances in the nonlinear regime. The influence of the important physical parameters on the thermal instability is investigated. The results are presented in terms of streamlines, isotherms, isoconcentrations, the Nusselt and the Sherwood numbers. The trapping region provide useful information about the trajectories. A limited phase space analysis with trajectories of the disturbances is presented.

Key words. Thermal instability, double-diffusive convection, inclined open cavity, multi-domain spectral collocation method.

1. Introduction

The thermal instability of a Rayleigh–Benard problem with various physical configuration is well reported in Chandrasekhar [1] and Drazin and Reid [2]. Also, Simó et al. [3] examined the dynamics of particle trajectories in a Rayleigh–Benard problem. Laroze and Pleiner [4] studied thermal convection in a nonlinear non-Newtonian magnetic fluid. Double diffusive convection in a fluid-saturated porous medium in a square cavity has received considerable attention in recent years due to its wide range of applications in engineering and science, for example in nuclear reactors, packed beds, the cooling of electronic devices, solar energy, drying technologies and

[1]The authors are grateful to the University of KwaZulu-Natal, South Africa and Amity University, Kolkata, India for the necessary support.

[2]School of Mathematics, Statistics & Computer Science University of KwaZulu-Natal, Pietermaritzburg-3209, South Africa

[3]Department of Mathematics, Amity University, Kolkata, Newtown-700135, West Bengal, India

[4]Corresponding author; e-mail: sabya.mondal.2007@gmail.com

high performance insulation buildings, etc. Studies on natural convective heat transfer in fluid-saturated porous media includes those by Nield and Bejan [5], Ingham and Pop [6, 7], Bejan et al. [8] and Vafai [9]. In these studies it was shown that the effect of the Lorentz force in an electrically conducting fluid is to suppress convection currents by reducing the fluid velocity. For this reason, it has been suggested that the presence of an external magnetic field can thus be an active control mechanism in manufacturing processes.

Le Quere et al. [10] studied thermally driven laminar flow in cavities of rectangular cross-section. Chamkha and Al-Naser [11] investigated the laminar double diffusive convective flow of a binary gas mixture in an inclined rectangular porous enclosure. Wang et al. [12] analyzed natural convection and heat transfer in an inclined porous cavity with time-periodic boundary conditions. Double diffusive convection in an electrically conducting fluid layer in inclined cavities was also studied by Polate et al. [13] and Khanafer et al. [14]. Double diffusive magneto-convection has received considerable attention because of its wide application in oceanography, geophysics, astrophysics and engineering problem, Turner [15] and Rudraiah [16]. Hydromagnetic convection in a conducting fluid flow through a porous medium has been studied by Bian et al. [17]. They found that the temperature and the velocity are significantly modified through the application of a magnetic field. Revnic et al. [18] studied the magnetic field effect on the unsteady free convection flow in a square cavity filled with porous medium and with a constant heat generation. Mansour et al. [19] investigated the effects of an inclined magnetic field on unsteady natural convection in a porous inclined cavity with a heat source in the solid phase.

Recently, Mondal and Sibanda [20] studied unsteady double diffusive convection in an inclined rectangular lid-driven enclosure for different magnetic field angles and non-uniform boundary conditions. They found that different angles of the magnetic field may suppress the convection flow with significant changes in the flow pattern. Narayana et al. [21] studied double diffusive magneto-convection in viscoelastic fluids. They found that the magnetic field has the effect of delaying the onset of convection. Siddheshwar and Pranesh [22, 23] investigated the effect of the magnetic field on the thermal instability under temperature and gravity modulation for an electrically conducting fluid with internal angular momentum. Rudraiah et al. [24] studied finite amplitude convection in a two-component fluid saturated porous layer. They found that subcritical instabilities are possible for such fluid flow. Gaikwad and Kouser [25] studied double diffusive convection in a porous layer saturated with a couple stress fluid with an internal heat source, using linear and weakly nonlinear stability analysis.

The interaction between the fluid velocity and electromagnetic forces gives rise to the flow structure. The electromagnetic effect tends to stabilize the flow and suppress the oscillatory instabilities. The instability in double diffusive convection can occur, depending on whether the solute gradient is stabilizing or destabilizing. If the solute gradient is destabilizing and the temperature gradient is stabilizing, the stationary conductive state becomes unstable through a super-critical bifurcation. On the contradictory, if the solute gradient is stabilizing and the temperature gradient is destabilizing,the instability occurs in the form of a sub-critical bifurcation where

the conductive state may lose stability to a growing oscillatory mode or may even lead to the formation of convection rolls well below the critical Rayleigh number [21]. Lehotzky et al. [26] studied the extension of the spectral element method for stability analysis of time-periodic delay-differential equations.

From the literature, there are many studies on double diffusive convection in square inclined open cavities. To the best of our knowledge none of the studies deal with the analysis of double diffusive convection in open square inclined cavity. The objective of this paper is to investigate thermal instability in double diffusive natural convection in an inclined open cavity. The non-oscillatory and oscillatory convection addressed in this work. The trapping region of the trajectories are determined. The general Lorenz types equations have been solved numerically. The multi-domain spectral collocation method (see [27]) has been used to solve the differential equations. The effects of various controlling parameters are discussed in terms of streamlines, isotherms and iso-concentrations and phase space analysis.

2. Mathematical formulation

Consider the two-dimensional laminar flow of an incompressible and electrically conducting Newtonian fluid which is permeated by a uniform magnetic field $\bar{B}$ with strength B_0 and an inclination angle ϕ. The inclined open square cavity has inclination angle φ from the horizontal plane in an anticlockwise direction. We assume that gravity acts in the vertical direction, all the fluid properties are constant and fluid density variations are neglected except in the buoyancy force term. Under these assumption the continuity, momentum, energy and concentrations equations are given as follows (see Fig. 1):

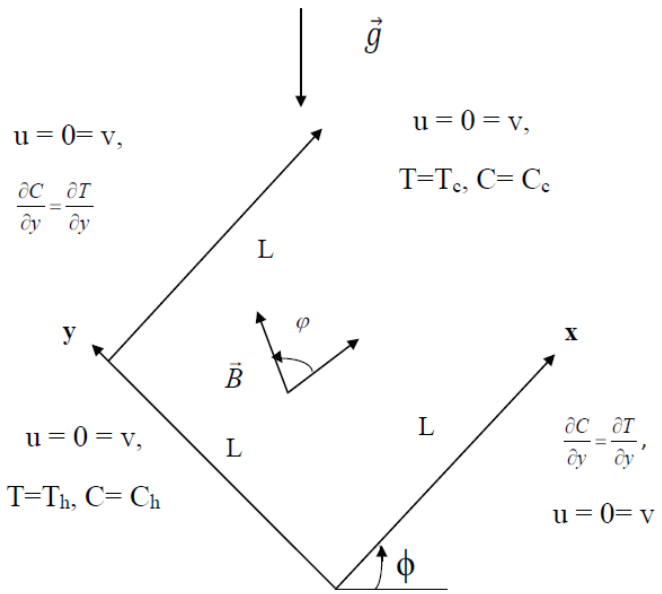

Fig. 1. Physical configuration and coordinate system

$$\frac{\partial u}{\partial x}+\frac{\partial v}{\partial y}=0, \tag{1}$$

$$\rho_0\Big(\frac{\partial u}{\partial t}+u\frac{\partial u}{\partial x}+v\frac{\partial u}{\partial y}\Big)=-\frac{\partial p}{\partial x}+\mu\nabla^2 u+\rho_0\beta_1 g(T-T_\infty)\cos\varphi - \rho_0\beta_2 g(C-C_\infty)\cos\varphi+\sigma|\boldsymbol{B}_0|^2(v\sin\phi\cos\phi-u\sin^2\phi), \tag{2}$$

$$\rho_0\Big(\frac{\partial v}{\partial t}+u\frac{\partial v}{\partial x}+v\frac{\partial v}{\partial y}\Big)=-\frac{\partial p}{\partial y}+\mu\nabla^2 v+\rho_0\beta_1 g(T-T_\infty)\sin\varphi - \rho_0\beta_2 g(C-C_\infty)\sin\varphi+\sigma|\boldsymbol{B}_0|^2(u\sin\phi\cos\phi-v\cos^2\phi), \tag{3}$$

$$\frac{\partial T}{\partial t}+u\frac{\partial T}{\partial x}+v\frac{\partial T}{\partial y}=\alpha\nabla^2 T, \tag{4}$$

$$\frac{\partial C}{\partial t}+u\frac{\partial C}{\partial x}+v\frac{\partial C}{\partial y}=D_{\mathrm{s}}\nabla^2 C. \tag{5}$$

The variables (u,v) are the velocity components in the x and y directions respectively, T, C are the temperature and concentration fields, respectively, g is the gravitation acceleration, p is the pressure and the $\mu, \rho_0, \beta_1, \beta_2, \sigma, \alpha, D_{\mathrm{s}}$ are the viscosity, density, thermal expansion coefficient, solute expansion coefficient, the electrical conductivity, thermal diffusivity and mass diffusivity, respectively.

Introducing the dimensionless variables

$$(X,Y)=\frac{(x,x)}{L},\quad (U,V)=\frac{(u,v)L}{\alpha},\quad P=\frac{pL^2}{\rho_0\alpha^2}, \tag{6}$$

$$\tau=\frac{\alpha t}{L^2},\quad \theta=\frac{T-T_\infty}{T_1-T_\infty},\quad S=\frac{C-C_\infty}{C_1-C_\infty} \tag{7}$$

and substituting equations (6)–(7) into equations (1)–(5) we have

$$\frac{\partial U}{\partial X}+\frac{\partial V}{\partial Y}=0, \tag{8}$$

$$\frac{\partial U}{\partial \tau}+U\frac{\partial U}{\partial X}+V\frac{\partial U}{\partial Y}=-\frac{\partial P}{\partial X}+\mathrm{Pr}\nabla^2 U+\mathrm{Pr}\,(\mathrm{Ra}\,\theta-\mathrm{Rs}\,S)\cos\varphi + \mathrm{Pr}\,\mathrm{Ha}^2(V\sin\phi\cos\phi-U\sin^2\phi), \tag{9}$$

$$\frac{\partial V}{\partial \tau}+U\frac{\partial V}{\partial X}+V\frac{\partial V}{\partial Y}=-\frac{\partial P}{\partial Y}+\mathrm{Pr}\nabla^2 V+\mathrm{Pr}\,(\mathrm{Ra}\,\theta-\mathrm{Rs})\sin\varphi + \mathrm{Pr}\,\mathrm{Ha}^2(U\sin\phi\cos\phi-V\cos^2\phi), \tag{10}$$

$$\frac{\partial \theta}{\partial \tau}+U\frac{\partial \theta}{\partial X}+V\frac{\partial \theta}{\partial Y}=\nabla^2\theta, \tag{11}$$

$$\frac{\partial S}{\partial \tau}+U\frac{\partial S}{\partial X}+V\frac{\partial S}{\partial Y}=\frac{1}{\mathrm{Le}}\nabla^2 S, \tag{12}$$

where $\mathrm{Pr} = \nu/\alpha$ is the Prandtl number, $\mathrm{Ha} = B_0 L/\sqrt{\nu}$ is the Hartmann number, $\mathrm{Ra} = g\beta_1(T_1 - T_\infty)L^3/(\alpha\nu)$ is the thermal Rayleigh number, $\mathrm{Le} = \alpha/D_\mathrm{s}$ is the Lewis number, and $\mathrm{Rs} = g\beta_1(C_1 - C_\infty)L^3/(\alpha\nu)$ is the concentration Rayleigh number.

The basic state solution is described as follows:

$$U_\mathrm{b} = V_\mathrm{b} = 0,\ P_\mathrm{b} = P_\mathrm{b}(Y),\ \theta_\mathrm{b}(Y) = 1 - Y,\ S_\mathrm{b}(Y) = 1 - Y. \tag{13}$$

We superimpose small perturbation on the basic state solution to determine the stability of the fluid and define the fluid quantities as follows:

$$U = U_\mathrm{b} + U',\ \ V = V_\mathrm{b} + V',\ \theta = \theta_\mathrm{b} + \theta',\ S = S_\mathrm{b} + S', \tag{14}$$

where the prime describes a perturbed quantity. Substituting (14) into equations (8)–(12), introducing the stream function ψ as $U' = \partial\psi'/\partial Y, V' = -\partial\psi'/\partial X$ and eliminating the pressure terms in equations (9)–(10) we obtain the perturbed equations

$$\begin{aligned}&\left\{\mathrm{Pr}\nabla^4 - \frac{\partial}{\partial\tau}\nabla^2 + \mathrm{Pr}\,\mathrm{Ha}^2\left(\frac{\partial^2}{\partial X\partial Y}\sin\phi\cos\phi + \frac{\partial^2}{\partial X^2}\cos^2\phi + \frac{\partial^2}{\partial Y^2}\sin^2\phi\right)\right\}\psi' \\ &+ \mathrm{Pr}\,\mathrm{Ra}\left(\frac{\partial\theta'}{\partial Y}\cos\varphi - \frac{\partial\theta'}{\partial X}\sin\varphi\right) - \mathrm{Pr}\,\mathrm{Rs}\left(\frac{\partial S'}{\partial Y}\cos\varphi - \frac{\partial S'}{\partial X}\sin\varphi\right) = \mathcal{J}(\psi', \nabla^2\psi'),\end{aligned} \tag{15}$$

$$\frac{\partial\psi'}{\partial X} + \left(\frac{\partial}{\partial\tau} - \nabla^2\right)\theta' = \mathcal{J}(\psi', \theta'), \tag{16}$$

$$\frac{\partial\psi'}{\partial X} + \left(\frac{\partial}{\partial\tau} - Le^{-1}\nabla^2\right)S' = \mathcal{J}(\psi', S'), \tag{17}$$

where $\mathcal{J}(.,.)$ is the Jacobian determinant.

3. Linear stability analysis

In this section we give a linear stability analysis of the fluid flow. We linearized equations (15)–(17) by neglecting the nonlinear terms. Assume that all perturbed quantities have the following form

$$\psi' = \Psi'(Y)\mathrm{e}^{s\tau}\sin ax, \tag{18}$$

$$\theta' = \Theta'(Y)\mathrm{e}^{s\tau}\cos ax, \tag{19}$$

$$S' = S'(Y)\mathrm{e}^{s\tau}\cos ax, \tag{20}$$

where a is the wave number, and $s = i\omega$, where ω is the frequency of the oscillations. We obtain the following eigenvalue problem by substituting (18)–(20) into (15)-(17)

$$\left\{\mathrm{Pr}(D^2-a^2)^2 - s(D^2-a^2) + \mathrm{Pr}\,\mathrm{Ha}^2(D^2\sin^2\phi - a^2\cos^2\phi)\right\}\Psi' + \mathrm{Pr}\,\mathrm{Ra}(D\Theta'\cos\varphi + a\sin\varphi\Theta') - \mathrm{Pr}\,\mathrm{Rs}(DS'\cos\varphi + a\sin\varphi S') = 0, \tag{21}$$

$$a\Psi' + \left\{(D^2-a^2) - s\right\}\Theta' = 0, \tag{22}$$

$$a\Psi' + \left\{\mathrm{Le}^{-1}(D^2-a^2) - s\right\}S' = 0, \tag{23}$$

where $D(\cdot) = \frac{d}{dY}(\cdot)$. Subject to the boundary conditions

$$\Psi' = D^2\Psi' = D\Theta' = DS' = 0 \ \text{ at } Y = 0 \ \text{ and } 1. \tag{24}$$

We employ a Galerkin type weighted residual method to obtain approximate solutions of the above system of ordinary differential equations by setting

$$\Psi' = \sum_{n=1}^{N_1} a_n\Psi_n, \ \Theta' = \sum_{n=1}^{N_1} b_n\Theta_n, \ S' = \sum_{n=1}^{N_1} c_nS_n, \tag{25}$$

and choosing the trial functions:

$$\Psi_n = \sin n\pi Y, \ \Theta_n = S_n = \cos n\pi Y. \tag{26}$$

Substituting (25)–(26) into (21)–(23), we obtain a system of $(3 \times N_1)$ linear algebraic equations with $(3 \times N_1)$ unknowns a_n, b_n, c_n for $n = 1, 2, \cdots, N_1$. For simplicity we confine ourselves to the one-term Galerkin approximation with $N_1 = 1$. Thus gives

$$A\tilde{X} = 0 \tag{27}$$

where $\tilde{X} = (a_1, b_1, c_1)$ and

$$A = \begin{pmatrix} \mathrm{Pr}\gamma^2 - s\gamma - \mathrm{Pr}\,\mathrm{Ha}^2\delta_1 & -\mathrm{Pr}\,\mathrm{Ra}\delta_2 & \mathrm{PrRs}\delta_2 \\ a & -\gamma - s & 0 \\ a & 0 & -\frac{\gamma}{\mathrm{Le}} - s \end{pmatrix}, \tag{28}$$

where $\gamma = \pi^2 + a^2$. For non-trivial solutions, we require the determinant of (28) to vanish. We obtain the thermal Rayleigh number Ra in terms of other parameters,

$$\mathrm{Ra} = \frac{\left(\gamma^2 - \frac{s}{\mathrm{Pr}}\gamma - \mathrm{Ha}^2\delta_1\right)(\gamma + s)}{a\delta_2} + \mathrm{Rs}\,\mathrm{Le}\frac{\gamma + s}{\gamma + s\,\mathrm{Le}}, \tag{29}$$

where $\delta_1 = \pi^2\sin^2\phi + a^2\cos^2\phi$ and $\delta_2 = \pi\cos\varphi - a\sin\varphi$.

Stationary convection occurs when $s = 0$ and oscillatory convection occurs when $s = iw$. The non-oscillatory and oscillatory convection regimes are discussed below.

3.1. Non-oscillatory convection

Non-oscillatory convection arise when $s = 0$, we obtain the stationary Rayleigh number,

$$\mathrm{Ra}^{st} = \frac{(\pi^2 + a^2)^3 - \mathrm{Ha}^2\delta_1(\pi^2 + a^2)}{a\delta_2} + \mathrm{Rs\,Le}. \tag{30}$$

When $\mathrm{Rs} = 0$, the magnetic field inclination angle $\phi = 3\pi/2$ and the inclination angle of the cavity $\varphi = \pi/2$, then we obtain the stationary Rayleigh number

$$\mathrm{Ra}^{\mathrm{st}} = \frac{\pi^2 + a^2}{a^2}((\pi^2 + a^2)^2 + \mathrm{Ha}^2\pi^2). \tag{31}$$

This result agrees with the result obtain by Chandreasekhar [1]. We obtain the critical wave number a_{c} and corresponding critical Rayleigh number $\mathrm{Ra_c}$ by minimizing the stationary Rayleigh number,

$$\frac{\partial}{\partial a^2}(\mathrm{Ra}^{\mathrm{st}}) = \frac{\partial}{\partial a^2}\left(\frac{(\pi^2 + a^2)^3 + \mathrm{Ha}^2\pi^2(\pi^2 + a^2)}{a^2}\right) = 0, \tag{32}$$

which implies that

$$2a^6 + 3\pi^2a^4 - \pi^6 - \pi^4\mathrm{Ha}^2 = 0. \tag{33}$$

By setting $x = a^2/\pi^2$ we obtain

$$2x^3 + 3x^2 - 1 - \mathrm{Ha}^2/\pi^2 = 0. \tag{34}$$

This equation depends only on the Hartmann number hence, the influence of the magnetic field on the onset of convection will be significant. If we assume Ha to be very large then we obtain $a_{\mathrm{c}} = \pi/\sqrt{2}$ and the corresponding critical Rayleigh number $\mathrm{Ra_c}$ is $Ra_{\mathrm{c}} = \frac{27}{4}\pi^4$.

This result again agrees with Chandrasekhar [1] and Nield and Kuznetsov [28].

3.2. Oscillatory convection

Substituting $s = i\omega$ into equation (29) and imposing the condition $\omega^2 > 0$ (which is required for ω to be real to get over stability) we obtain

$$\mathrm{Ra}^{\mathrm{osc}} = \frac{\left(\gamma^2 - \frac{i\omega}{\mathrm{Pr}}\gamma - \mathrm{Ha}^2\delta_1\right)(\gamma + i\omega)}{a\delta_2} + \mathrm{Rs\,Le}\frac{\gamma + i\omega}{\gamma + i\omega\mathrm{Le}}. \tag{35}$$

Equation (35) can be reduced to

$$\mathrm{Ra}^{\mathrm{osc}} = \Delta_1 + i\omega\Delta_2, \tag{36}$$

where Δ_1 and Δ_2 are the real and imaginary parts given as follows:

$$\Delta_1 = \frac{\gamma\left(\mathrm{Pr}\left(\gamma^2 - \delta_1\mathrm{Ha}^2\right) + \omega^2\right)}{a\delta_2\mathrm{Pr}} + \frac{\mathrm{Le}\,\mathrm{Rs}\left(\gamma^2 + \omega^2\mathrm{Le}\right)}{\gamma^2 + \omega^2\mathrm{Le}^2}, \tag{37}$$

$$\Delta_2 = \omega\left(\frac{\mathrm{Pr}\left(\gamma^2 - \delta_1\mathrm{Ha}^2\right) - \gamma^2}{a\delta_2\mathrm{Pr}} - \frac{\gamma\left(\mathrm{Le}-1\right)\mathrm{Le}\,\mathrm{Rs}}{\gamma^2 + \omega^2 Le^2}\right). \tag{38}$$

Since the Rayleigh number is always real, this implies that $\Delta_2 = 0$. Therefore, we obtain the angular frequency ω of the oscillatory convection as

$$\omega^2 = \frac{a\delta_1\mathrm{Pr}(\gamma(\mathrm{Le}-1)\mathrm{Le}\,\mathrm{Rs} - \gamma^2(\mathrm{Pr}(\gamma^2 - \delta_1\mathrm{Ha}^2) - \gamma^2)}{\mathrm{Le}^2(\mathrm{Pr}(\gamma^2 - \delta_2\mathrm{Ha}^2) - \gamma^2)}. \tag{39}$$

The oscillatory convection is then defined by

$$\mathrm{Ra}^{\mathrm{osc}} = \frac{\gamma\left(\mathrm{Pr}\left(\gamma^2 - \delta_1\mathrm{Ha}^2\right) + \omega^2\right)}{a\delta_2\mathrm{Pr}} + \frac{\mathrm{Le}\,\mathrm{Rs}\left(\gamma^2 + \omega^2\mathrm{Le}\right)}{\gamma^2 + \omega^2\mathrm{Le}^2}. \tag{40}$$

4. Nonlinear stability

The nonlinear stability analysis is presented using a minimal truncated Fourier series that consists of two terms. The linear stability analysis fails to provide insights into the convection amplitudes and the rate of heat and mass transfer.

We assume a minimal truncated Fourier series to describe the finite amplitude convection defined by

$$\psi' = A_{11}(\tau)\sin ax \sin \pi y, \tag{41}$$

$$\theta' = B_{11}(\tau)\cos ax \sin \pi y + B_{02}(\tau)\sin 2\pi y, \tag{42}$$

$$S' = C_{11}(\tau)\cos ax \sin \pi y + C_{02}(\tau)\sin 2\pi y, \tag{43}$$

where $A_{11}, B_{02}, B_{02}, C_{11}$ and C_{02} are time dependent convective amplitudes. Nonlinear autonomous equations are obtained after substituting equations (41)–(43) into (15)–(17) and introducing new variables

$$Y_1 = \frac{a\pi}{\gamma}A_{11},\ Y_2 = -\pi R B_{11},\ Y_3 = -\pi R B_{02}, \tag{44}$$

$$Y_4 = -\pi R C_{11},\ Y_5 = -\pi R C_{02},\ \tau^* = \gamma\tau, G = \frac{4\pi^2}{\gamma}. \tag{45}$$

After dropping the asterisk from τ for clarity, we obtain

$$\dot{Y_1} = Pr(-bY_1 + \sin\varphi(Y_2 - NY_4)), \tag{46}$$

$$\dot{Y_2} = RY_1 - Y_2 - Y_1Y_3, \tag{47}$$

$$\dot{Y_3} = \frac{1}{2}Y_1Y_2 - GY_3, \tag{48}$$

$$\dot{Y_4} = RY_1 - Y_1Y_5 - Le^{-1}Y_4, \tag{49}$$

$$\dot{Y_5} = \frac{1}{2}Y_1Y_4 - \frac{G}{\mathrm{Le}}Y_5, \tag{50}$$

where $b = \mathrm{Ha}^2(a^2\cos^2\phi + \pi^2\sin^2\phi)/\gamma^2 - 1$, $R = a^2\mathrm{Ra}/\gamma^3$ is revised Rayleigh number and $N = \mathrm{Rs}/\mathrm{Ra}$ is the buoyancy ratio.

4.1. Steady finite amplitude convection

The general Lorenz type model (46)–(50) has the steady state solutions

$$Y_1^2 = \frac{-B \pm \sqrt{B^2 - 4AC}}{2A}, \quad Y_2 = \frac{2GRY_1}{2G + Y_1^2},$$
$$Y_3 = \frac{RY_1^2}{2G + Y_1^2}, \quad Y_4 = \frac{2G\,\mathrm{Le}\,RY_1}{2G + \mathrm{Le}^2Y_1^2}, \quad Y_5 = \frac{\mathrm{Le}^2RY_1^2}{2G + \mathrm{Le}^2Y_1^2}, \tag{51}$$

where $A = b\,\mathrm{Le}^2$, $B = 2G(b(1+Le) + R\,\mathrm{Le}(\mathrm{Le} - N)\sin\varphi)$ and $C = 4G^2(1 + R(1 - N\,\mathrm{Le})\sin\varphi)$. The equations (46)–(50) are uniformly bounded in time and dissipative in the phase space. To this end, we obtain

$$\sum_{n=1}^{5}\frac{\partial\dot{Y_n}}{\partial Y_n} = -\left(\mathrm{Pr}b + 1 + G + \mathrm{Le}^{-1} + G\,Le^{-1}\right) \tag{52}$$

Equation (52) will always be negative if and only if $b \geq 0$ implies that $\mathrm{Ha}^2 \geq \gamma/(a^2\cos^2\phi + \pi^2\sin^2\phi)$. Therefore, the trajectories may be attracted to a fixed point or limit cycle or any strange attractor. Also, from equations (46)–(50), the volume V_0 at time $t = 0$ is contracted by the flow into a volume element defined by

$$V = V_0\exp\left\{-\left(\mathrm{Pr}\,b + 1 + G + \mathrm{Le}^{-1} + G\mathrm{Le}^{-1}\right)t\right\} \tag{53}$$

in time t. Thus, each volume containing the trajectory of this system of equations shrink to zero as $t \to \infty$. Further, the system of equations (46)–(50) are invariant under the transformation $S(Y_n) = -Y_n$ for $n = 1, 2, \cdots, 5$.

4.2. The trapping region

In the classical Lorenz model, the trajectories are known to remain within a finite volume. The trapping region of the trajectories of the system of equations (46)–(50) is a smooth real-valued function $\Sigma(\Lambda(t))$, where $\Lambda(t)$ is the solution of the system of equations (46)–(50) (see [29]). This function has to satisfy the condition $\Sigma(\Lambda(t)) \longrightarrow \infty$ as $\| \Lambda \| \longrightarrow \infty$. The nonlinear terms keep the trajectories confined. We follow the procedure of Sidddheshwar and Titus [29] to find the trapping region $\Sigma(\Lambda)$ as follows

$$\frac{\mathrm{d}\Sigma}{\mathrm{d}t} = Y_1\frac{\mathrm{d}Y_1}{\mathrm{d}t} + \frac{1}{2}Y_2\frac{\mathrm{d}Y_2}{\mathrm{d}t} + (Y_3 - R - \frac{\sin\varphi}{2})\frac{\mathrm{d}(Y_3 - R - \frac{\sin\varphi}{2})}{\mathrm{d}t} + \frac{1}{2}Y_4\frac{\mathrm{d}Y_4}{\mathrm{d}t} + (Y_5 - R + \frac{N\sin\varphi}{2})\frac{\mathrm{d}(Y_5 - R + \frac{N\sin\varphi}{2})}{\mathrm{d}t}. \tag{54}$$

We obtain the trapping region of the system (46)–(50) as an ellipsoid in five dimensions by integrating the above equations which gives

$$Y_1^2 + \frac{Y_2^2}{2} + (Y_3 - R - \frac{\sin\varphi}{2})^2 + \frac{Y_4^2}{2} + (Y_5 - R + \frac{N\sin\varphi}{2})^2 = 2. \tag{55}$$

For the stability of the fixed point we linearized the general autonomous Lorenz-type equations (46)–(50) around the fixed point, we obtain

$$\boldsymbol{J}(0,0,0,0,0) = \begin{pmatrix} -\mathrm{Pr}\,b & \mathrm{Pr}\sin\varphi & 0 & -N\mathrm{Pr}\sin\varphi & 0 \\ R & -1 & 0 & 0 & 0 \\ 0 & 0 & -G & 0 & 0 \\ R & 0 & 0 & -\mathrm{Le}^{-1} & 0 \\ 0 & & 0 & 0 & -G\,\mathrm{Pr}^{-1} \end{pmatrix}. \tag{56}$$

The eigenvalues of equation (56) are

$$\lambda_1 \;=\; -1,\;\; \lambda_2 = -G,\;\; \lambda_3 = -G\,\mathrm{Le}^2,\;\; \lambda_{\pm 4} = \frac{-\zeta \pm \sqrt{\zeta^2 - 4\mathrm{Pr}\eta}}{2}, \tag{57}$$

where $\zeta = \mathrm{Pr}\,b + \mathrm{Le}^{-1}$ and $\eta = b$
$, \mathrm{Le}^{-1} + R\sin\varphi(N - \mathrm{Le}^{-1})$. It's clear that λ_1, λ_2 and λ_3 all have negative real parts. While $\lambda_{\pm 4}$ are have negative real part if and only if $\zeta^2 - 4\mathrm{Pr}\eta < 0$. Hence, the fixed point $(0,0,0,0,0)$ is stable.

5. Method of solution

Since an analytical solution of equations (46)–(50) is not possible, we solved the equations numerically. We used a newly developed multi-domain spectral collocation method to solve this system of equations [27]. To apply the method first divided the interval $[0,T]$ into sub-intervals $\Omega_i = [t_{i-1}, t_i]$ for $i = 1, 2, \cdots, p$ and use the

transformation

$$t = \frac{t_i - t_{i-1}}{2}\tau + \frac{t_i + t_{i-1}}{2} \tag{58}$$

to transform each sub-interval to $[-1, 1]$. The Gauss-Lobatto collocation points are defined by

$$\tau_j^i = \cos\frac{\pi j}{M}, \quad \text{for } j = 0, 1, \cdots M. \tag{59}$$

The derivatives at the collocation points of the unknown functions $Y_{n,r+1}^i(t)$ are given by

$$\frac{\mathrm{d}Y_{n,r+1}^i}{\mathrm{d}t}(\tau_j^i) = \sum_{k=0}^{M} \boldsymbol{D}_{jk} Y_{n,r+1}^i(\tau_j^j) = \boldsymbol{D}\boldsymbol{U}_{n,r+1}^i, \tag{60}$$

where $\boldsymbol{D} = 2D/(t_i - t_{i-1})$. D is the Chebyshev derivative which is given in [27] and $\boldsymbol{U}_{n,r+1}^i = (Y_{n,r+1}^i(\tau_0^i), \cdots Y_{n,r+1}^i(\tau_M^i))$ is the vector of the unknown functions at the collocation points and r is the number of iteration. Now substituting these into equations (46)–(50) and reducing the outcomes in the matrix form

$$\begin{pmatrix} A_{11} & A_{12} & A_{13} & A_{14} & A_{15} \\ A_{21} & A_{22} & A_{23} & A_{24} & A_{25} \\ A_{31} & A_{32} & A_{33} & A_{34} & A_{35} \\ A_{41} & A_{42} & A_{43} & A_{44} & A_{45} \\ A_{51} & A_{52} & A_{53} & A_{54} & A_{55} \end{pmatrix} \begin{pmatrix} \boldsymbol{U}_{1,r+1}^i \\ \boldsymbol{U}_{2,r+1}^i \\ \boldsymbol{U}_{3,r+1}^i \\ \boldsymbol{U}_{4,r+1}^i \\ \boldsymbol{U}_{5,r+1}^i \end{pmatrix} = \begin{pmatrix} \boldsymbol{R}_{1,r}^i \\ \boldsymbol{R}_{2,r}^i \\ \boldsymbol{R}_{3,r}^i \\ \boldsymbol{R}_{4,r}^i \\ \boldsymbol{R}_{5,r}^i \end{pmatrix} \tag{61}$$

where the matrices A_{ij} and $\boldsymbol{R}_n^i$ are given as follows:

$$A_{11} = \boldsymbol{d}(-b\,\mathrm{Pr}), \quad A_{12} = \boldsymbol{d}(\mathrm{Pr}\sin\varphi), \quad A_{14} = \boldsymbol{d}(-N\,\mathrm{Pr}\sin\varphi), \quad A_{13} = A_{15} = \boldsymbol{0}$$

$$A_{21} = \boldsymbol{d}(R - Y_{3,r}^i), \quad A_{22} = \boldsymbol{d}(-1), \quad A_{23} = \boldsymbol{d}(-Y_{1,r}^i), \quad A_{24} = A_{25} = \boldsymbol{0}$$

$$A_{31} = \boldsymbol{d}(\frac{Y_{2,r}^i}{2}), \quad A_{32} = \boldsymbol{d}(\frac{Y_{1,r}^i}{2}), \quad A_{33} = \boldsymbol{d}(-G), \quad A_{34} = A_{35} = \boldsymbol{0}$$

$$A_{41} = \boldsymbol{d}(R - Y_{5,r}^i), \quad A_{44} = \boldsymbol{d}(-\frac{1}{Le}), \quad A_{45} = \boldsymbol{d}(-Y_{1,r}^i), \quad A_{42} = A_{43} = \boldsymbol{0}$$

$$A_{51} = \boldsymbol{d}(\frac{Y_{4,r}^i}{2}), \quad A_{54} = \boldsymbol{d}(\frac{Y_{1,r}^i}{2}), \quad A_{55} = \boldsymbol{d}(-\frac{G}{\mathrm{Le}}), \quad A_{52} = A_{53} = \boldsymbol{0},$$

($\boldsymbol{d}$ denoting diagonal matrix) and the right-hand side matrices are

$$\boldsymbol{R}_{1,r}^i = 0, \quad \boldsymbol{R}_{2,r}^i = -Y_{1,r}^i Y_{3,r}^i, \quad \boldsymbol{R}_{3,r}^i = 1/2(Y_{1,r}^i Y_{2,r}^i),$$

$$\boldsymbol{R}_{4,r}^i = -Y_{1,r}^i Y_{5,r}^i, \quad \boldsymbol{R}_{5,r}^i = 1/2(Y_{1,r}^i Y_{4,r}^i).$$

6. Heat and mass transfers

Heat and mass transfer rates in terms of the Nusselt number (Nu) and Sherwood number (Sh) can be calculated with the help of the above solution method. The dimensionless temperature gradient and concentration gradient of the hot wall are defined as

$$\mathrm{Nu} = -\frac{a}{2\pi}\int_0^{\frac{a}{2\pi}} \left(\frac{\partial \Theta}{\partial Y}\right)|_{Y=0}\,\mathrm{d}X = -2\pi C = \frac{2}{R}Y_3 \tag{62}$$

$$\mathrm{Sh} = -\frac{a}{2\pi}\int_0^{\frac{a}{2\pi}} \left(\frac{\partial S}{\partial Y}\right)|_{Y=0}\,\mathrm{d}X = -2\pi E = \frac{2}{R}Y_5. \tag{63}$$

7. Results and discussion

The main purpose of our investigation was to study the thermal instability in double-diffusive convection in an electrically conducting fluid in an inclined open square cavity using linear and weakly nonlinear stability analysis. Analytical expressions for the stationary and oscillatory Rayleigh numbers have been obtained using linear stability analysis. Moreover, the critical Rayleigh number and corresponding critical waver number for the onset of non-oscillatory convection are determined here. The linear stability theory fails to give a good analysis of nonlinear regime. Therefore, the finite amplitude convection is employed here to study the chaotic behavior of the system and investigate the heat and mass transfer rate of the fluid. So, the nonlinear stability analysis has been discussed here numerically using multi-domain spectral collocation method. Also, the effects of various parameters on heat and mass transfer in terms of Nusselt number and Sherwood number are seen here. In this study, the Lewis number has to change its value from 0.1 to 10, the buoyancy ratio various its value from -10 to 10 and Prandtl number has the value 0.7 and above.

Figure 2 shows the stationary Rayleigh stability curves for various parameters.

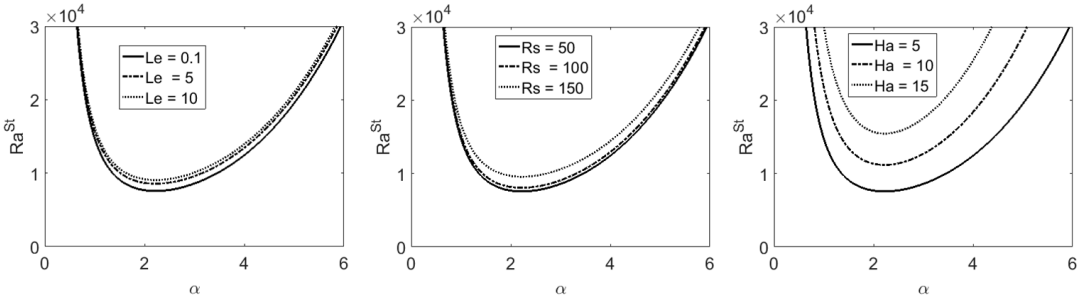

Fig. 2. Effect of critical Rayleigh number Ra with wave number α for various values of the Lewis number Le–left, of the concentration Rayleigh number Rs–middle, of the Hartmann number Ha–right

Its left and middle parts show the effect of increasing the Lewis number Le and concentration Rayleigh number Rs on stationary Rayleigh number. It can be seen

that an increasing value of Le and Rs increase the value of stationary Rayleigh number, which means that both Le and Rs have significant effect on stabilizing the system. The right part of Fig. 2 shows the effect of different values of Hartmann number Ha on the stationary Rayleigh number. It can be observed that an increasing values of Ha increases the value of stationary Rayleigh number which stabilize the system. It is conventional that the magnetic field offers a resistance to the motion of the fluid due to Lorenz force. As a result a huge amount of energy is used by the system to overcome this resistance. Then the convection is delayed the stabilization effect of those parameters on fluid.

Figure 3 shows the effect of different values of Ha on oscillatory Rayleigh number with respect to the concentration Rayleigh number, Lewis number and Prandtl number, respectively. It is seen that increasing value of Ha has a significant effect on increasing oscillatory Rayleigh number which stabilize the system. Hence, the influence of these parameters are used to stabilize the double diffusive convection on an inclined cavity.

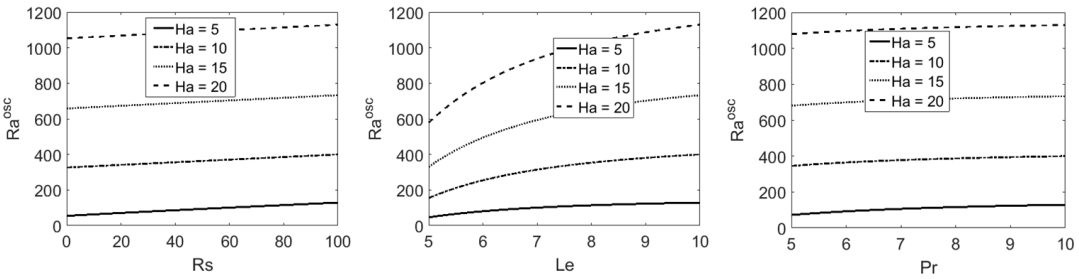

Fig. 3. Effect of Hartmann number Ha on critical oscillatory Rayleigh number $\mathrm{Ra}^{\mathrm{osc}}$ for various values of the concentration Rayleigh number Rs–left, of the Lewis number Le–middle, of the Prandlt number Pr–right

Figure 4 shows the effect of Ha on behavior of the Nusselt and Sherwood numbers with respect to time.

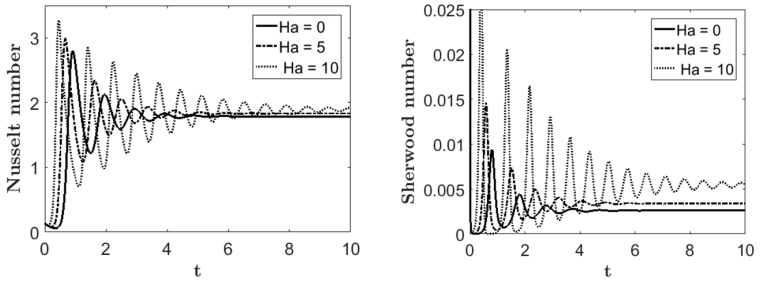

Fig. 4. Variation of average Nusselt number Nu (left) and average Sherwood number Sh (right) with time t for different values of Hartmann number Ha

It was found that increasing Ha increases both the rate of heat and mass transfer. It was also observed that both the Nusselt and Sherwood numbers tend to the state steady faster for small values of Ha than for large values of Ha.

Figure 5 shows the influence of Pr on the Nusselt and Sherwood numbers with respect to time. It is seen that increasing Pr increases both the Nusselt and Sherwood

numbers. Also, it is seen that the rates of heat and mass transfers tend to their steady state after some time faster for large value of Pr than small value of Pr.

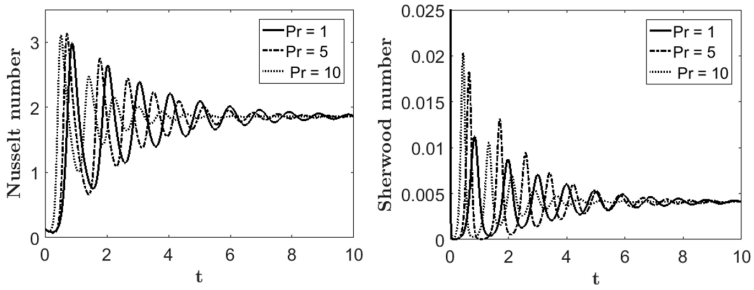

Fig. 5. Variation of average Nusselt number Nu (left) and average Sherwood number Sh (right) with time t for different values of Prandtl number Pr

Figure 6 displays the transient behavior of Nusselt number and Sherwood number for various values of Le.

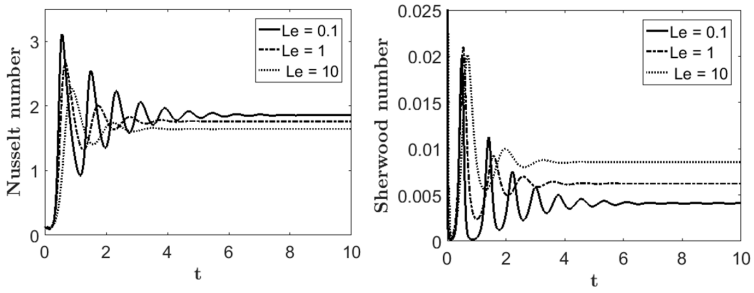

Fig. 6. Variation of average Nusselt number Nu (left) and average Sherwood number Sh (right) with time t for different values of Lewis number Le

The Nusselt number and Sherwood number decrease with increasing value of Le from 0.1 to 10. It is seen that the Nusselt number and Sherwood number attain their steady state faster for the larger values of Le. It is seen that initially Nusselt number and Sherwood number fluctuate and this fluctuation decrease as the time increases to the steady state values. Again, it is observed that increasing Pr increases the amplitude of fluctuations in these transient curves but also helps Nusselt and Sherwood numbers to reach their steady state values much earlier where the opposite trend can be found for Ha. But for increasing values of Le increases the amplitude of fluctuations in these transient curves and the Nusselt and Sherwood numbers reach their steady state values much earlier than small value of Le.

Figures 7–10 display the phase space of Y_iY_j plane for the sensitivity of different revised Rayleigh number Ra. However, these phase space plots are staying within the finiteness of an ellipsoid nature given by equation (55) (within the trapping region). It can be observed that the trajectories occupies a finite phase space region. However this finiteness of the phase space region is due to the nonlinear terms in the system of equations (46)–(50), which turn the trajectories into a finite region. Furthermore, these trajectories enter into trapping region and look like an ellipsoid given by equation (55) toggling between the phase space around the critical points.

The "saddle points" can be observed in "butterfly diagrams". Its seem that various bifurcations reported in Sparrow [30] and Siddheshwar and Titus [29] hold good comparison with the present results. Also our results show that there exist closed orbits.

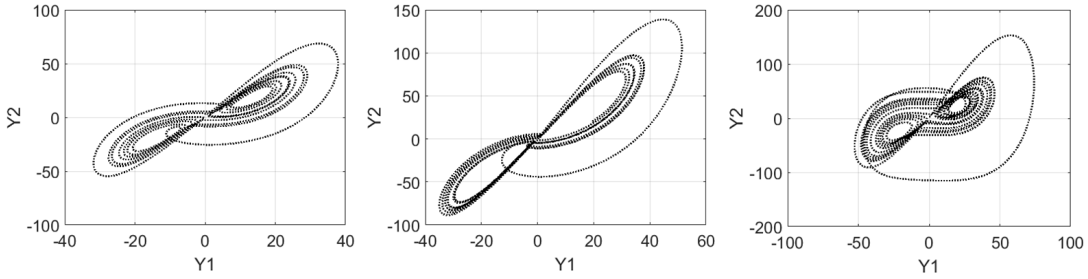

Fig. 7. Evolution of system of nonlinear equation solution shown the sensitivity to Rayleigh number when the solution is projected into Y_1Y_2 plane: left–$R = 50$, middle–$R = 100$, right–$R = 150$

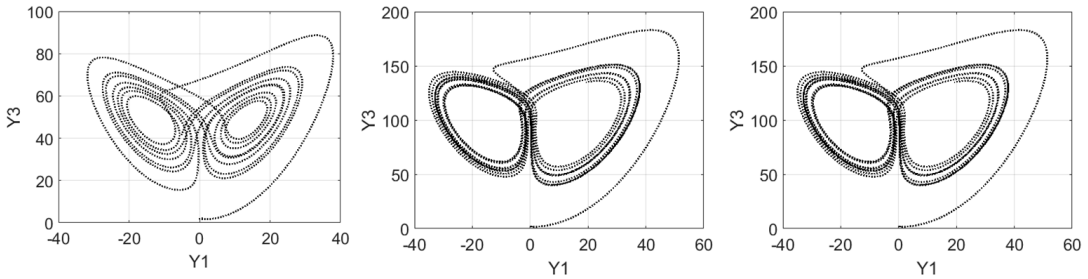

Fig. 8. Evolution of system of nonlinear equation solution shown the sensitivity to Rayleigh number when the solution is projected into Y_1Y_3 plane: left–$R = 50$, middle–$R = 100$, right–$R = 150$

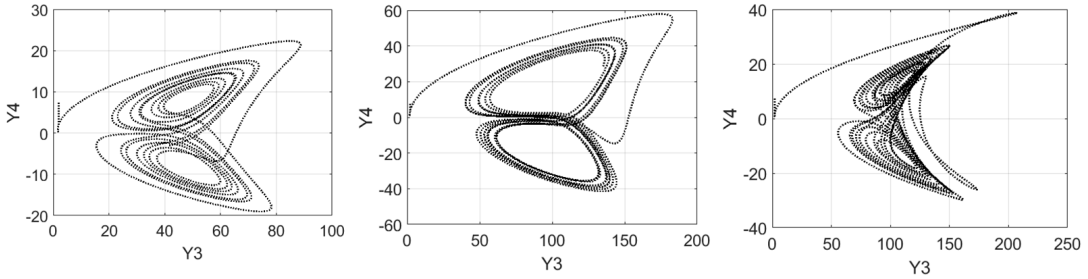

Fig. 9. Evolution of system of nonlinear equation solution shown the sensitivity to Rayleigh number when the solution is projected into Y_3Y_4 plane: left–$R = 50$, middle–$R = 100$, right–$R = 150$

Figure 11 displays the three-dimensional bifurcations which are solution of equations (46)–(50) as the revised Rayleigh number changed from 50 to 150 with fixed Prandtl number $\mathrm{Pr} = 10$ and Lewis number 0.1. These chaotic structures are similar to those in the two-phase space. The only differences are in the shape of the phase space. The phase space in three-dimensional bifurcations are different for different

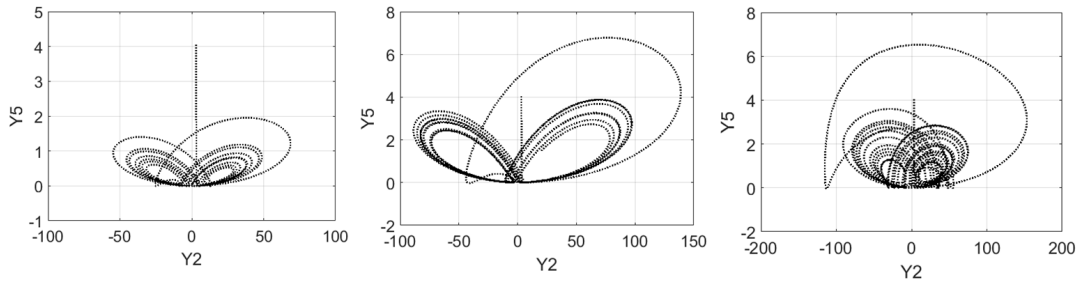

Fig. 10. Evolution of system of nonlinear equation solution shown the sensitivity to Rayleigh number when the solution is projected into Y_2Y_5 plane: left–$R = 50$, middle–$R = 100$, right–$R = 150$

space combinations. Some of these bifurcations have not been seen in literature before. It can, however, be observed that the system stabilizes with increasing values of R.

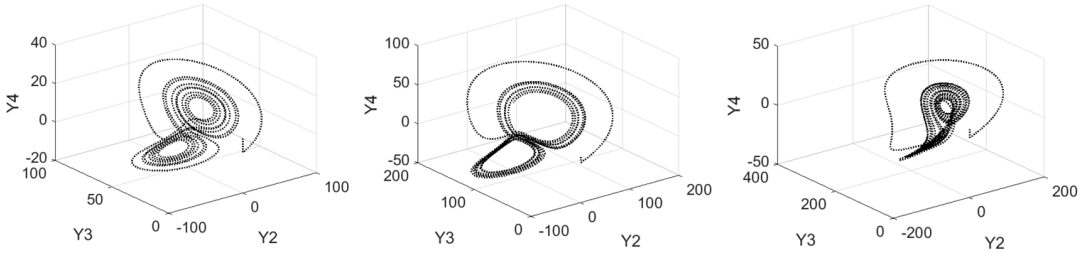

Fig. 11. Evolution of system of nonlinear equation solution shown the sensitivity to Rayleigh number when the solution is projected into $Y_2Y_3Y_4$ plane: left–$R = 50$, middle–$R = 100$, right–$R = 150$

The relative importance of the thermal and solutal buoyancy forces is denoted by the buoyancy ratio N, and is defined as the ratio of the solutal buoyancy force and the thermal buoyancy force. Here, this parameter is varied through the range $-10 < N < 10$. The concentration-dominated opposing flow can be seen when $N = -10$, pure thermal convection dominated flow for $N = 0$, and concentration-dominated aiding flow can be seen for $N = 10$. The flow is steady when $N = 1$, this is because the two buoyancy forces are equal and oppose each other. The buoyancy forces that drive the fluid motion are mainly due to the gradients of temperature if N is sufficiently small which indicates that the mass buoyancy is greater than the thermal buoyancy. Negative value of N represents the opposing nature of two buoyancy forces due to the negative coefficient of concentration expansion. In this limit, the so-called heat transfer-driven flows, the distribution of constituent does not influence the flow pattern and the heat transfer rate. The flow are mainly due to gradients of solute concentration due to solutal gradients if $N > 1$. The negative values of streamlines, isotherms and iso-concentration indicate clockwise rotation and positive value indicate anticlockwise rotation.

Figures 12–14 display the effect of different buoyancy ratios on the streamline, isotherm and iso-concentration profiles for different magnetic field angle when the inclination angle of the cavity is fixed at angle 90° and the bottom wall is heated.

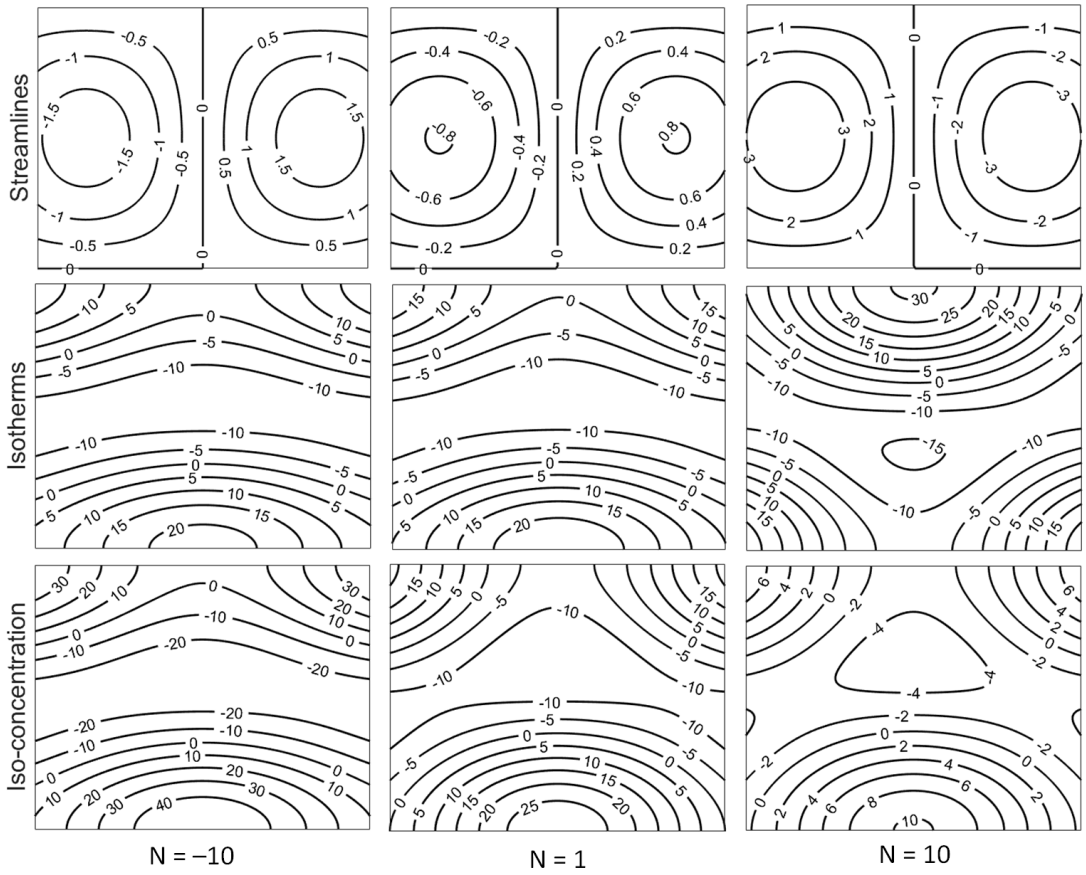

Fig. 12. The streamlines, isotherms and iso-concentration for different values of the buoyancy ratio N, inclination angle $\varphi = 90^\circ$ and magnetic angle $\phi = 45^\circ$

As expected, due to the cold vertical walls, fluids rise up from middle portion of the bottom wall and flow down along the two vertical walls forming two symmetric rolls clockwise and anticlockwise rotations inside the cavity. Actually, the fluid circulation is strongly dependent on buoyancy ratio and different magnetic field angles. Figure 12 illustrates that the streamlines, isotherms and iso-concentrations for magnetic field angle $\phi = 45^\circ$ and different values of N which are mentioned above. It is seen from this figure that the flow is seen to be very week for $N = -10$ and $N = 1$ compared to other streamline graph for $N = 10$. Therefore, the temperature distribution is similar to that with stationary fluid and the heat transfer will be purely conduction. During conduction dominant heat transfer, some isotherms ≤ 5 occur symmetrically near the top corners of the side walls in the enclosure and some isotherm are concentrated at the bottom wall. The other isotherms are smooth curves which span entire enclosure in clockwise and anticlockwise directions. But the isotherms are mainly concentrated near two bottom edges and top wall of the cavity when $N = 0$. And single eddy with clockwise rotation can be found at the center of the cavity with highest value 15. The similar type of iso-concentrations can be found as isotherms for $N = -10$ and $N = 1$. But, it can be seen five different

types of iso-concentration contours due to the higher value of N i.e, $N = 10$ and magnetic field angle $\phi = 45°$.

Figures 13 and 14 show the streamlines,isotherms and iso-concentration for high values of the magnetic field angle ϕ and different values of N compared to Fig. 12. Figure 13 depicts the effect of changing the magnetic field angle to $\phi = 90°$ and different values of N on streamlines, isotherms and iso-concentrations. The main difference compared to Fig. 12 is that the flow is stronger for any value of N compared to the streamline values in Fig. 12. The isotherms are due to heat conduction when $N = -10$ and similar patterns as in Fig. 12 can be observed. However, the isotherms patterns change as N increases in value, showing that the isotherm pattern depends on N. It is also observed that the iso-concentrations depend mainly on the magnetic field angle since large changes can be seen as the magnetic field angles. We found at least four eddies with different patterns of iso-concentrations due to the increasing value of the magnetic field angle.

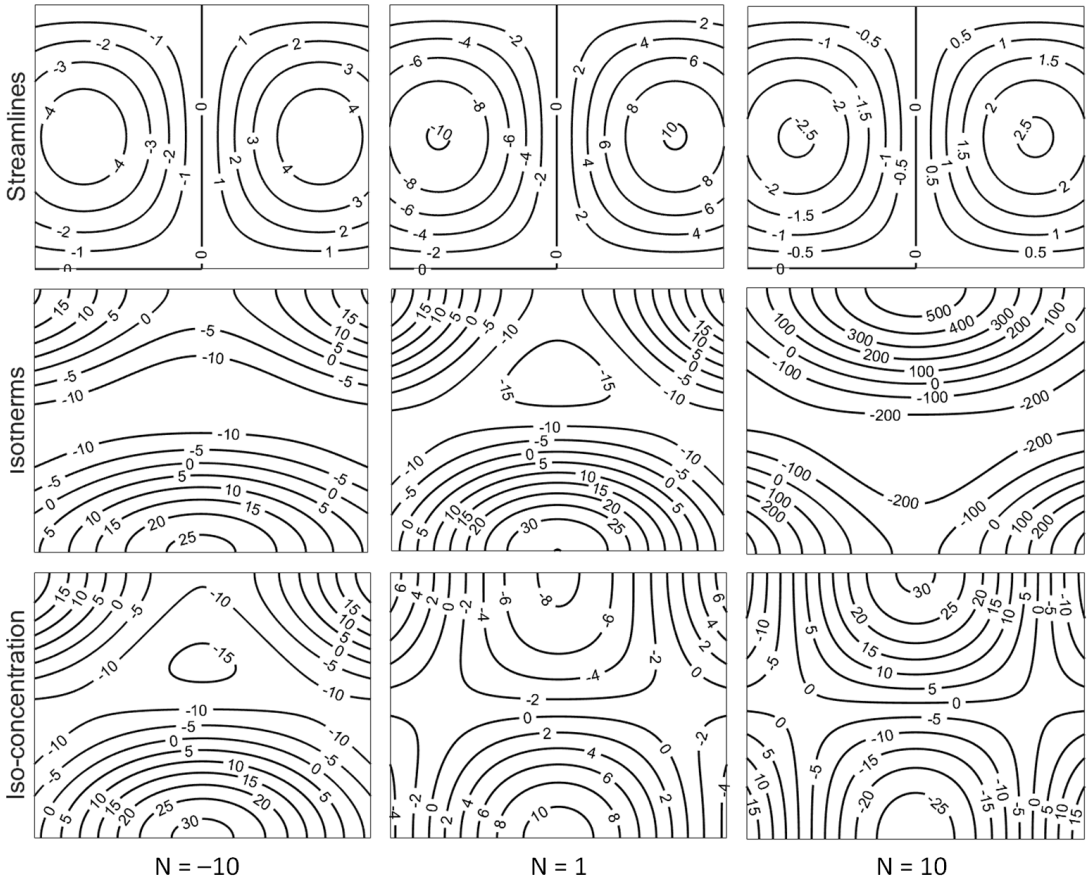

Fig. 13. The streamlines, isotherms and iso-concentration for different values of the buoyancy ratio N, inclination angle $\varphi = 90°$ and magnetic angle $\phi = 90°$

Figure 14 displays the effect of a higher magnetic field angle i.e., 135° for different values of N on the streamlines, isotherms and iso-concentrations. When the magnetic field angle changes from $\phi = 90°$ to $\phi = 135°$, the streamlines pattern does

no change while the values of central eddies changed. As the magnetic field angle increased from 45° to 135°, the isotherm and iso-concentration patterns changed and the values of the central eddies increased. The isotherms are smooth curves which span the entire enclosure in clockwise and anticlockwise directions for higher values of N. Also, as the buoyancy ratio increased from 1 to 10, the iso-concentration eddies became larger due to increasing solutal concentration gradients.

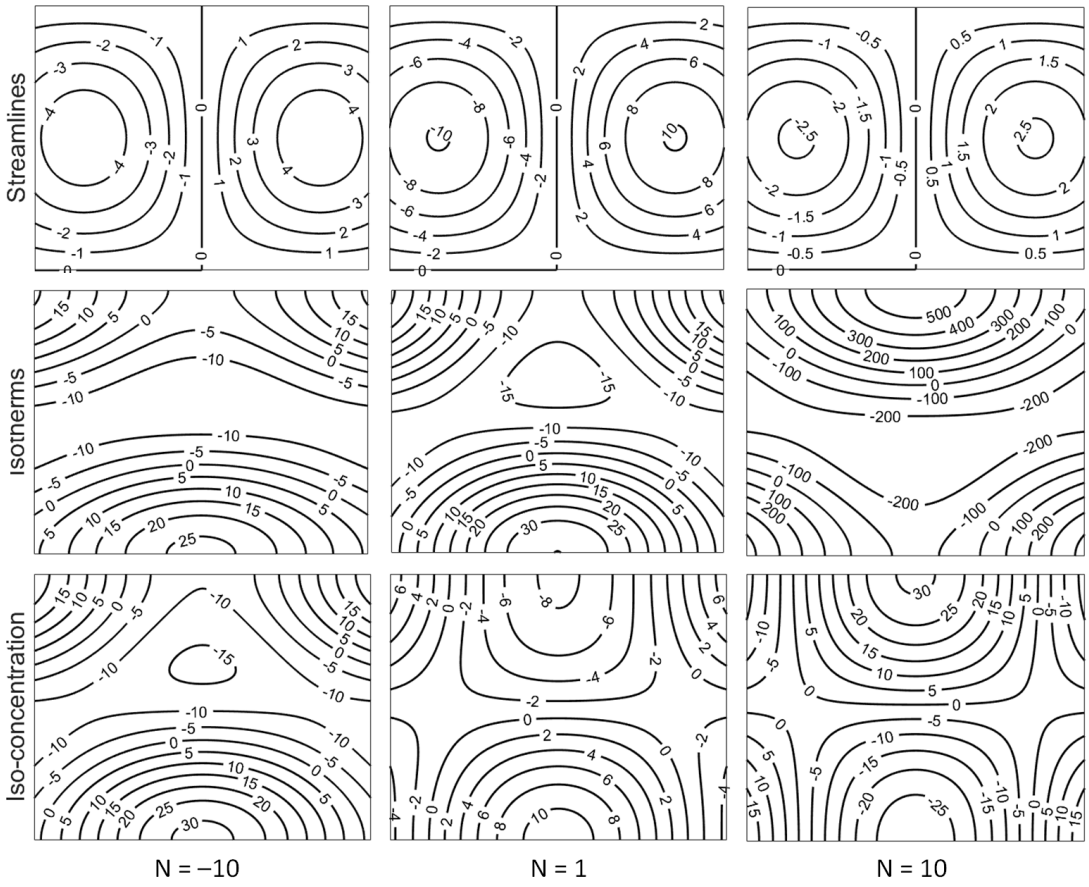

Fig. 14. The streamlines, isotherms and iso-concentration for different values of the buoyancy ratio N, inclination angle $\varphi = 135°$ and magnetic angle $\phi = 90°$

8. Conclusion

In this paper, the focus of the study was on the linear and nonlinear stability analysis of flow in an open inclined square cavity. The effect of Hartmann number on the stationary and oscillatory convection has been presented graphically. The stability of general Lorenz types equations has been studied. The nonlinear equations were solved numerically using a multi-domain spectral collocation approach. The influence of various parameters on the flow has been discussed. The following conclusion can drawn from this study.

1 . The magnetic field parameter has the effect of increasing both stationary and oscillatory convection, hence this has the effect of stabilizing the fluid motion.

2 . The trajectories in phase space of the general Lorenz types equations has been shown to be bounded within a finite ellipsoidal trapping region. Also, the chaotic behaviour is shown for the inclined open square cavity.

3 . The streamlines are seen to be weak when $\phi = 45°$ but stronger for higher value of ϕ than $\phi = 45°$. While some isotherms occur symmetrically near the top corners of the side walls in the enclosure and some isotherm are concentrated at the bottom wall due to the conduction dominant heat transfer for $N = -10$ when $\phi = 45°$ and $90°$ but opposite trend is observed for $\phi = 45°$ and $\phi = 135°$.

References

[1] S. Chandrasekhar: *Hydrodynamic and hydromagnetic stability.* Oxford University Press (1961).

[2] P. G. Drazin, W. H. Reid: *Hydrodynamic stability.* Combridge University Press (1981).

[3] C. Simó, D. Puigjaner, J. Herrero, F. Giralt: *Dynamics of particle trajectories in a Rayleigh–Bénard problem.* Communications in Nonlinear Science and Numerical Simulation *15* (2010), No. 1, 24–39.

[4] D. Laroze, H. Pleiner: *Thermal convection in a nonlinear non-Newtonian magnetic fluid.* Communications in Nonlinear Science and Numerical Simulation *26* (2015), Nos. 1–3, 167–183.

[5] D. A. Nield, A. Bejan: *Convection in porous media.* Springer-Verlag New York (2006).

[6] D. B. Ingham, I. Pop: *Transports phenomena in porous media.* Pergamon, Oxford *3* (2005).

[7] I. Pop, D. B. Ingham: *Convective heat transfer: Mathematical and computional modeling of viscous fluid and porous media.* Pergamon, Oxford (2001).

[8] A. Bejan, I. Dincer, S. Lorente, A. F. Miguel, A. H. Reis: *Porous and complex flows structures in modern technologies.* Springer Nature, Berlin (2004).

[9] K. Vafai: *Handbook of porous media.* CRC Press, Taylor & Francis Group (2005).

[10] P. Le Quere, J. A. C. Humphrey, F. S. Sherman: *Numereical calculation of thermally driven two-dimensinal unsteady laminar flow in cavities of rectangular cross section.* Numerical Heat Transfer *4* (1981), No. 3, 249-283.

[11] A. J. Chamkha, H. Al-Naser: *Double-diffusive convection in an inclined porous enclosure with opposing temperature and concentration gradients.* International Journal of Thermal Sciences *40* (2001), No. 3, 227–244.

[12] G. Wang, Q. Wang, M. Zeng, H. Ozoe: *Numerical study of natural convection heat transfer in an inclined porous cavity with time-periodic boundary conditions.* Transport in Porous Media *74* (2008), No. 3, 293–309.

[13] O. Polat, E. Bilgen: *Laminar natural convection in inclined open shallow cavities.* International Journal of Thermal Sciences *41* (2002), No. 4, 360–368.

[14] K. M. Khanafer, A. J. Chamkha: *Hydromagnetic natural convection from an inlinced porous square enclosure with heat generation.* Numerical Heat Transfer, Part A: Applications *33* (1998), No. 8, 891–910.

[15] J. S. Turner: *Buoyancy effects in fluids.* Cambridge University Press (1979).

[16] N. Rudraiah: *Double-diffusive magnetoconvection*. Pramana *27* (1986), Nos. 1–2, 233–266.

[17] W. Bian, P. Vasseur, E. Bilgen, F. Meng: *Effect of an electromagnetic field on natural convection in an inclined porous medium*. International Journal of Heat and Fluid Flow *17* (1996), No. 1, 36–44.

[18] C. Revnic, T. Grosan, I. Pop, D. B. Ingham: *Magnetic field effect on the unsteady free convection flow in a square cavity filled with a porous medium with a constant heat generation*. International Journal of Heat and Mass Transfer *54* (2011), Nos. 9–10, 1734–1742.

[19] M. A. Mansour, A. J. Chamkha, R. A. Mohamed, M. M. Abd, El-Aziz, S. E. Ahmed: *MHD natural convection in an inclined cavity filled with a fluid saturated porous medium with heat source in the solid phase*. Nonlinear Analysis: Modelling and Control *15* (2010), No. 1, 55–70.

[20] S. Mondal, P. Sibanda: *Unsteady double diffusive convection in an inclined rectangular lid-driven enclosure with different magnetic field angles and non-uniform boundary conditions*. International Journal of Heat and Mass Transfer *90* (2015), 900-910.

[21] M. Narayana, S. N. Gaikwad, P. Sibanda, R. B. Malge: *Double diffusive magneto-convection in viscoelastic fluids*. International Journal of Heat and Mass Transfer *67* (2013), 194–201.

[22] P. G. Siddheshwar, S. Pranesh: *Effect of temperature/gravity modulation on the onset of magneto-convection in weak electrically conducting fluids with internal angular momentum*. Journal of Magnetism and Magnetic Materials *192* (1999), No. 1, 159–176.

[23] P. G. Siddheshwar, S. Pranesh: *Effect of temperature/gravity modulation on the onset of magneto-convection in electrically conducting fluids with internal angular momentum*. Journal of Magnetism and Magnetic Materials *219* (2000), No. 2, 153–162.

[24] N. Rudraiah, P. K. Srimani, R. Friedrich: *Finite amplitude convection in a two-component fluid saturated porous layer*. International Journal of Heat and Mass Transfer *25* (1982), No. 5, 715–722.

[25] S. N. Gaikwad, S. Kouser: *Double diffusive convection in a couple stress fluid saturated porous layer with internal heat source*. International Journal of Heat and Mass Transfer *78* (2014), 1254–1264.

[26] D. Lehotzky, T. Insperger, G. Stepan: *Extension of the spectral element method for stability analysis of time-periodic delay-differential equations with multiple and distributed delays*. Communications in Nonlinear Science and Numerical Simulation *35* (2016), 177–189.

[27] S. S. Motsa, P. Dlamini, M. Khumalo: *A new multistage spectral relaxation method for solving chaotic initial value systems*. Nonlinear Dynamics *72* (2013), Nos. 1–2, 265–283.

[28] A. V. Kuznetsov, D. A. Nield: *Thermal instability in a porous medium layer saturated by a nanofluid: Brinkman model*. Transport in Porous Media *81* (2010), No. 1, 409–422.

[29] P. G. Siddheshwar, P. S. Titus: *Nonlinear Rayleigh-Bénard convection with variable heat source*. Journal of Heat Transfer *135* (2013), No. 12, 122502, Paper No: HT-13-1010.

[30] C. Sparrow: *The Lorenz equations: Bifurcations, chaos and strange attractors*. Springer-Verlag New York (1981).

Received October 12, 2017

Chapter 5

Thermoconvective instability in a rotating ferromagnetic fluid layer with temperature modulation

In this chapter, we study the thermoconvective instability in ferromagnetic fluid confined between two parallel infinite plates with temperature modulation at the walls. Analytical expressions for the Rayleigh number and the magnetic Rayleigh number are obtained. The heat transfer coefficient is analyzed in both in-phase and out-of-phase modulation. The bifurcation solutions for some values of the Rayleigh number are presented. In addition, streamlines and heat transfer coefficients for different Rayleigh numbers are presented.

Research Article

Precious Sibanda* and Osman Adam Ibrahim Noreldin

Thermo-convective instability in a rotating ferromagnetic fluid layer with temperature modulation

https://doi.org/10.1515/phys-2018-0109
Received Dec 18, 2017; accepted Sep 27, 2018

Abstract: We study the thermoconvective instability in a rotating ferromagnetic fluid confined between two parallel infinite plates with temperature modulation at the boundaries. We use weakly nonlinear stability theory to analyze the stationary convection in terms of critical Rayleigh numbers. The influence of parameters such as the Taylor number, the ratio of the magnetic force to the buoyancy force and the magnetization on the flow behaviour and structure are investigated. The heat transfer coefficient is analyzed for both the in-phase and the out-of-phase modulations. A truncated Fourier series is used to obtain a set of ordinary differential equations for the time evolution of the amplitude of convection for the ferromagnetic fluid flow. The system of differential equations is solved using a recent multi-domain spectral collocation method that has not been fully tested on such systems before. The solutions sets are presented as sets of trajectories in the phase plane. For some supercritical values of the Rayleigh number, spiralling trajectories that transition to chaotic solutions are obtained. Additional results are presented in terms of streamlines and isotherms for various Rayleigh numbers.

Keywords: Thermal instability, Ferromagnetic Fluids, Weakly nonlinear stability, Rotation, Multi-domain spectral collocation method

PACS: 47.11.Kb; 47.20.Bp

1 Introduction

Ferromagnetic fluids are colloids consisting of nanometer-sized magnetic particles suspended in a fluid carrier. The magnetization of a ferromagnetic fluid depends on the temperature, the magnetic field, and the density of the fluid. The magnetic force and the thermal state of the fluid may give rise to convection currents. Studies on the flow of ferromagnetic fluids include, for example, Finalyson [1] who studied instabilities in a ferromagnetic fluid using free-free and rigid-rigid boundaries conditions. He used the linear stability theory to predict the critical Rayleigh number for the onset of instability when both a magnetic and a buoyancy force are present. The generalization of Rayleigh Benard convection under various assumption is reported by Chandrasekhar [2]. In the last few decades the study of heat transfer in ferromagnetic fluids has attracted many researchers due to the potential application of these fluids in industry, such as in the sealing of rotating shafts, ink, and so on. An authoritative introduction to research on magnetic fluids is given by Rosensweig [3].

Schwab *et al.* [4] studied the Finlayson problem experimentally in the case of a strong magnetic field and determined the parameters for the onset of convection. Their results were shown to be in good agreement with those of Finlayson [1]. Stiles and Kagan [5] extended the experimental problem reported by Schwab *et al.* [4] by introducing a strong magnetic field. A weakly nonlinear stability analysis was used by Russell *et al.* [6] for magnetized ferrofluids heated from above with the Rayleigh number as the control parameter for the onset of convection. They showed that heat transfer depends on the temperature difference between the bounding surfaces.

The rotation of fluids is an interesting topic that has been studied by, for example, Greenspan [7]. The classical Rayleigh-Benard problem when the fluid layer is rotating is well known in the case of ordinary viscous fluids and has been reported by Chandrasekhar [2]. However, ferromagnetic fluids are known to exhibit very peculiar characteristics when set to rotate. Demonstrating the effect of

***Corresponding Author: Precious Sibanda:** School of Mathematics, Statistics and Computer Science, University of KwaZulu-Natal, Private Bag X01, Scottsville, Pietermaritzburg 3209, South Africa; Email: sibandaP@ukzn.ac.za
Osman Adam Ibrahim Noreldin: School of Mathematics, Statistics and Computer Science, University of KwaZulu-Natal, Private Bag X01, Scottsville, Pietermaritzburg 3209, South Africa; Email: noreldino@ukzn.ac.za

rotation on convection in ferromagnetic fluids is scientifically important to researchers. Gupta and Gupta [8] examined the onset of convection in a ferromagnetic fluid heated from below and rotating about a vertical axis subject to a uniform magnetic field. They concluded that overstability may not occur for Prandtl numbers smaller than unity. The thermo-convective instability in a rotating ferrofluid was further analyzed by Venkatasubramanian and Kaloni [9]. They presented both analytical and numerical results for free and rigid boundary conditions. Their results were in good agreement with those of Finlayson [1] and Chandrasekhar [2] for some limiting cases. Thermoconvection in a ferromagnetic fluid has been studied by other researchers, for instance, [10, 12].

The problem associated with convection in ferromagnetic fluids is both relevant and mathematically challenging. The unmodulated Rayleigh Benard problem of a ferromagnetic fluid has been extensively studied. The effect of a magnetic modulation on the stability of a magnetic liquid layer heated from above was studied by Aniss *et al.* [13]. They used the Floquet theory for their study of the onset of convection. The study showed the possibility of a competitive interaction between harmonic and subharmonic modes at the onset of convection. Convective instability in a ferromagnetic fluid layer with time-periodic modulation in the temperature field was investigated by Singh and Bajaj [14] using the linear stability theory and the classical Floquet theory. Their result agrees with those of Aniss *et al.* [13].

Convection in a rotating horizontal fluid layer confined in a porous medium with temperature modulation at the boundary was studied by Bhadauria [19]. He investigated the stability of the flow using the Galerkin method and the Flouquet theory. In this study we analyze thermoconvective instability in a rotating ferromagnetic fluid layer with time periodic temperature boundary conditions. The fluid layer is heated from below and rotates about the vertical axis subject to a uniform magnetic field. We assume two stress free and two rigid boundary conditions. The Ginzburg Landau equation is obtained, see [20] for details on the relevance of the Ginzburg Landau equation. Nonlinear ordinary differential equations of the Lorenz type are obtained and solved numerically using the multidomain spectral collocation method [16–18]. This method has not been fully tested before on evolution equations of this nature, hence the accuracy of solutions obtained using this method is also a matter of concern in this study. Heat transfer in the rotating horizontal fluid layer is discussed.

2 Mathematical formulation

Consider a ferromagnetic fluid confined between two infinite horizontal plates at $z = -h/2$ and $z = h/2$. The layer is heated from below and cooled from above, and is rotating uniformly about the vertical axis with constant angular velocity Ω. The lower and upper plates are subjected to an oscillatory temperature $T_0 + \Delta T[1 + \epsilon^2 \cos(\omega t + \varphi)]$ where ω is the modulation frequency and φ is the phase angle. The Oberbeck-Boussinesq approximation is assumed to be applicable. The magnetization $\mathbf{M}$ of the ferrofluid is assumed to be parallel to the magnetic field $\mathbf{H}$. The equations describing the fluid motion under these assumptions are the continuity equation, modified momentum equation, energy equation and Maxwell's equations (Finlayson [1] and Gupta and Gupta [8]):

$$\nabla \cdot V = 0, \tag{1}$$

$$\rho_0 \frac{DV}{Dt} = -\nabla P' + \mu \nabla^2 V + \rho \mathbf{g}$$

$$+ \nabla \cdot (\mathbf{HB}) + 2\rho_0 V \times \Omega) + \frac{\rho_0}{2} \nabla(|\Omega \times \mathbf{r}|), \tag{2}$$

$$\left[\rho_0 C_{V.H} - \mu_0 \mathbf{H} \cdot \left(\frac{\partial \mathbf{M}}{\partial T}\right)_{V,H}\right] \frac{DT}{Dt}$$

$$+\mu_0 T \left(\frac{\partial \mathbf{M}}{\partial T}\right)_{V,H} \cdot \frac{D\mathbf{H}}{Dt} = \kappa \nabla^2 T + \Phi, \tag{3}$$

$$\nabla \cdot \mathbf{B} = 0; \quad \nabla \times \mathbf{H} = 0, \tag{4}$$

where V is the velocity field, ρ_0 is the density at the ambient temperature, $P' = P + \frac{\mu_0}{2}\mathbf{H}^2$ is the pressure, μ is the viscosity, $\mathbf{g}$ is the gravitational body force, $\mathbf{B}$ is the magnetic induction, μ_0 is the magnetic permeability, T is the temperature, κ is the thermal conductivity, $C_{V,H}$ is the heat capacity at constant volume and magnetic field, α is the thermal expansion coefficient and Φ is the viscous dissipation. The magnetization and magnetic field are related by the formula

$$\mathbf{B} = \mu_0(\mathbf{H} + \mathbf{M}). \tag{5}$$

The magnetization is dependent on the temperature and magnitude of magnetic field, so that

$$\mathbf{M} = \frac{\mathbf{H}}{H}\mathbf{M}(H, T). \tag{6}$$

Equation (6) is linearized using the Taylor expansion

$$\mathbf{M} = \mathbf{M_0} + \chi(\mathbf{H} - \mathbf{H_0}) - K(T - T_1), \tag{7}$$

where $\chi \equiv (\partial \mathbf{M}/\partial \mathbf{H})_{H_0,T_1}$ is the magnetic susceptibility and $K \equiv -(\partial \mathbf{M}/\partial T)_{H_0,T_1}$ is pryomagnetic coefficient, H_0 is the uniform magnetic field and $T_1 = (T_\infty + T_0)/2$, T_∞ and T_0 are the temperatures at $h/2$ and $-h/2$, respectively. The study is restricted to the case when magnetization induced by the temperature variation is much smaller than that induced by the external magnetic field. The density varies linearly with temperature as

$$\rho = \rho_0(1 - \alpha(T - T_1)). \tag{8}$$

3 Weakly nonlinear stability

In this section we use weakly nonlinear stability analysis to study the evolution of disturbances in a ferromagnetic fluid with two free and two rigid boundary conditions and temperature modulation. Using Eqs. (4) and (5) and assuming that the magnetic field $\mathbf{H}$ is collinear with the magnetic induction $\mathbf{B}$, Eq. (2) reduces to

$$\rho_0 \frac{DV}{Dt} = -\nabla P + \mu \nabla^2 V + \rho \mathbf{g} + \mu_0 \mathbf{M} \cdot \nabla \mathbf{H} + 2\rho_0 V \times \Omega) + \frac{\rho_0}{2} \nabla(|\Omega \times \mathbf{r}|). \tag{9}$$

The basic state solution of Eqs. (1)–(4) with (9) is obtained as

$$V = 0, \tag{10}$$
$$T_b(z,t) = T_1 + \frac{\Delta T}{2} - \beta z + \epsilon^2 (F(z,t)),$$

where

$$F(z,t) = Re\left\{ \frac{\Delta T}{\sinh \lambda} \left[e^{i\varphi} \sinh \lambda(1/2 - z/h) + \sinh \lambda(1/2 - z/h) \right] e^{i\omega t} \right\},$$
$$\lambda^2 = i\omega \rho_0 C h^2/\kappa, \quad \beta = \frac{\Delta T}{h}.$$

Following [1, 3] we define

$$\mathbf{M}_b + \mathbf{H}_b = \text{ constant}, \tag{11}$$

and

$$\mathbf{H}_b = \left(\mathbf{H}_0 - \frac{K(T_b - T_1))}{1+\chi} \right) \hat{e}_z, \tag{12}$$
$$\mathbf{M}_b = \left(\mathbf{M}_0 + \frac{K(T_b - T_1))}{1+\chi} \right) \hat{e}_z.$$

We superimpose small perturbations on the basic state. The perturbed quantities are defined as

$$T = T_b + T', \quad \mathbf{H}_i = \mathbf{H}'_i, \quad \mathbf{M}_i = \mathbf{M}'_i \text{ for i =1,2;} \tag{13}$$
$$\mathbf{H}_3 = \mathbf{H}_b + \mathbf{H}'_3, \quad \mathbf{M}_3 = \mathbf{M}_b + \mathbf{M}'_3,$$

where the prime represents a perturbed quantity. The linearization of Eqs. (6) and (7) gives

$$\mathbf{H}'_i + \mathbf{M}'_i = \left(1 + \frac{\mathbf{M}_0}{\mathbf{H}_0}\right) \mathbf{H}'_i, \quad i = 1, 2. \tag{14}$$

$$\mathbf{H}'_3 + \mathbf{M}'_3 = (1+\chi)\mathbf{H}' - KT'. \tag{15}$$

We assume that $K\Delta T << (1+\chi)\mathbf{H}_0$. For more details see [1]. Substituting Eq. (13) and using the curl operator on Eq. (9) we obtain the vorticity equation

$$\rho_0 \frac{\partial \zeta'}{\partial t} = \mu \nabla^2 \zeta' + \rho_0 \Omega \frac{\partial w'}{\partial z}. \tag{16}$$

Substituting Eqs. (12), (14) and (15) in Eq. (9) and using $\mathbf{H}' = \nabla \phi'$ where ϕ is the magnetic potential, the z–component of the resulting equation can be written as,

$$\rho_0 \frac{\partial}{\partial t} \nabla^2 w' - \mu \nabla^4 w' = \rho_0 g \alpha \nabla_l^2 T' + \frac{\mu_0 K^2 \beta}{1+\chi} \nabla_l^2 T' - \mu_0 K \beta \frac{\partial}{\partial z} \nabla_l^2 \phi' - 2\rho_0 \Omega \frac{\partial \zeta'}{\partial z}. \tag{17}$$

On using Eq. (13) in Eq. (3) and linearizing we obtain

$$\rho_0 C \frac{\partial T'}{\partial t} + \rho_0 C w' \frac{\partial T'}{\partial z} - \mu_0 T_0 K \left(\frac{\partial}{\partial t} \left(\frac{\partial \phi'}{\partial z} \right) + w' \frac{\partial^2 \phi'}{\partial z^2} \right) + \left(\rho_0 C \beta - \frac{\mu_0 T_0 K^2 \beta}{1+\chi} \right) \left(-1 + \epsilon \frac{\partial F}{\partial z} \right) w = \nabla^2 T'. \tag{18}$$

Finally, substituting Eqs. (14) and (15) into Eq. (4) we have

$$(1+\chi) \frac{\partial^2 \phi'}{\partial z^2} - \left(1 + \frac{\mathbf{M}_0}{\mathbf{H}_0}\right) \nabla_l^2 \phi' - K \frac{\partial T'}{\partial z} = 0, \tag{19}$$

where $\rho_o C = \rho_0 C_{V,H} + \mu_0 K \mathbf{H}_0$ and $\nabla_l^2 = \partial^2/\partial x^2 + \partial^2/\partial y^2$ is the Laplace operator in two dimension. For the clarity we drop the prime from the perturbed quantities and introduce the following dimensionless variables

$$(x^\star, y^\star, z^\star) = (x, y, x)/h, \; w^\star = w'h/\nu, \quad t^\star = \mu t/\rho_0 h^2, \quad \zeta^\star = \zeta' h^2/\nu, \quad \theta^\star = (\kappa R a^{\frac{1}{2}} T')/(\rho_0 C \beta \nu h), \quad \phi^\star = ((1+\chi)\kappa R a^{\frac{1}{2}} \phi')/(\rho_0 C \beta \nu h^2). \tag{20}$$

The linearized perturbed Eqs. (16)–(19) in the dimensionless form can be written as,

$$\frac{\partial}{\partial t^\star} \nabla^2 w^\star - \nabla^4 w^\star + T a^{\frac{1}{2}} \frac{\partial \zeta^\star}{\partial z} \tag{21}$$

$$-Ra^{\frac{1}{2}}(1+M_1)\nabla_l^2\theta^\star + Ra^{\frac{1}{2}}M_1\frac{\partial}{\partial z}\nabla_l^2\phi^\star = 0,$$

$$-Ta^{\frac{1}{2}}\frac{\partial w^\star}{\partial z^\star} + \frac{\partial \zeta^\star}{\partial t^\star} - \nabla^2\zeta^\star = 0, \tag{22}$$

$$\left(Ra^{\frac{1}{2}} - Ra^{\frac{1}{2}}M_2\right)\left(-1+\epsilon^2\frac{\partial F}{\partial z^\star}\right)w^\star + Pr\frac{\partial\theta^\star}{\partial t^\star} \tag{23}$$
$$+ Prw^\star\frac{\partial\theta^\star}{\partial z^\star} - \nabla^2\theta^\star - PrM_2\frac{\partial}{\partial t^\star}\left(\frac{\partial\phi^\star}{\partial z^\star}\right)$$
$$- PrM_2w^\star\frac{\partial^2\phi^\star}{\partial z^{\star 2}} = 0,$$

$$-\frac{\partial\theta^\star}{\partial z^\star} + \frac{\partial^2\phi^\star}{\partial z^2} + M_3\nabla_l^2\phi^\star = 0, \tag{24}$$

where $Ta = \frac{4\Omega h^4}{\nu^2}$ is the Taylor number, $Ra = \frac{\rho_0 C\beta\alpha g h^4}{\nu\kappa}$ is the Rayleigh number, $M_1 = \frac{\mu_0 K^2\beta}{(1+\chi)\rho_0\alpha g}$ is the ratio of the magnetic force to the buoyancy force, $M_2 = \frac{\mu_0 T_0 K^2}{(1+\chi)\rho_0 C}$ is a nondimensional parameter, $Pr = \frac{\mu C}{\kappa}$ is the Prandtl number and $M_3 = (1+\frac{\mathbf{M}_0}{\mathbf{H}_0})/(1+\chi)$ is a measure of nonlinearity of the magnetization. The magnetic Rayleigh number can be obtained from the formula $N = RaM_1$. Hereafter the asterisk will be dropped from Eqs. (21)-(24).

The associated boundary conditions for the system of Eqs. (21)-(24) are

– Free boundary conditions

$$w = 0,\ D^2w = 0,\ D\zeta = 0,\ \theta = 0,\ D\phi = 0, \quad \text{at } z = \pm\frac{1}{2}. \tag{25}$$

– Rigid boundary conditions

$$w = 0,\ Dw = 0,\ \zeta = 0,\ \theta = 0, \quad \text{at } z = \pm\frac{1}{2}, \tag{26}$$

where

$$D = \partial/\partial z.$$

3.1 The solution for stress free boundaries

The solution for stress free boundaries has been discussed in [1, 3, 9]. Here we only emphasize the solution aspects which have not been discussed before. We solve the eigenvalue problem with two stress free boundaries to study the onset of instability in the ferromagnetic fluid. We consider a small variation in time scale $\tau = \epsilon^2 t$ such that stationary convection occurs at lower orders of ϵ and introduce the following asymptotic expansions

$$Ra^{\frac{1}{2}} = (Ra^\alpha)^{\frac{1}{2}} + \epsilon^2 Ra_2^{\frac{1}{2}} + \epsilon^4 Ra_4^{\frac{1}{2}} + \cdots, \tag{27}$$

$$w = \epsilon w_1 + \epsilon^2 w_2 + \epsilon^3 w_3 + \cdots, \tag{28}$$

$$\zeta = \epsilon\zeta_1 + \epsilon^2\zeta_2 + \epsilon^3\zeta_3 + \cdots, \tag{29}$$

$$\theta = \epsilon\theta_1 + \epsilon^2\theta_2 + \epsilon^3\theta_3 + \cdots, \tag{30}$$

$$\phi = \epsilon\phi_1 + \epsilon^2\phi_2 + \epsilon^3\phi_3 + \cdots. \tag{31}$$

Substituting Eqs. (27)–(31) into Eqs. (21)–(24), at the lowest order of ϵ we obtain

$$BZ_1 = R_1, \tag{32}$$

where

$$B = \begin{pmatrix} -\nabla^4 & \sqrt{Ta}\frac{\partial}{\partial z} & -\sqrt{Ra^\alpha}(1+M_1)\nabla_l^2 & \sqrt{Ra^\alpha}M_1\frac{\partial}{\partial z}\nabla_l^2 \\ -\sqrt{Ta}\frac{\partial}{\partial z} & -\nabla^2 & 0 & 0 \\ -\sqrt{Ra^\alpha}(1-M_2) & 0 & -\nabla^2 & 0 \\ 0 & 0 & -\frac{\partial}{\partial z} & \frac{\partial^2}{\partial z^2} + M_3\nabla_l^2 \end{pmatrix},$$

$Z_1 = \begin{pmatrix} w_1 \\ \zeta_1 \\ \theta_1 \\ \phi_1 \end{pmatrix}$ and $R_1 = \begin{pmatrix} 0 \\ 0 \\ 0 \\ 0 \end{pmatrix}$. This equation corresponds to the linear equations in [1, 9]. Solving Eq. (32) we obtain the solution

$$w_1 = A(\tau)\sin ax\cos\pi z, \tag{33}$$

$$\zeta_1 = -\frac{Ta^{\frac{1}{2}}\pi}{\pi^2+a^2}A(\tau)\sin ax\sin\pi z, \tag{34}$$

$$\theta_1 = \frac{(Ra^\alpha)^{\frac{1}{2}}(1-M_2)}{\pi^2+a^2}A(\tau)\sin ax\cos\pi z, \tag{35}$$

$$\phi_1 = -\left(\frac{(Ra^\alpha)^{\frac{1}{2}}(1-M_2)\pi}{(\pi^2+a^2)(\pi^2+a^2M_3)}\right) A(\tau)\sin ax\sin\pi z, \tag{36}$$

where a is a dimensionless wave number. Thus, the stationary Rayleigh number is given as

$$Ra^\alpha = \frac{((\pi^2+a^2)^3+\pi^2 Ta)(\pi^2+a^2M_3)}{(1-M2)(a^2\pi^2M_1 + a^2(M_1+1)(\pi^2+a^2M_3))}. \tag{37}$$

To find the critical wave number and the corresponding critical Rayleigh number we set $a^2 = \pi^2 x$. Then the stationary Rayleigh number can be written as

$$Ra^\alpha = \frac{(\pi^4(1+x)^3+Ta)(1+xM_3)}{(1-M2)x(1+xM_3(M_1+1))}. \tag{38}$$

This result agrees with [1, 3, 9]. Since M_2 is very small as indicated in [1, 9] it can be neglected in the subsequent analysis.

The critical wave number and the corresponding critical Rayleigh number are obtained from

$$\frac{\partial Ra^{\alpha}}{\partial x} = 0,$$

then we have

$$\begin{aligned} &- Ta - 2Ta\,(xM_3 + xM_1M_3) \\ &- Ta\left(x^2M_3^2 + x^2M_1M_3^2\right) \\ &+ \pi^4\,(1+x)^2\left(-1 + 2x - 2xM_3 - 2xM_1M_3 - 4x^2M_3\right. \\ &\left. + x^2M_3^2M_1 + 2x^3M_3^2 + 2x^3M_1M_3^2\right) = 0. \end{aligned} \tag{39}$$

For the case $Ta = 0, M_1 = 0$ and $M_3 = 0$, the classical critical wave number is

$$a_c = \frac{\pi}{\sqrt{2}}$$

with corresponding classical critical Rayleigh number

$$Ra_c^{\alpha} = \frac{27}{4}\pi^4.$$

The magnetic Rayleigh number is also of an interest and can be expressed as

$$N^{\alpha} = Ra^{\alpha}M_1 = \frac{(\pi^4(1+x)^3 + Ta)M_1(1+xM_3)}{x(1+xM_3(M_1+1))}. \tag{40}$$

For large values of M_1 the magnetic Rayleigh number in the absence of buoyancy effects is obtained as

$$N^{\alpha} = \frac{(\pi^4(1+x)^3 + Ta)(1+xM_3)}{x^2M_3}. \tag{41}$$

The critical wave number and corresponding critical magnetic Rayleigh number are obtained from solving the equation

$$-2Ta + M3x + \pi^4(1+x)^2(-2+x-M3x+2M3x^2) = 0. \tag{42}$$

The critical wave number and corresponding Rayleigh numbers are given for different values of the Taylor number Ta in Tables 1 and 2.

At second order $O(\epsilon^2)$ we obtain the following equations:

$$BZ_2 = R_2 \tag{43}$$

where $Z_2 = \begin{pmatrix} w_2 \\ \zeta_2 \\ \theta_2 \\ \phi_2 \end{pmatrix}$ and $R_2 = \begin{pmatrix} R_{21} \\ R_{22} \\ R_{23} \\ R_{24} \end{pmatrix}$ with

$$R_{21} = 0, \quad R_{22} = 0, \quad R_{24} = 0, \tag{44}$$

Table 1: Comparison of the critical wave number and corresponding Rayleigh number for $M_1 = 1$ and $M_3 = 5$.

	Present study		**Ref** [9]	
Ta	a_c	Ra_c^{α}	a_c	Ra_c^{α}
1	2.11212	269.6382	2.7348	461.5368
10	2.15849	275.0998	3.7827	883.4022
100	2.49953	322.9328	5.7215	2727.2022
1000	3.65242	608.4028	8.6174	10619.856
10000	5.66466	1862.582	12.8255	45606.430

Table 2: Comparison of the critical wave number and corresponding Magnetic Rayleigh number for $M_1 \to \infty$ and $M_3 = 3$.

	Present study		**Ref** [9]	
Ta	a_c	N_c^{α}	a_c	N_c^{α}
1	2.6084	880.7959	2.7348	1037.8896
10	2.62069	897.4541	3.8770	1885.6592
100	2.72574	1050.072	5.7736	5617.3574
1000	3.2225	2083.258	8.6487	21520.978
10000	4.28305	7315.093	12.8455	91759.273

$$R_{23} = -\frac{Pr\pi(Ra^{\alpha})^{\frac{1}{2}}}{2(\pi^2+a^2)}A^2(\tau)\sin^2 ax \sin 2\pi z.$$

The solution at the second order is

$$w_2 = 0, \quad \zeta_2 = 0, \tag{45}$$

$$\theta_2 = -\left(\frac{Pr\pi(Ra^{\alpha})^{\frac{1}{2}}}{4(\pi^2+a^2)(2\pi^2+a^2)}\right) A^2(\tau)\sin^2 ax \sin 2\pi z, \tag{46}$$

$$\phi_2 = -\left(\frac{Pr\pi^2(Ra^{\alpha})^{\frac{1}{2}}}{4(2\pi^2+a^2)(\pi^2+a^2)(2\pi^2+a^2M_3)}\right) A^2(\tau)\sin^2 ax \cos 2\pi z. \tag{47}$$

At the third order, we obtain

$$BZ_3 = R_3, \tag{48}$$

where $Z_3 = \begin{pmatrix} w_3 \\ \zeta_3 \\ \theta_3 \\ \phi_3 \end{pmatrix}$ and $R_2 = \begin{pmatrix} R_{31} \\ R_{32} \\ R_{33} \\ R_{34} \end{pmatrix}$ with

$$R_{31} = \left\{ -\gamma^2\frac{dA}{d\tau} + \frac{a^2(Ra^{\alpha})^{\frac{1}{2}}R_{a2}^{\frac{1}{2}}(1+M_1)}{\gamma^2(\pi^2+a^2M_3)} ((1+M_1)\pi^2 + a^2M_3)A(\tau)\right\} \sin ax \cos \pi z, \tag{49}$$

$$R_{32} = -\frac{Ta^{\frac{1}{2}}\pi^2}{\gamma^2}\frac{dA}{d\tau}\sin ax \sin \pi z, \tag{50}$$

$$R_{33} = -\Bigg(\Big((Ra^{\alpha})^{\frac{1}{2}}\frac{\partial F}{\partial z} - Ra_2^{\frac{1}{2}}\Big)A(\tau) + \frac{Pr(Ra^{\alpha})^{\frac{1}{2}}}{\gamma^2}\frac{dA}{d\tau}\Bigg)\sin ax\cos \pi z + \frac{Pr^2\pi^2(Ra^{\alpha})^{\frac{1}{2}}}{2\gamma^2(2\pi^2+a^2)} A^3(\tau)\sin^3 ax\cos \pi z\cos 2\pi z, \tag{51}$$

$$R_{34} = 0. \tag{52}$$

Here, $\gamma^2 = a^2 + \pi^2$. To obtain the Ginzburg Landau equation we applied the Fredholm solvability condition [11, 18]

$$\int_0^{\frac{1}{2}}\int_0^{\frac{2\pi}{a}}\Big[\hat{w}_1 R_{31} + \hat{\zeta}_1 R_{32} + \hat{\theta} R_{33}\Big]dxdz = 0, \tag{53}$$

where $\hat{w}_1$, $\hat{\zeta}_1$ and $\hat{\theta}_1$ are the solutions of the adjoint system of the first order. This gives

$$\Big[\frac{\pi\gamma^2}{4a} + \frac{PrRa^{\alpha}\pi}{4a\gamma^4} - \frac{Ta\pi^4}{4a\gamma^4}\Big]\frac{dA}{d\tau} = \Big\{\frac{\pi Ra^{\alpha\frac{1}{2}}Ra_2^{\frac{1}{2}}}{4a\gamma^2} - \frac{\pi Ra^{\alpha}}{a\gamma^2}\mathbf{I} + \frac{a\pi Ra^{\alpha\frac{1}{2}}Ra_2^{\frac{1}{2}}(1+M_1)}{4\gamma^2(\pi^2+a^2M_3)} \Big((1+M_1)\pi^2 + a^2M_3\Big)\Big\}A - \frac{3Pr^2\pi^3Ra^{\alpha}}{64a\gamma^4(2\pi^2+a^2)}A^3. \tag{54}$$

The above equation reduces to

$$\frac{dA}{d\tau} = \Delta_1 A - \Delta_2 A^3, \tag{55}$$

where $\Delta_1 = \gamma^2/(\gamma^6 + PrRa^{\alpha} - Ta\pi^3)$ $\Big(Ra^{\star} - 4Ra^{\alpha}\mathbf{I} + \frac{a^2Ra^{\star}(1+M_1)((1+M_1)\pi^2+a^2M_3)}{\pi^2+a^2M_3}\Big)$, $Ra^{\star} = Ra^{\alpha\frac{1}{2}}Ra_2^{\frac{1}{2}}$, $\Delta_2 = 3\,\mathrm{Pr}^2\,\pi^3 Ra^{\alpha}/\left(16\left(2\pi^2+a^2\right)\right)$, and

$$\mathbf{I} = \int_0^{\frac{1}{2}}\frac{dF}{dz}\cos^2(\pi z)dz.$$

In this study we are also interested in heat transfer in ferromagnetic fluids. The Nusselt number for ferromagnetic fluids is defined as

$$Nu(\tau) = \frac{\text{Heat transfer by conduction+convection}}{\text{Heat transfer by conduction}} = 1 + \frac{Pr\pi^2(Ra^{\alpha})^{\frac{1}{2}}}{4\gamma^2(2\pi^2+a^2)}A^2(\tau). \tag{56}$$

3.2 The general Lorentz type equations

We restrict the analysis to the case of two-dimensional disturbances so that all physical quantities are independent of y. Using the stream function defined by

$$u = \frac{\partial\psi}{\partial z} \text{ and } w = -\frac{\partial\psi}{\partial x}$$

equations (1)–(4) reduce to

$$\frac{\partial}{\partial t}\nabla_L^2\psi - |\mathcal{J}(\psi,\nabla_L^2\psi)| = \nabla_L^4\psi - M_1Ra^{\alpha\frac{1}{2}}\frac{\partial^2\phi}{\partial x\partial z} - Ra^{\alpha\frac{1}{2}}(1+M_1)\frac{\partial\theta}{\partial x} + Ta^{\frac{1}{2}}\frac{\partial\zeta}{\partial z}, \tag{57}$$

$$\frac{\partial\zeta}{\partial t} + |\mathcal{J}(\psi,\zeta)| = \nabla_L^2\zeta - Ta^{\frac{1}{2}}\frac{\partial\psi}{\partial z}, \tag{58}$$

$$Pr\left(\frac{\partial\theta}{\partial t} + |\mathcal{J}(\psi,\theta)|\right) = \nabla_L^2\theta - Ra^{\alpha\frac{1}{2}}\frac{\partial\psi}{\partial x}, \tag{59}$$

$$\frac{\partial^2\phi}{\partial z^2} + M_3\frac{\partial^2\phi}{\partial x^2} = \frac{\partial\theta}{\partial z}, \tag{60}$$

where $\mathcal{J}$ is the Jacobian matrix. The solution of Eqs. (57)–(60) represented as a minimal double Fourier series of modes (1,1) for the stream function and magnetic potential and modes (0,2) and (1,1) for temperature and vorticity of the finite amplitude convection of the ferromagnetic fluid flows as

$$\psi =_{11} \sin ax\sin \pi z, \tag{61}$$

$$\theta = B_{11}\cos ax\sin \pi z + B_{02}\sin 2\pi z, \tag{62}$$

$$\zeta = C_{11}\sin ax\cos \pi z + C_{02}\sin 2\pi z, \tag{63}$$

$$\phi = D_{11}\cos ax\cos \pi z, \tag{64}$$

where $A_{11}, B_{11}, B_{02}, C_{11}, C_{02}$ and D_{11} are time t dependent amplitudes. This is equivalent to a truncated Galerkin method. Substituting and integrating over the domain, we obtain a set of four ordinary differential equations for the time evolution of the amplitudes of convection of a ferromagnetic fluid in the form

$$\frac{dA_{11}}{dt} = -\gamma^2A_{11} - \frac{a\pi Ra^{\alpha\frac{1}{2}}}{\gamma^2(\pi^2+a_3^M)}B_{11} - \frac{aRa^{\alpha\frac{1}{2}}(1+M_1)}{\gamma^2}B_{11} + \frac{\pi Ta^{\frac{1}{2}}}{\gamma^2}C_{11}, \tag{65}$$

$$\frac{dC_{11}}{dt} = -\gamma^2 - \pi Ta^{\frac{1}{2}}A_{11}, \tag{66}$$

$$\frac{dB_{11}}{dt} = \frac{aRa^{\alpha\frac{1}{2}}}{Pr}A_{11} - \frac{\gamma^2}{Pr}B_{11} - a\pi A_{11}B_{02}, \tag{67}$$

$$\frac{dB_{02}}{dt} = \frac{a\pi}{2}A_{11}B_{11} - \frac{4\pi^2}{Pr}B_{02}. \tag{68}$$

To simplify the equations we introduce new variables

$$X_1 = \frac{a\pi}{\gamma^2}A_{11},\ X_2 = \frac{-a^2\pi Ra^{\alpha\frac{1}{2}}}{\gamma^6}B_{11},\ \tau = \gamma^2 t, \tag{69}$$

$$X_3 = \frac{-a^2\pi Ra^{\alpha\frac{1}{2}}}{\gamma^6}B_{02} \text{ and } X_4 = \frac{a\pi^2 Ta^{\frac{1}{2}}}{\gamma^6}C_{11}. \tag{70}$$

This reduces Eqs. (65)-(68) to general Lorentz type equations

$$\frac{dX_1}{d\tau} = -X_1 + KX_2 + X_4, \tag{71}$$

$$\frac{dX_2}{d\tau} = RX_1 - Pr^{-1}X_2 - X_1X_3, \tag{72}$$

$$\frac{dX_3}{d\tau} = \frac{1}{2}X_1X_2 - bPr^{-1}X_3, \tag{73}$$

$$\frac{dX_4}{d\tau} = -TaX_1 - X_4, \tag{74}$$

where $R = \frac{a^2}{\gamma^6}Ra^{\alpha}$, $b = \frac{4\pi^2}{\gamma^2}$,
and $K = \frac{(2\pi^2+a^2M_3)+M_1(\pi^2+a^2M_3)}{\pi^2+a^2M_3}$.

3.3 Stability of Lorentz equations

In this section we discuss the stability of the nonlinear systems of differential equations that describe the evolution of the convection amplitudes for a ferromagnetic fluid flow. Firstly, we note that the nonlinear Eqs. (71)–(74) are invariant under the transformation

$$S(X_1, X_2, X_3, X_4) = (-X_1, -X_2, -X_3, -X_4). \tag{75}$$

These equations are also uniformly bounded and dissipative in the phase space

$$\sum_{i=1}^{4}\frac{\partial \dot{X}_i}{X_i} = -\left[1 + Pr^{-1} + bPr^{-1}\right] < 0 \tag{76}$$

Thus the volume of the phase space moving with the flow for time $\tau > 0$ is given by

$$V(t) = V(0)\exp\left(-\left[1 + Pr^{-1} + bPr^{-1}\right]\tau\right). \tag{77}$$

We find that the stationary points of the system of nonlinear Eqs. (71)–(74) are:

– The motionless conduction solutions (0, 0, 0, 0).

– The steady solution represented by the point

$$(x_1^\star, x_2^\star, x_3^\star, x_4^\star) = \left(\pm\sqrt{\frac{2b(PrKR-(Ta+1))}{Pr^2(1+Ta)}}, \pm\frac{Ta+1}{K}\sqrt{\frac{2b(PrKR-(Ta+1))}{Pr^2(Ta+1)}}, \frac{kPrR-(Ta+1)}{kPr}, \mp\sqrt{\frac{2b(PrKR-(Ta+1))}{Ta^2Pr^2(1+Ta)}}\right).$$

The stability of the stationary point associated with the motionless solution $X^\star = (0, 0, 0, 0)$ is determined by roots of the following characteristic polynomial equation

$$P(\xi) = \xi^3 + d_1\xi^2 + d_2\xi + d_3 = 0, \tag{78}$$

where

$$d_1 = Pr^{-1},\quad d_2 = Ta - 1 - KR$$

and

$$d_3 = \frac{Ta - PrKR - 1}{Pr}$$

for the eigenvalues ξ_i, $(i = 2, 3, 4)$ and $\xi_1 = -\frac{b}{Pr}$. It is clear that ξ_1 is always negative as $Pr > 0$. The remaining eigenvalues are obtained from Eq. (78), and using the Routh-Hurwitz criteria [21], the polynomial Eq. (78) has negative real roots if and only if

$$R < \frac{Ta-1}{KPr}$$

and $Pr > 1$. This implies that the stationary solution is a stable node. Hence the critical value of R where the stationary solution of ferromagnetic fluid flow loses stability and steady convective flow takes over is

$$R = \frac{Ta-1}{KPr}.$$

The stability of the stationary point corresponding to the steady convective flow is determined by the roots of the characteristic equation

$$p(\xi) = \xi^4 + c_1\xi^3 + c_2\xi^2 + c_3\xi + c_4 = 0, \tag{79}$$

where

$$\begin{aligned}
c_1 &= 2Pr + 2bPr,\\
c_2 &= 2b - 2Pr^2 - 2KPr^2R + 2Pr^2Ta\\
&\quad + Pr^2x_1^{\star 2} + 2KPr^2x_3^\star,\\
c_3 &= -2Pr - 2bPr - 2bKPrR - 2KPr^2R + 2PrTa\\
&\quad + 2bPrTa + KPr^3x_1^\star x_2^\star + 2bKPrx_3^\star + 2KPr^2x_3^\star,\\
c_4 &= -2b - 2bKPrR + 2bTa - Pr^2x_1^{\star 2} + Pr^2Tax_1^{\star 2}\\
&\quad + KPr^2x_1^\star x_2^\star + 2bKPrx_3^\star.
\end{aligned}$$

Applying the Routh-Hurwitz criteria to Eq. (79), it is clear that $c_1 > 0$, and $c_3 > 0$ if and only if

$$Ta + 1 < PrKR$$

and

$$R < -\left(\frac{b+1}{bK+Pr}\right).$$

Also, $c_4 > 0$ if and only if

$$x_1^{\star 2} < -\left(\frac{2b(1+PrKR)}{Pr^2}\right)$$

with

$$Ta + 1 < PrKR.$$

Hence the fixed point is stable if the condition

$$\begin{aligned} &Pr^3 c_3^\star + Pr^2 c_2^\star + Prc_1^\star + c_0^\star \\ &> Pr^3 d_3^\star + Pr^2 d_2^\star + Prd_1^\star + d_0^\star, \end{aligned} \tag{80}$$

is satisfied where

$$\begin{aligned} c_3^\star &= \Big(8KR + 8K^2R^2 + 4KTax_1^\star x_2^\star \\ &\quad + 2Kx_1^{\star 3}x_2^\star + 4Kx_1^{\star 2}x_3^\star + 4K^2x_1^\star x_2^\star x_3^\star \\ &\quad + 8K^2x_3^{\star 2} + 8KTax_3^\star\Big)\Big(1+b\Big), \\ c_2^\star &= 8(KR+1) + 16b + 8b^2 + 8KR(3+2b) \\ &\quad + 8K^2R^2(b+1) + 8Ta^2(b^2+2b+1) \\ &\quad + 8KTax_3^\star(2b^2+3b+1) + (4Kx_1^{\star 2}x_3^\star \\ &\quad + 8K^2x_3^{\star 2})(b+b^2) + 4K^2R(x_1^{\star 2}x_2^\star + 2x_3^\star), \\ c_1^\star &= 8KR(b^3+b^2) + 4Kx_1^{\star 2}x_2^\star(2b+b^2) \\ &\quad + (8Kx_3^\star + 8KRTa + 4K^2Rx_1^{\star 2}x_2^\star)(1+b) \\ &\quad + 16bK^2Rx_3^\star, \quad c_0^\star = 8b + 4b^2 + 8Ta(b^2 \\ &\quad + 2b + 1) + 8Kx_3^\star(b^3 + 2b^2 + b) \\ &\quad + 8KRTa(b^2+b) + 8b^2K^2Rx_3^\star, \end{aligned}$$

and

$$\begin{aligned} d_3^\star &= \Big(8KRTa + 4KRx_1^{\star 2} + 4(K+K^2)x_1^{\star 2}x_2^\star \\ &\quad + 8Kx_3^\star + 16K^2Rx_3^\star\Big)\Big(1+b\Big), \\ d_2^\star &= \Big(16Ta + 4Kx_1^\star x_2^\star\Big)\Big(b^2+2b+1\Big) \\ &\quad + \Big(8KRTa + 8Kx_3^\star\Big)\Big(2b^2+3b+1\Big) \\ &\quad + 16K^2Rx_3^\star\Big(b^2+b\Big) + K^2(x_1^{\star 2}x_2^{\star 2} + 4x_1^\star x_2^\star x_3^\star + 4x_3^\star), \\ d_1^\star &= 8Kx_3^\star(b^3+b^2) + \big(\star KTax_3^\star + 4KTax_1^\star x_2^\star \\ &\quad + 8K^2R^2\big)(b+1) + 4bK^2(x_1^\star x_2^\star x_3^\star + 2x_3^{\star 2}), \\ d_0^\star &= 8KR(b^3+2b^2+b) + 4Ta(b^2+2b+1) \\ &\quad + 8KTax_3^\star(b^2+b) + 4b^2K^2x_3^{\star 2}. \end{aligned}$$

3.4 The method of solution

In this section, we describe the multi-domain spectral collocation method [15–18] used to obtain the solutions to Eqs. (71)–(74). The multi-domain technique assumes that the interval $\Lambda = [0, T]$ can be decomposed into p non overlapping sub-intervals. The sub-intervals are defined as

$$\Lambda_i = [\tau_{i-1}, \tau_i], \quad i = 1, 2, \cdots, p. \tag{81}$$

In each sub-interval, the system of Eqs. (71)–(74) is written in the form

$$\begin{aligned} &\dot{X}^i_{1,s+1} + \alpha_{1,1}X^i_{1,s+1} + \alpha_{1,2}X^i_{2,s} + \alpha_{1,3}X^i_{3,s} \\ &+ \alpha_{1,4}X^i_{4,s} + f_1(X^i_{2,s}, X^i_{3,s}, X^i_{4,s}) = g_1 \\ &\dot{X}^i_{2,s+1} + \alpha_{2,1}X^i_{1,s+1} + \alpha_{2,2}X^i_{2,s+1} + \alpha_{2,3}X^i_{3,s} \\ &+ \alpha_{2,4}X^i_{4,s} + f_2(X^i_{1,s+1}, X^i_{3,s}, X^i_{4,s}) = g_2 \\ &\dot{X}^i_{3,s+1} + \alpha_{3,1}X^i_{1,s+1} + \alpha_{3,2}X^i_{2,s+1} + \alpha_{3,3}X^i_{3,s+1} \\ &+ \alpha_{3,4}X^i_{4,s} + f_3(X^i_{1,s+1}, X^i_{2,s+1}, X^i_{4,s}) = g_3 \\ &\dot{X}^i_{4,s+1} + \alpha_{4,1}X^i_{1,s+1} + \alpha_{4,2}X^i_{2,s+1} + \alpha_{4,3}X^i_{3,s+} \\ &+ \alpha_{4,4}X^i_{4,s+1} + f_4(X^i_{1,s+1}, X^i_{2,s+1}, X^i_{3,s+1}) = g_4, \end{aligned} \tag{82}$$

with initial conditions

$$X^i_{n,s+1}(\tau_{i-1}) = X^{i-1}_n(\tau_{i-1}), \quad n = 1, 2, 3, 4. \tag{83}$$

Here $\alpha_{n,k}$ and g_n $(n, k = 1, 2, 3, 4)$ are constants while f_n is the nonlinear component of each equation. Each sub-interval Λ_i is transformed to $[-1, 1]$ using the transformation

$$\tau = \frac{\tau_{i-1} - \tau_i}{2}t^\star + \frac{\tau_{i-1} + \tau_i}{2}, \quad t^\star \in [-1, 1]. \tag{84}$$

The Chebyshev-Gauss-Lobatto collocation points are used to discretize the unknown functions

$$t_j^{\star i} = \cos\left(\frac{\pi j}{N}\right), \quad j = 0, 1, \cdots, N. \tag{85}$$

The derivative of the unknown function at the collocation point is given by

$$\frac{dX^i_{n,s+1}}{d\tau}(\tau^i) = \sum_{k=0}^{N} \mathbf{D}_{jk}X^i_{n,s+1}(t_k^{\star i}) = \mathbf{D}\mathbf{X}^i_{n,s+1} \tag{86}$$

where

$$\mathbf{D} = 2D/\delta\tau_i$$

with $\delta\tau_i = \tau_{i-1} - \tau_i$ and D is Chebyshev differentiation matrix. The vector functions at the collocation points are

$$\mathbf{X}^i_{n,s+1} = \left(X^i_{n,s+1}(t_0^{\star i}), \cdots, X^i_{n,s+1}(t_N^{\star i})\right)^T.$$

Substituting Eq. (86) into Eq. (82) and reducing to matrix form we obtain the system

$$\mathbf{A}_n \mathbf{X}^i_{n,s+1} = \mathbf{R}^i_n \tag{87}$$

with $\mathbf{A}_n = \mathbf{D} + \alpha_{n,n}\mathbf{I}$ and

$$\mathbf{R}^i_1 = \mathbf{g}_1 - \Big[\alpha_{1,2}\mathbf{X}^i_{2,s} + \alpha_{1,3}\mathbf{X}^i_{3,s} + \alpha_{1,4}\mathbf{X}^i_{4,s} + f_1(\mathbf{X}^i_{2,s}, \mathbf{X}^i_{3,s}, \mathbf{X}^i_{4,s})\Big] \tag{88}$$

$$\mathbf{R}^i_2 = \mathbf{g}_2 - \Big[\alpha_{2,1}\mathbf{X}^i_{1,s+1} + \alpha_{2,3}\mathbf{X}^i_{3,s} + \alpha_{2,4}\mathbf{X}^i_{4,s} + f_2(\mathbf{X}^i_{1,s+1}, \mathbf{X}^i_{3,s}, \mathbf{X}^i_{4,s})\Big] \tag{89}$$

$$\mathbf{R}^i_3 = \mathbf{g}_3 - \Big[\alpha_{3,1}\mathbf{X}^i_{1,s+} + \alpha_{3,2}\mathbf{X}^i_{2,s+1} + \alpha_{3,4}\mathbf{X}^i_{4,s} + f_3(\mathbf{X}^i_{1,s+1}, \mathbf{X}^i_{2,s+1}, \mathbf{X}^i_{4,s})\Big] \tag{90}$$

$$\mathbf{R}^i_4 = \mathbf{g}_4 - \Big[\alpha_{4,1}\mathbf{X}^i_{1,s+1} + \alpha_{4,2}\mathbf{X}^i_{2,s+1} + \alpha_{4,3}\mathbf{X}^i_{3,s+1} + f_4(\mathbf{X}^i_{1,s+1}, \mathbf{X}^i_{2,s+1}, \mathbf{X}^i_{3,s+1})\Big] \tag{91}$$

where $\mathbf{g}_n$ is g_n multiplied by a vector of ones of size $(N + 1) \times 1$ and $\mathbf{I}$ is an identity matrix of size $(N + 1) \times (N + 1)$.

4 Results and discussion

We have presented a weakly nonlinear stability analysis of a rotating layer of a ferromagnetic fluid with temperature modulation at the boundary. We have obtained mathematical expressions for the stationary Rayleigh number Ra^α and the magnetic Rayleigh number N^α. Our results agree qualitatively with the results in [1, 9]. To provide a measure of validation of our results we give a comparison with [9] in Tables 1 and 2 of the influence of the Taylor number on the critical wave number and the corresponding Rayleigh numbers. Although the results in the two studies are not directly comparable, of interest is the general trend observed, namely that in both cases, increasing Ta increases the critical wave number and the Rayleigh numbers suggesting that the influence of Taylor number is to stabilize the system.

The instability curves are given in Figures 1–3. Figure 1(a)–1(d) shows the influence of various parameters

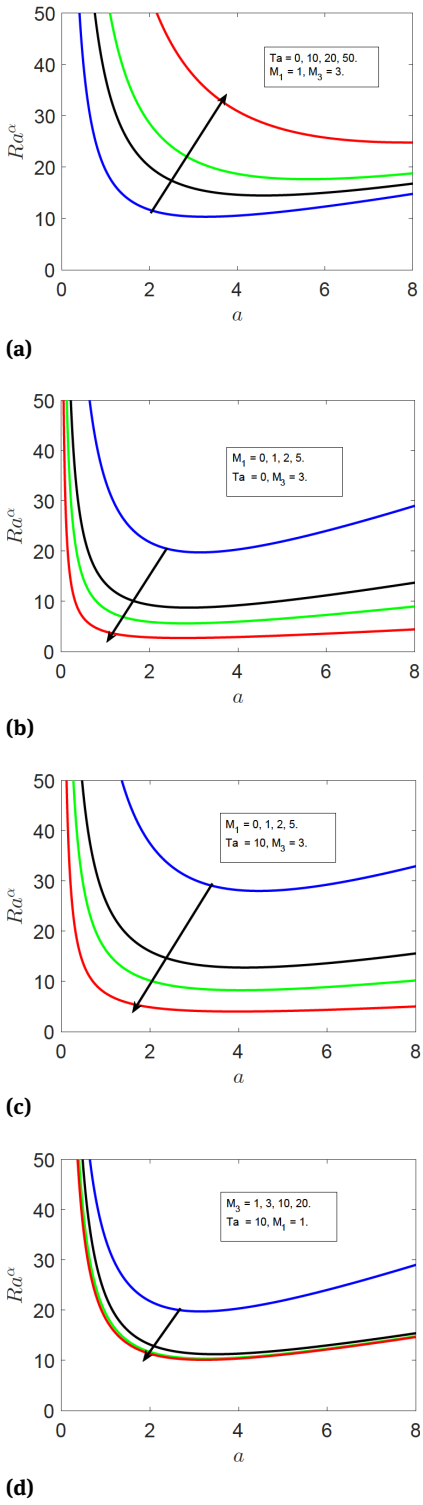

(a) (b) (c) (d)

Figure 1: The effect of stationary Rayleigh number Ra^α versus wave number a for various values of (a) the Taylor number Ta, (b)the ratio of magnetic force to the buoyancy force parameter M_1 with $Ta = 0$ (c) the ratio magnetic force to the buoyancy force parameter M_1 with $Ta = 10$ (d) the nonlinearity of magnetization parameter M_3

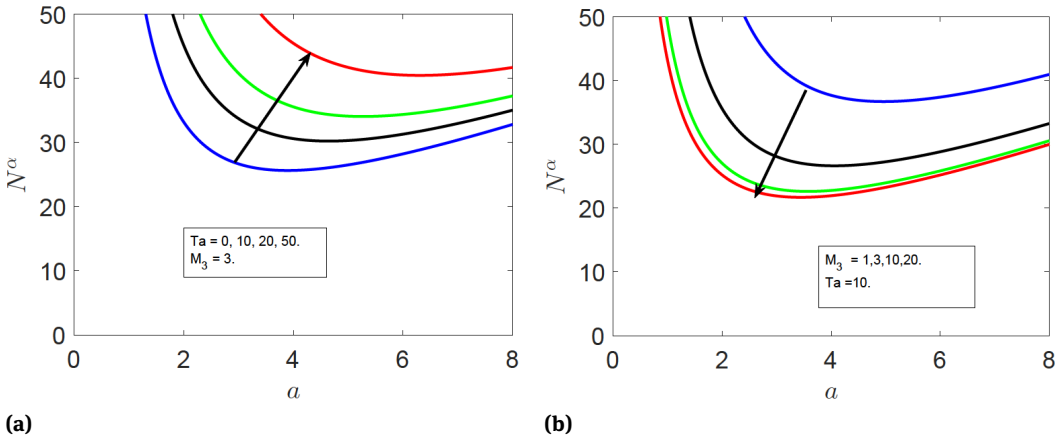

Figure 2: The effect of magnetic Rayleigh number N^{α} versus wave number a for various values of (a) the Taylor number Ta (b) the nonlinearity of magnetization parameter M_3

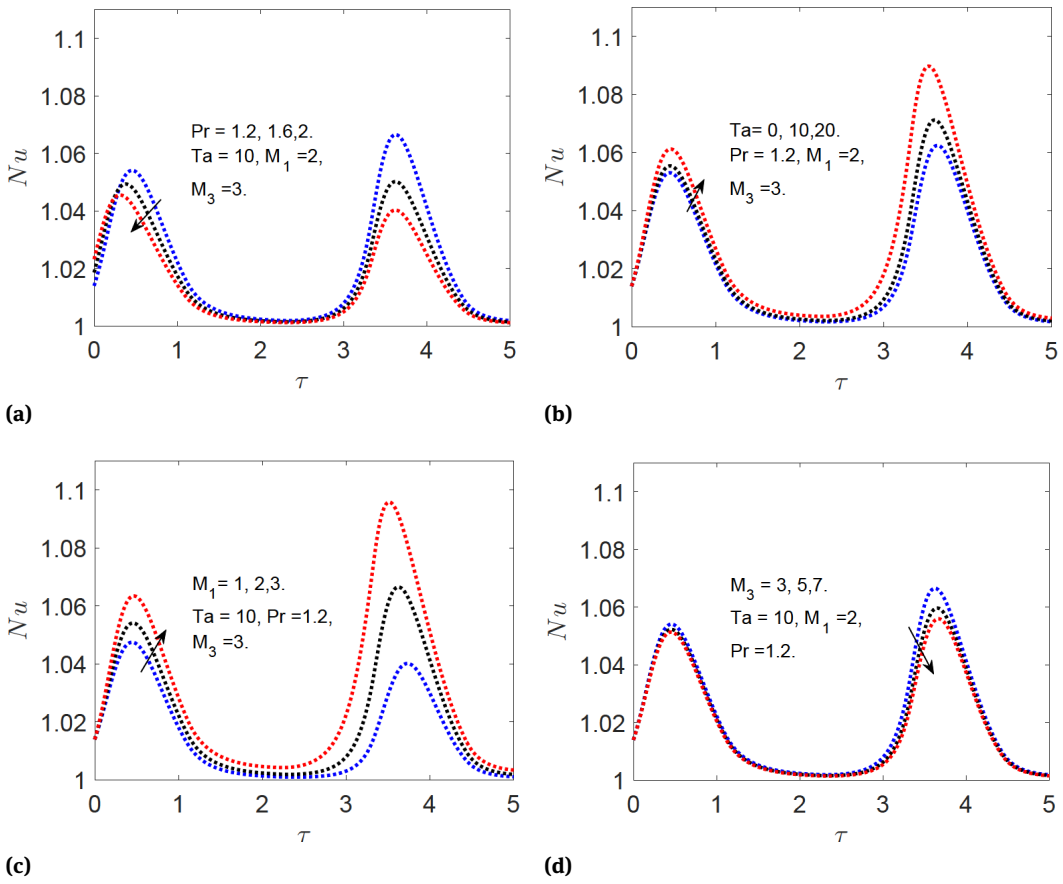

Figure 3: The variation of Nusselt number Nu with time τ in in-phase modulation ($\phi = 0$) for different values of : (a) the Prandtl number Pr, (b)the Taylor number Ta, (c) the ratio of magnetic force to buoyancy force M_1 and (d) the nonlinearity of magnetization M_3

on the stationary Rayleigh number. It can be seen in Figures 1(a)and 2(a) that as Ta increases from 0 to 50 the values of the stationary Rayleigh and the magnetic Rayleigh numbers both increase. This shows that rotation has a stabilizing effect on the system. This result is similar to that of an ordinary viscous fluid. Rotation has a stabilizing influence on ferromagnetic fluid flow. Figures 1(b) and 2(c) show the relative influence of the size of the magnetic

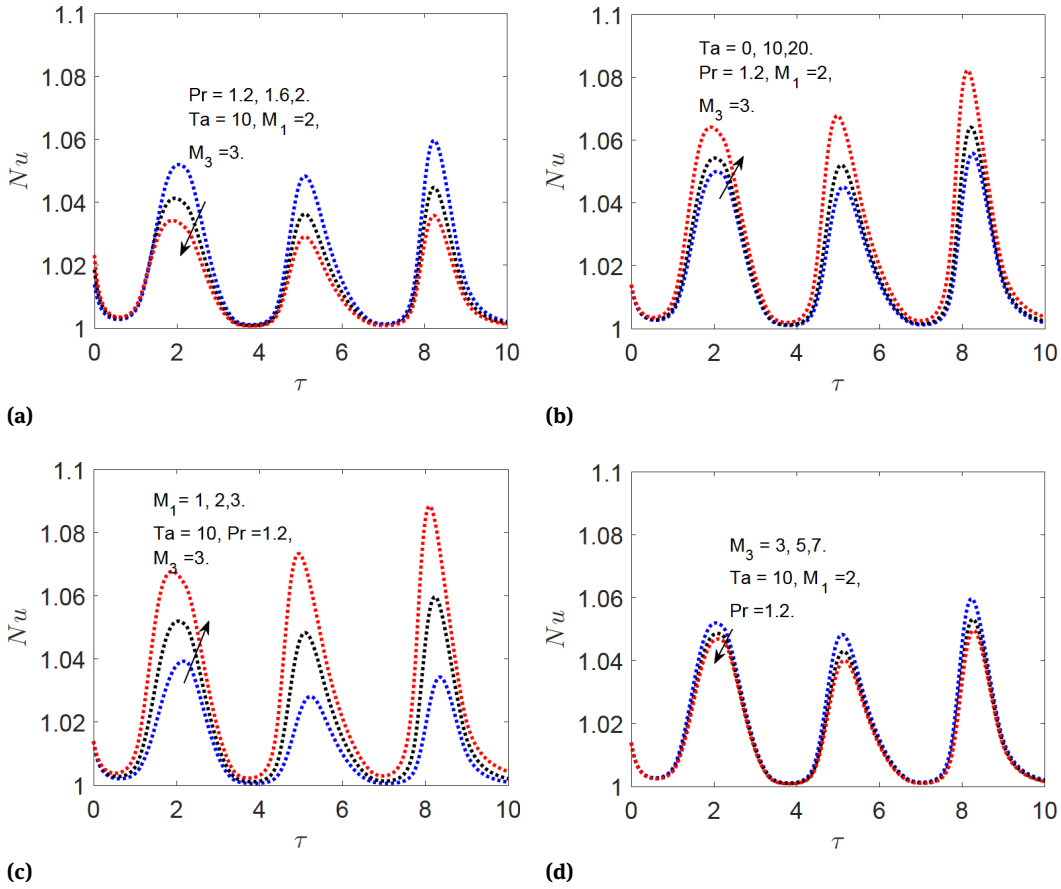

Figure 4: The variation of Nusselt number Nu with time τ in out-phase modulation ($\phi = \pi$) for different values of : (a) the Prandtl number Pr, (b)the Taylor number Ta, (c) the ratio of magnetic force to buoyancy force M_1 and (d) the nonlinearity of magnetization M_3

force to the buoyancy force parameter M_1. As M_1 increases from 0 to 5 the stationary Rayleigh number is reduced. This suggest the magnetic and the buoyancy force are both destabilizing to the ferromagnetic fluid flow. Further, as M_1 increases with $Ta = 10$ fixed, the stationary Rayleigh number decreases, suggesting M_1 has a destabilizing effect for both low and high Taylor numbers. From Figures 1(d) and 2(b) it is observed that increasing M_3 from 1 to 20 reduces both the Rayleigh number and the magnetic Rayleigh number, this is destabilization to the system.

The Ginzburg-Landau equation is obtained using the nonlinear stability analysis at the third order of ϵ. The equation was solved using a multi-domain spectral method. The heat transfer coefficient, represented by the Nusselt number, is presented graphically for in-phase and out-phase modulation in Figures 3–4. Figure 3(a)–3(d) show the effect of Pr, Ta, M_1 and M_3 on the Nusselt number with time τ. It can be observed that on increasing the Pr and M_3, the Nusselt number decreases. Hence increasing these parameters reduces the rate of heat transfer. Increasing Ta and M_1 increases the Nusselt number, thus the rate of heat transfer increases. Figures 4(a)–4(d) show changes in the Nusselt number with respect to time τ due to the influence of various parameters in the case of out of phase modulation. It can be observed that the Nusselt number for in-phase modulation is less than for out of phase modulation.

A multi-domain spectral collocation method was used to find the nonlinear amplitudes in ferromagnetic fluid convection equations for various values of R. The solution sets were obtained using initial conditions selected in the neighborhood of the stationary points corresponding to the motionless solutions. The simulations were done to a maximum time $\tau_{max} = 20$. For a sense of the accuracy of the method, the solutions were compared with solutions obtained using the Runge-Kutta based ode45 routine. Figures 5(a)–5(d) show the time series solution of $X_1(\tau)$ for different supercritical values of R. As R increases, periodic solutions are obtained. Here a comparison between the multi-domain spectral collo-

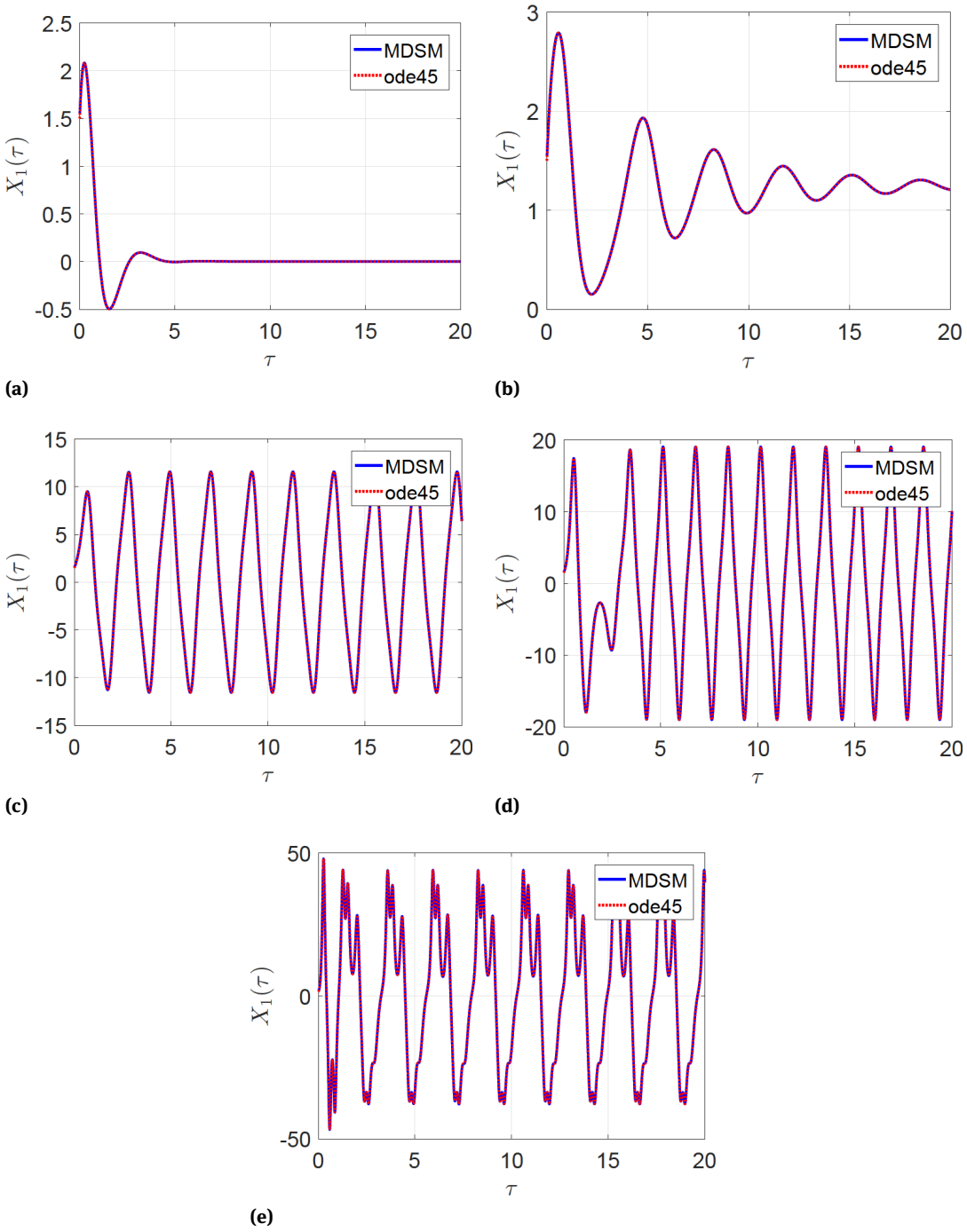

Figure 5: Comparison between a Multi-domain spectral collocation methods and ode45 methods for the solution of $X_1(\tau)$ for different values of R (a) $R = 2$, (b) $R = 4$, (c) $R = 10$, (d) $R = 20$ and (e)$R = 100$

cation method and the ode45 is given. In Figures 6–11 we present a projection of the trajectories onto the $(X_1, X_2), (X_1, X_3), (X_1, X_4), (X_2, X_3), (X_2, X_4)$ and (X_3, X_4) phase planes, respectively. The initial supercritical convective solution $R = 2$ is presented in part a in each figure. We observe that the trajectories attracted to equilibrium points that correspond to the motionless solution are stable spirals. The solutions are presented in part c and d of each figure when $R = 20$ and $R = 25$, respectively. For these Rayleigh numbers, chaotic solutions are obtained. These changes in solutions are further presented in Figures 6(c)–6(d), 7(c)–7(d) and 9(c)–9(d). The results pre-

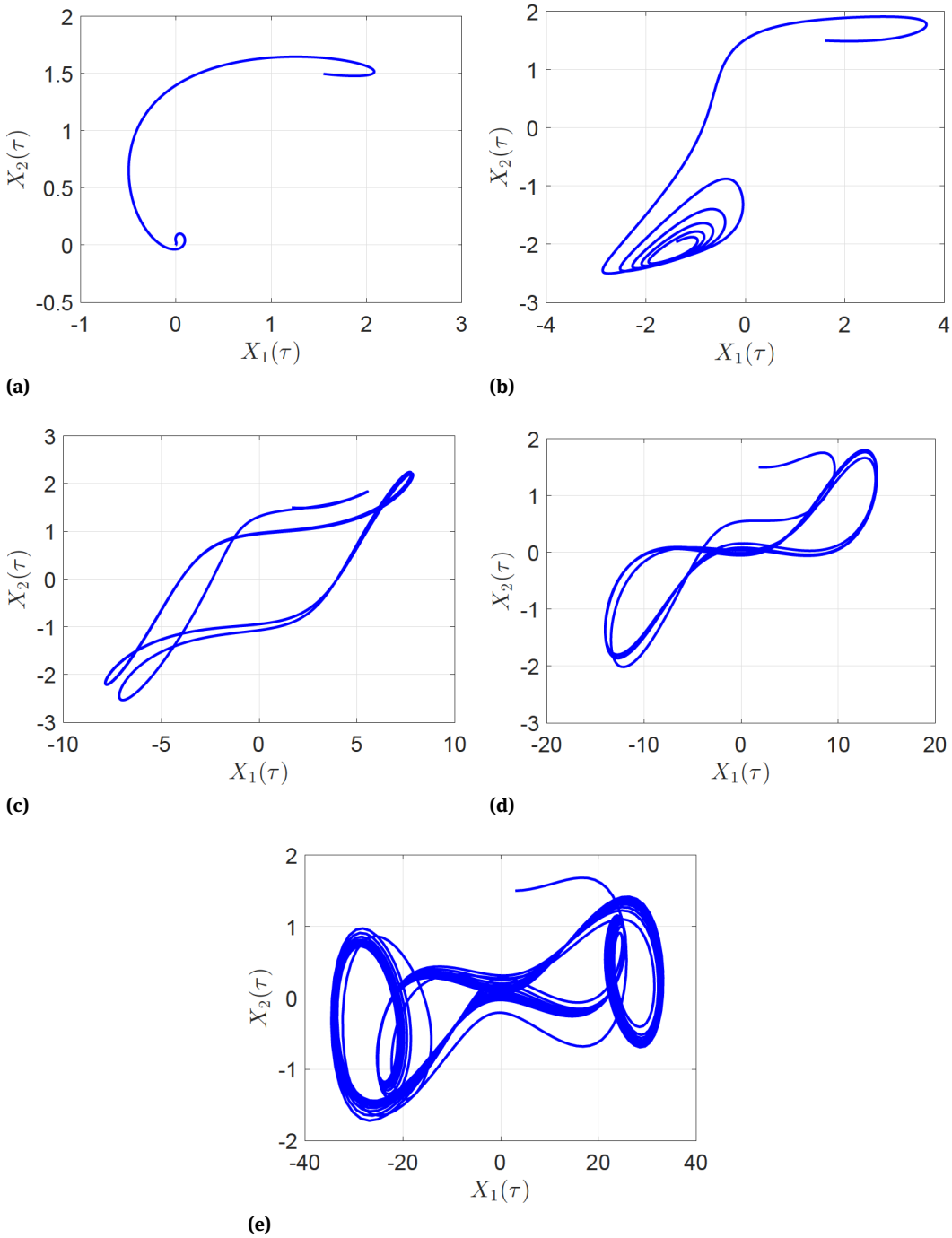

Figure 6: The evolution of trajectory over times in phase space for increasing values of Rayleigh number.(in term of R) corresponding to (a)$R = 2$, (b)$R = 4$, (c)$R = 10$, (d) $R = 20$ and (e)$R = 100$. The graph represented the projection of the solution into X_1X_2 plane

sented in Figures 8(c)–8(d) and 10(c)–10(d) show a transition to a limit cycle. Increasing the values of R, for example, when $R = 100$ the results are complex with a significant level of unpredictability.

Figure 12 shows the streamlines patterns for the flow of a ferromagnetic fluid. Two different eddies are observed. The clockwise and anti-clockwise flows are shown via negative and positive stream function values, respectively. With the Rayleigh number increasing from 2 to 200, the magnitude of the stream function values increase. The sense of motion in the subsequent cells is opposite that of an adjoining cell, indicating symmetry in the forma-

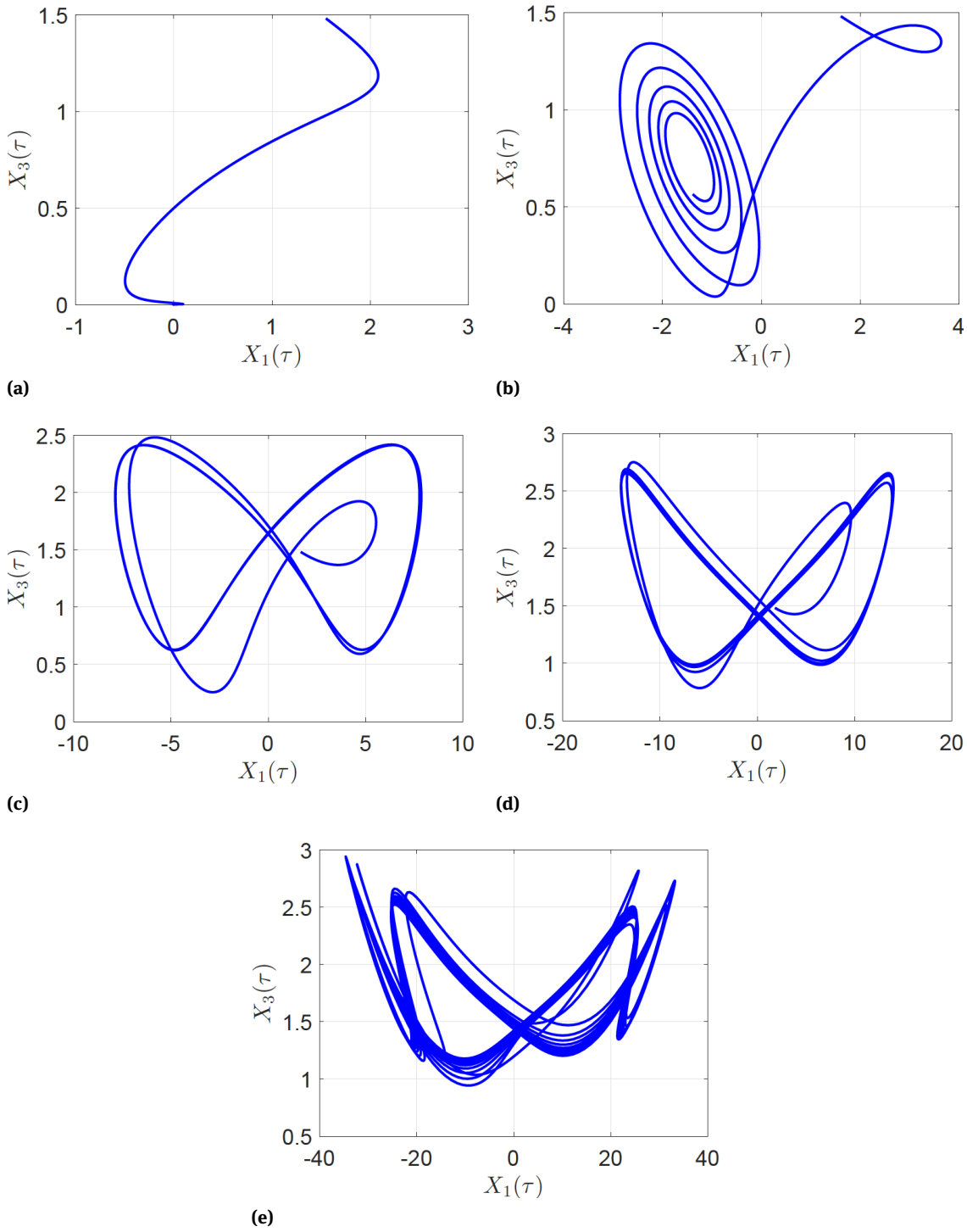

Figure 7: The evolution of trajectory over times in phase space for increasing values of Rayleigh number. (in term of R) corresponding to (a) $R = 2$, (b) $R = 4$, (c) $R = 10$, (d) $R = 20$ and (e) $R = 100$. The graph represented the projection of the solution into X_1X_3 plane

tion of ferromagnetic convective cells. Figure 13 shows the isotherm patterns as the Rayleigh number changes from 2 to 200. Three different eddies are observed. The small eddy at the left corner diminishes as R increases from 2 to 200. Also, increasing R reduces the density of the isotherms implying a delay of the onset of instability.

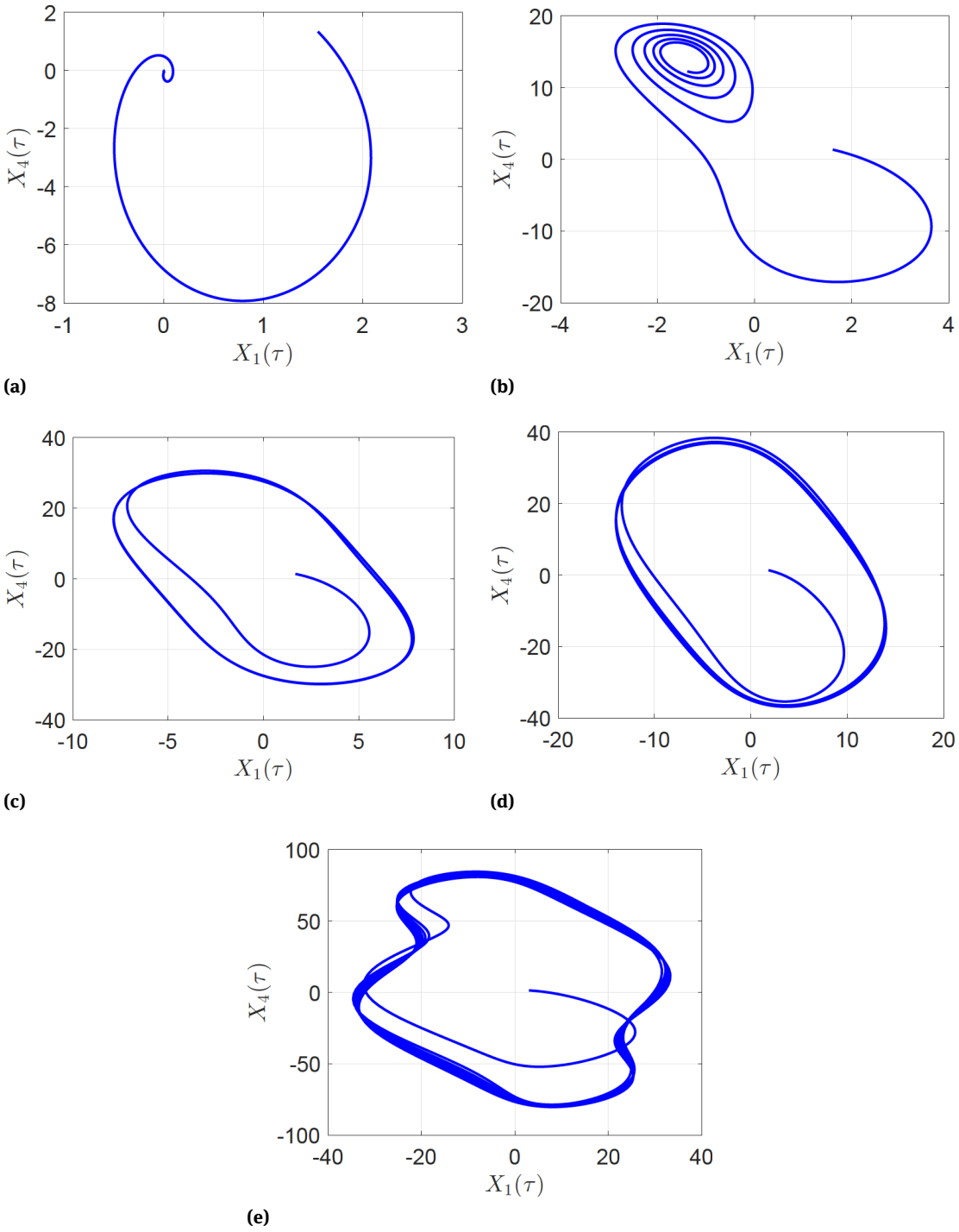

Figure 8: The evolution of trajectory over times in phase space for increasing values of Rayleigh number. (in term of R) corresponding to (a) $R = 2$, (b) $R = 4$, (c) $R = 10$, (d) $R = 20$ and (e) $R = 100$. The graph represented the projection of the solution into X_1X_4 plane

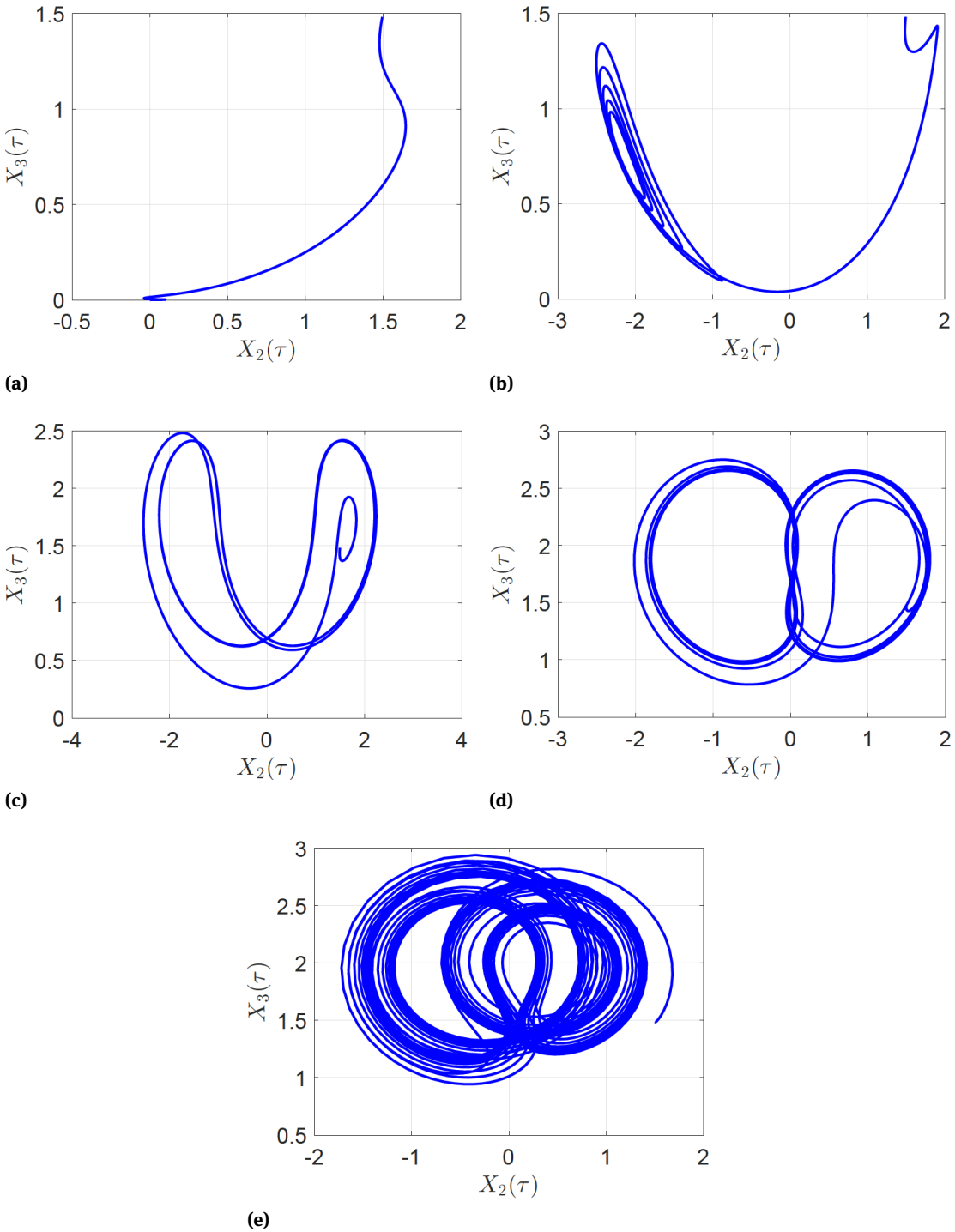

Figure 9: The evolution of trajectory over times in phase space for increasing values of Rayleigh number. (in term of R) corresponding to (a) $R = 2$, (b) $R = 4$, (c) $R = 10$, (d) $R = 20$ and (e) $R = 100$. The graph represented the projection of the solution into X_2X_3 plane

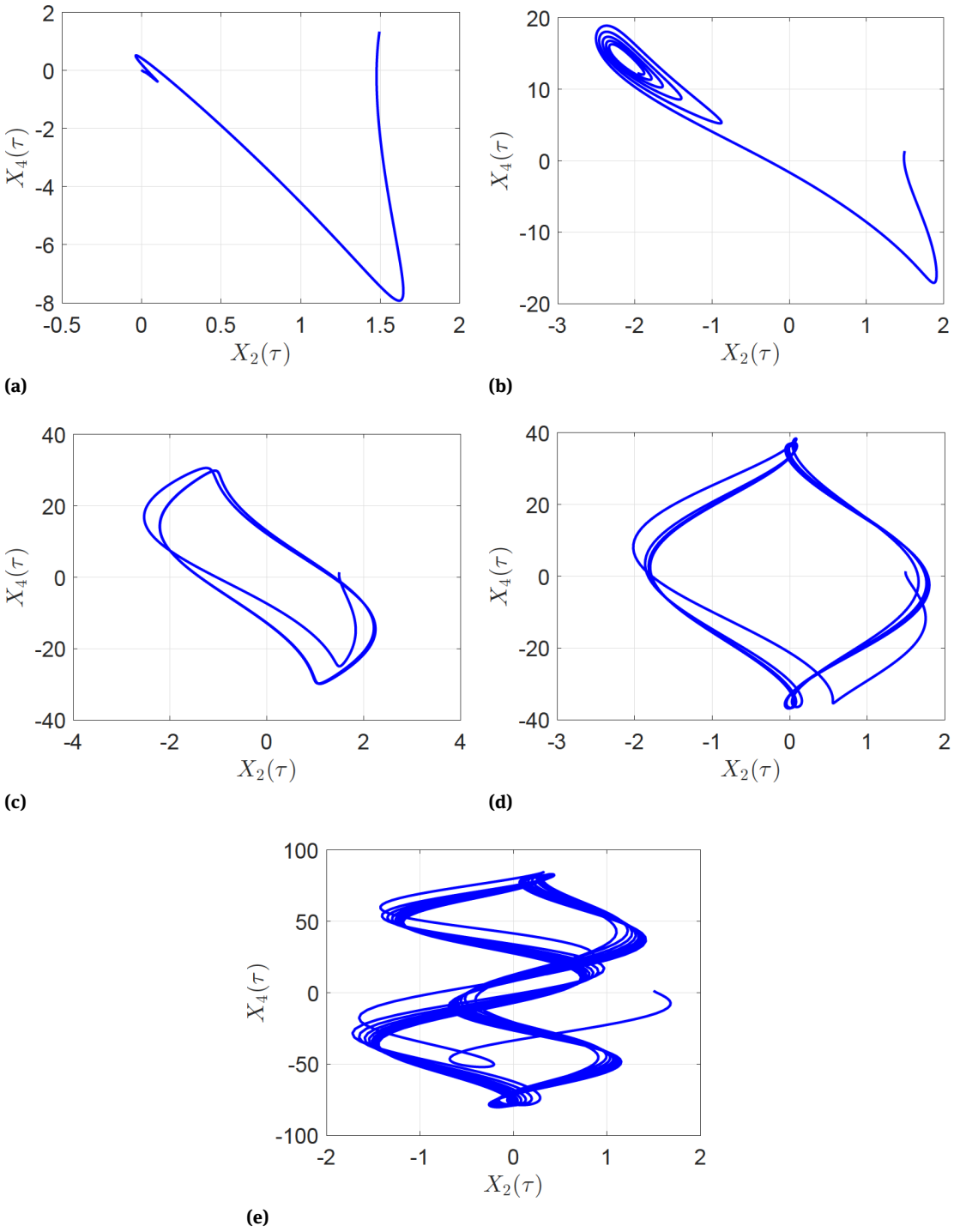

Figure 10: The evolution of trajectory over times in phase space for increasing values of Rayleigh number. (in term of R) corresponding to (a) $R = 2$, (b) $R = 4$, (c) $R = 10$, (d) $R = 20$ and (e) $R = 100$. The graph represented the projection of the solution into X_2X_4 plane

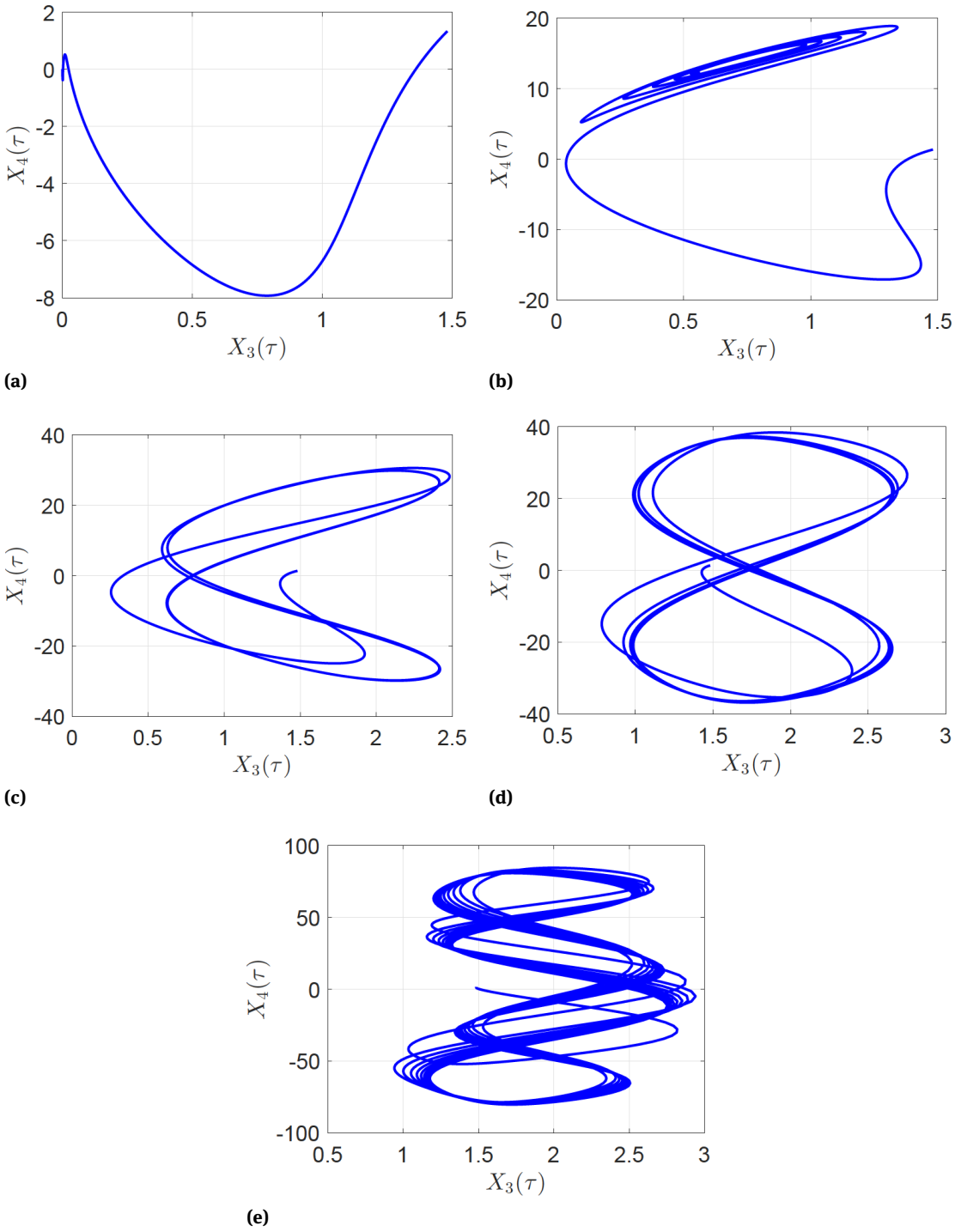

Figure 11: The evolution of trajectory over times in phase space for increasing values of Rayleigh number. (in term of R) corresponding to (a) $R = 2$, (b) $R = 4$, (c) $R = 10$, (d) $R = 20$ and (e) $R = 100$. The graph represented the projection of the solution into X_3X_4 plane

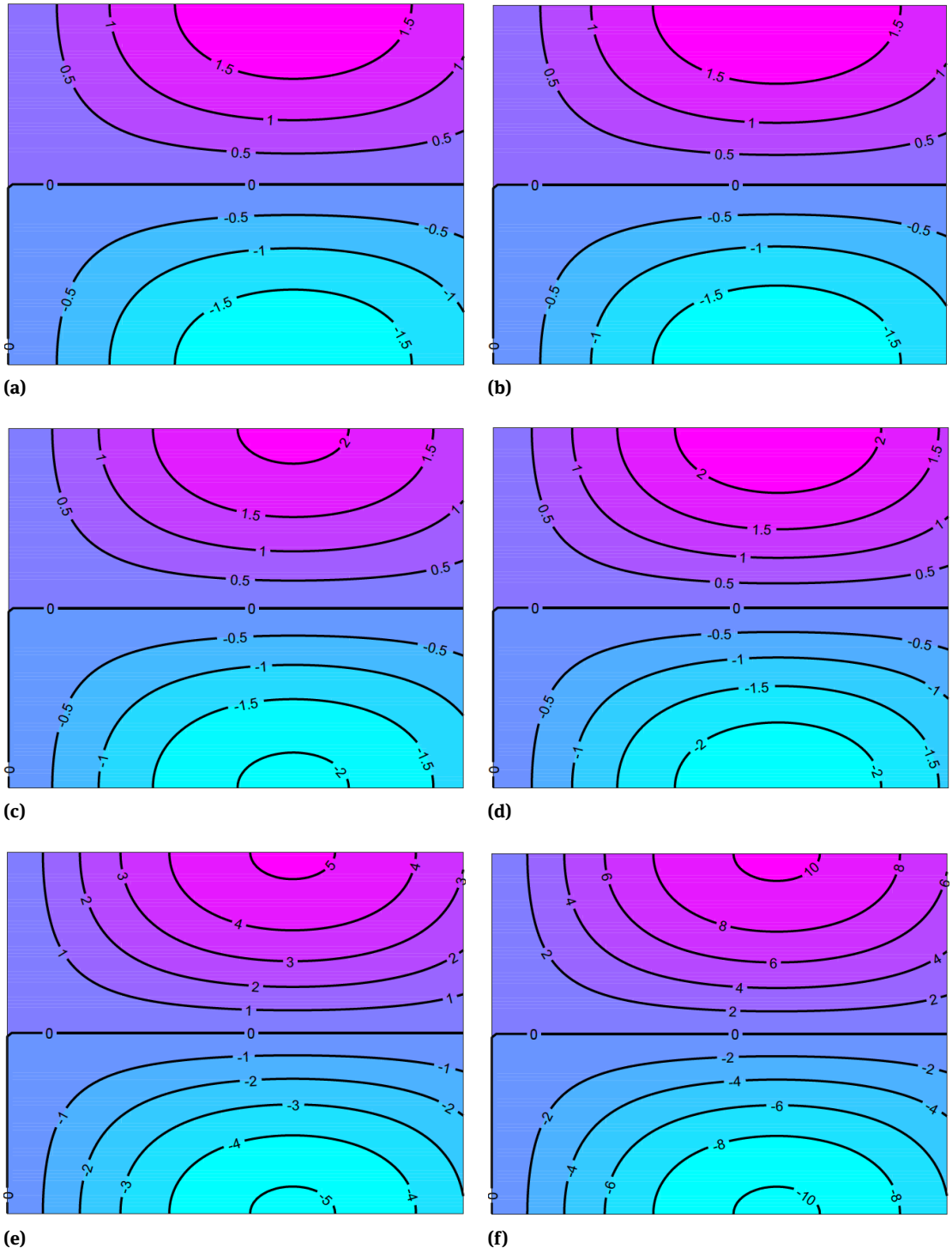

Figure 12: The streamlines for different values of the Rayleigh number R *e.g.* $R = 2, 4, 10, 20, 100, 200$

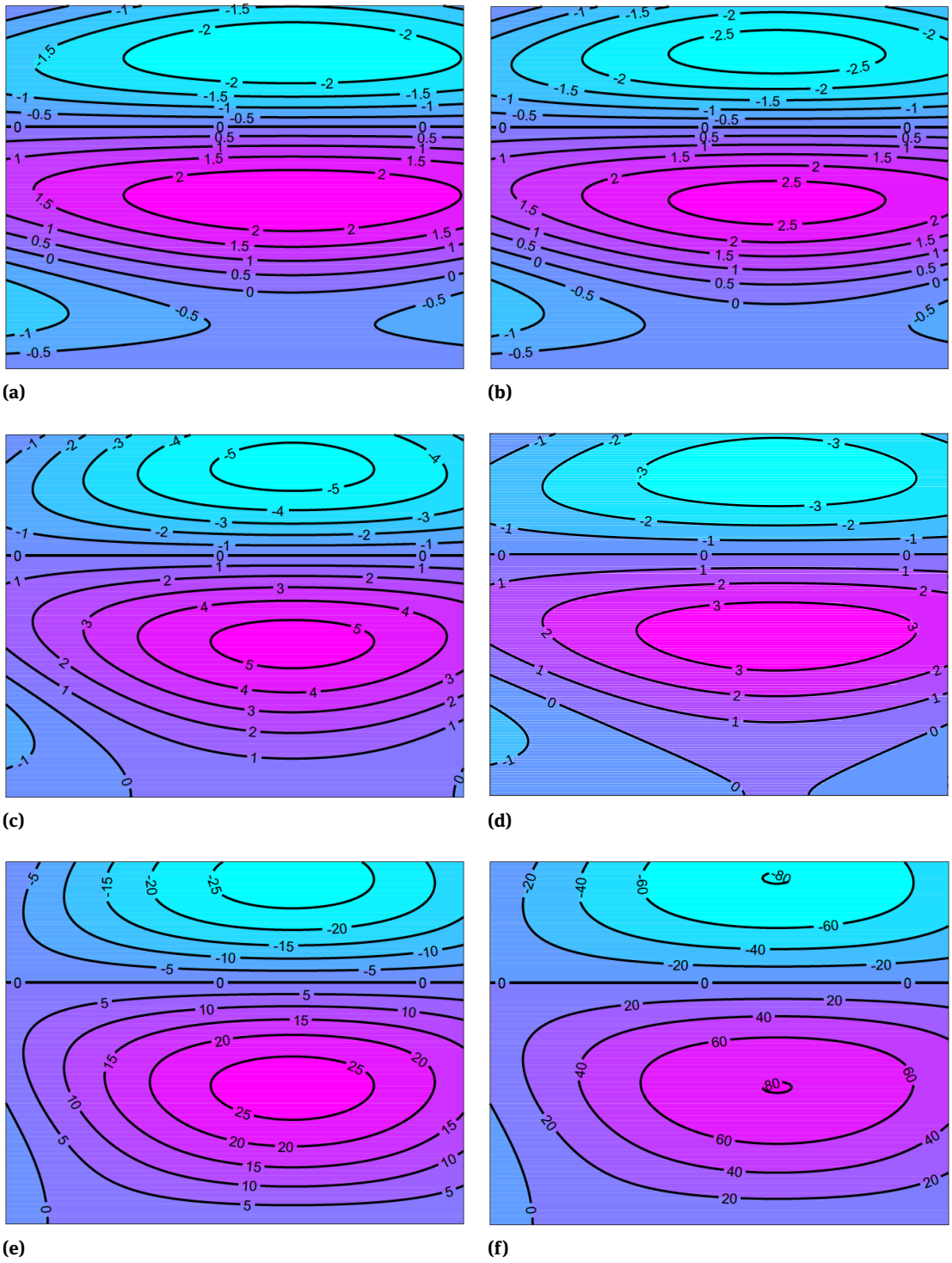

Figure 13: The isotherms for different values of the Rayleigh number R *e.g.* $R = 2, 4, 10, 20, 100, 200$

5 Conclusion

We investigated the thermoconvective instability in a rotating ferromagnetic fluid layer with time periodic temperature boundary conditions. The influence of flow parameters such as the Rayleigh number on the onset of instability was determined using a weakly nonlinear stability analysis. The results are broadly in line with the earlier findings in [1, 3, 8]. The heat transport has been analyzed for both the in-phase and out of phase temperature modulations. The influence of the parameters such as the Prandtl number, Taylor number and the magnetization parameter on the Nusselt number for the in-phase modulation was found to be less significant compared to the case of out of phase modulation.

The set of nonlinear differential equations for convection amplitude was solved using a multi-domain spectral collocation method. The accuracy of the solutions was determined by comparison with solutions using a different independent method, namely the Runge-Kutta based ode45 Matlab solver. The stability of the equilibrium solutions of the nonlinear differential equations has been analyzed. Transitions from different states have been demonstrated for different parameter values, for example from steady convection to chaotic solutions at high Rayleigh numbers.

References

[1] Finlayson, B.A., Convective instability of ferromgnetic fluids, J. Fluid Mech., 1970, 40(4), 755–767.
[2] Chandrasekhar, S., Hydrodynamic and hydromagnetic stability, 1961, Oxford University Press, Oxford.
[3] Rosensweig, R.E.,Ferrohydrodynamics, 1985, Cambridge University Press.
[4] Schwab L., Hildebrandt U., Stierstadt K., Magnetic Benard convection, J. Magn. Magn. Mat., 1983, 39(1-2), 113–114.
[5] Stiles P.J., Kagan M., Thermoconvective instability of a horizontal layer of ferrofluid in a strong magnetic field, J. Magn. Magn. Mat., 1990, 85(1-3), 196–198.
[6] Ruessll C.L., Blnnerhassett P.J., Stiles P.J., Large wave number convection in magnetized ferrofluids, J. Magn. Magn. Mat., 1995, 149(1-2), 196–121.
[7] Greenspan H.P., The theory of rotating fluids, 1968, Cambridge University press, London.
[8] Gupta M.D., Gupta A.S., Convective instability of a layer of a ferromagnetic fluid rotating about a vertical axis, Int. J. Eng, Sci., 1979, 17(3), 271–277.
[9] Venkatasubramanian S., Kaloni P.N., Effects of rotation on the thermo-convective instability of a layer of a ferrofluids, Int. J. Eng. Sci., 1994, 32(2), 237–256.
[10] Gotoh K., Yamada M., Thermal convective in a horizontal layer of magnetic fluid, J. Phys. Soc. Japan, 1982, 51(9), 3042–3048.
[11] Bhasauria B.S., Siddheshwar P.G., Kumar J., Suthar O.P., Weakly nonlinear stability analysis of temerature/gravity modulated stationary Rayleigh-Benard convection in a rotating porous medium, Transp. Porous Med., 2012,92(3), 633–647.
[12] Rudraiah N., Sekhar N.G., Convective on magnetic fluids with internal heat generation, ASME J. Heat Transfer, 1991, 113(1), 122–127.
[13] Aniss S., Belhaq M., Souhar M., Effects of amagnetic mod- ulation on the stability of a magnetic liquid layer heated from above, J. Heat Transfer, 2001,123(3) 428–432.
[14] Singh J., Bajaj R., convective instability ina ferrofluids layer with temperature modulation rigid boundaries, Fluid Dyn. Res., 2011, 43(2), 025502.
[15] Trefethen L.N., Spectral methods in MATLAB, SIAM, Philadelphia, 2000, 26(2), 199.
[16] Motsa S.S., Dlamini P., Khumalo M., A new multistage spectral relaxation method for solving chaotic initial value systems, Nonlin. Dyn., 2013, 72(1-2) 265–83.
[17] Motsa S.S., Magagula V.M., Goqo P.S., Oyelakin I.S., Sibanda P., A multi-domain spectral collocation approach for solving Lane-Emden type equations, Chaper 7, Numerical Simulation - From Brain Imaging to Turbulent flows, 2016, 10, 5772-63016.
[18] Noreldin O.A.I., Sibanda P., Mondal S., Weakly Nonlinear Stability in a Horizontal Porous Layer Using a Multi-domain Spectral Collocation Method, chapter 9, Complexity in Biological and Physical Systems, 2018, 71066.
[19] Bhadauria B.S., Fluid convection in a rotating porous layer under modulated temperature on the boundaries, Transp. Porous Med., 2007, 67 297–315.
[20] Mielke A., The Ginzburg-Landau Equation in Its Role as a Modulation Equation, Chapter 15, Handbook of Dynamical Systems, 2002, 2, 759–834.
[21] Routh-Hurwitz criterion, Encyclopedia of Mathematics, http://www.encyclopediaofmath.org/index.php?title=Routh-Hurwitz_criterion&oldid=33371

Chapter 6

Conclusion

In this study we have formulated and given an analysis of the behaviours and solutions of mathematical models that describe Rayleigh-Bénard type convection in various fluid flows using linear and weakly nonlinear stability theories. We have, in particular, investigated thermal instability in a horizontal nanofluid layer, double-diffusive convection in an inclined open cavity and thermoconvective instability in a rotating ferromagnetic fluid with temperature modulation. We have determined criteria necessary for the onset of convective instabilities in terms of certain fluid parameters such as the Darcy, Hartman, Prandtl, Taylor and Rayleigh numbers. We have solved the Lorentz type convective amplitude equations using the recently published multidomain spectral method.

In Chapter 2, we used the linear stability theory to study the onset of convection in a porous medium of infinite extent saturated with a nanofluid and subjected to a magnetic field. Here we assumed stress-free conditions, constant temperature and solute concentration, and zero nanoparticle flux at the boundaries. An analytic expression for the critical stationary Rayleigh number was derived. The effects of both the Darcy number and magnetic field parameter on the onset of convection were investigated. It has been shown that increasing both the Darcy number and the magnetic field parameter increases the critical Rayleigh number, which has the effect of delaying the onset of

stationary convection. Hence, increasing both the Darcy number and the magnetic field parameter has the effect of stabilizing the nanofluid flow. The effect of the magnetic field parameter on the onset of convection in a cross-diffusive nanofluid is similar to that observed in pure thermal convection, as reported by [2]. We also noted that an increase in the value of nanofluid Lewis number increases both the stationary and oscillatory Rayleigh numbers. This has the effect of increasing the value of the Rayleigh number at the turning point of the neutral stability curve. Hence, increasing the nanofluid Lewis number has a stabilizing effect the system. Further, increasing the Soret and Dufour parameters has the effect of, respectively, reducing and increasing the critical Rayleigh number.

In Chapter 3, we studied convective instability for a nanofluid flow in a horizontal porous medium. Using a stress-free boundary condition, and assuming zero nanoparticle flux at walls, and applying a truncated Fourier series expansion, a system of nonlinear ordinary differential equations that describe the convection amplitudes for the nanofluid flow was derived. The multidomain spectral collocation was used to solve the system of equations. A limited phase space analysis was presented for different Rayleigh numbers. As the Rayleigh number Ra increased to 10^4 the trajectories of the amplitude convection are spirals that approach a fixed point. The flow is far more complex and unpredictable for Rayleigh numbers higher than 10^4. We have presented the flow structure in terms of streamlines, isotherms and iso-concentrations for different values of the Darcy numbers and the buoyancy ratio parameter. As the Darcy number increases from 0.05 to 0.07, the rotation of the flow circulations changes. Increasing the Darcy number has the effect of increasing the effective nanofluid viscosity and reducing the thermal and solute concentration boundary layers. The nanofluid flow structure is significantly influenced by buoyancy within the fluid layer. Increasing the buoyancy ratio decreased the boundary layer thickness. A high buoyancy ratio changes the nanofluid flow structure, which impacts on the concentration field that builds up a vertical stratification in the layer. Additionally, a change in the system parameters, such as an increase in the flow Lewis number, improves the rate of heat and mass transfer in the nanofluid flow. Increasing the Dufour parameter also has the effect of increasing the rate of heat transfer, and increasing the Soret parameter increases the rate of mass transfer.

In Chapter 4, we investigated thermal instability in double-diffusive convection in an inclined open cavity with an inclined magnetic field. For the linear case, we obtained an analytical expression for the critical wave number and corresponding critical Rayleigh number at the onset of double-diffusive convective instability. The influence of parameters such as the Hartman, Prandtl, Lewis and solute concentration Rayleigh numbers on the onset of the stationary and oscillatory convection were investigated. We noted, for example, that on increasing the Hartman number from $Ha = 5$ to 20 the critical Rayleigh number for the onset of both the stationary and oscillatory convection increased. This shows that increasing the Hartman number delays the onset of the double-diffusive convective instability. We note that the magnetic field offers resistance to the motion of the fluid in the inclined cavity due to the Lorenz force generated and, as a result, a considerable amount of energy is used by the system to overcome this resistance.

We further used the weakly nonlinear stability to investigate the evolution of flow perturbations in double-diffusive convection. The influence of the parameters such as the Lewis number, Hartman number, Prandtl number, buoyancy ratio parameter and the inclination angles of the cavity and magnetic field was investigated. We determined the steady state solutions and the trapping region for the trajectories in the phase space. The rates of heat and mass transfer were further analyzed. It was observed that increasing the Hartman and Lewis numbers increases both heat and mass transfer coefficients. A limited phase space analysis is presented for Rayleigh numbers from $R = 100$ to $R = 150$. For the higher Rayleigh number a chaotic state of the system was observed, showing the unpredictability of double-diffusive convective flow for high Rayleigh numbers. We presented the flow structure in terms of streamlines, isotherms and iso-concentrations contours for buoyancy ratio of $N = -10, 1, 10$ with a fixed cavity inclination angle φ and varying the magnetic field inclination angle ϕ. It was ascertained that the fluid circulation strongly depends on the buoyancy ratio and magnetic field parameters. Further, we observed that the streamlines are weak for $\phi = \frac{\pi}{4}$, but are stronger for higher values of ϕ. The isotherms and iso-concentrations occur symmetrically near the top corners of the side walls in the cavity and are also concentrated at the bottom walls of the cavity for buoyancy ratio $N = -10$ when $\phi = \frac{\pi}{4}$ and, $\frac{\pi}{2}$ but the opposite trend is observed for $\frac{3\pi}{4}$.

In Chapter 5, we investigated thermoconvective instability in a rotating ferromagnetic fluids in a horizontal layer with time periodic temperature at the walls. The effects of parameters such as the Taylor number, the ratio of the magnetic and buoyancy forces, and the magnetization parameter on the onset of convection are analyzed. Increasing the Taylor number increased both the critical Rayleigh number and the magnetic Rayleigh number. Hence, increasing the Taylor number delays the onset of convective instability in ferromagnetic fluid flow. This shows that Taylor number has the effect of stabilizing the system. On the other hand, the effect of increasing the magnetization parameter is to reduce the critical Rayleigh number, showing that the magnetization parameter increase has a destabilizing effect on the system.

For the nonlinear stability regime, we obtained Ginzburg-Landau equation and analyzed the flow for both in-phase and out-of-phase modulation. The influence of parameters such as the Taylor number, Prandtl number and magnetization parameter on the rate of heat transfer for in-phase modulation was found to be significantly less than that for out-of-phase modulation. The system of nonlinear differential equations that describes the amplitude evolution for a ferromagnetic fluid in a rotating horizontal layer was solved numerically. The stability of the equilibrium solutions of this system was analyzed. A limited phase space analysis was presented and transition between different states was demonstrated for changes in bifurcation parameters. We observed a transition from steady convection to chaotic convective flow at higher Rayleigh number. The flow pattern is further shown in terms of streamlines and isotherms. For large Rayleigh numbers, we observed three types of flow circulation as well as symmetry in the formulation of ferromagnetic convection cells in the rotating layer.

We have investigated flow instabilities in nanofluid and ferromagnetic flows, both in a horizontal layer and an inclined cavity. We have demonstrated how instabilities set in for different parameters and how the parameters influence the flow patterns. In these studies we have confined our analysis mostly to stress-free boundary conditions. In future, it is suggested to extend this study to include both free-rigid and rigid-rigid boundary conditions with temperature and gravity modulation. Further, we have used linear and weakly nonlinear stabilities to study double-diffusive con-

vection, with the key parameter being the buoyancy ratio, which has applications in, for instance, ocean studies. It is suggested to extend this work to triple-diffusive convection in Newtonian and non-Newtonian fluid flow for different settings, such as a rotating cylinder and rotating spherical shells. Triple-diffusive convection is found in many applications; for example aqueous suspension of deoxyribonucleic acid (DNA) contain more than two independently diffusive components, each having different diffusivities. It would therefore be interesting to study the effects of Soret and Dufour for triple-diffusive convection in an inclined cavity, subjected to both temperature and solute concentration modulation.

References

[1] L. Rayleigh. On convection currents in a horizontal layer of fluid, when the higher temperature is on the under side. *The London, Edinburgh, and Dublin Philosophical Magazine and Journal of Science*, 32:529–546, 1916.

[2] S. Chandrasekhar. *Hydrodynamic and Hydromagnetic Stability*. New York: Courier Corporation, 2013.

[3] J. Thomson. On a changing tesselated structure in certain liquids. *Proceedings of the Philosophical Society, Glasgow*, 13:464–468, 1882.

[4] P. G. Drazin and W. H. Reid. *Hydrodynamic stability*. Cambridge: Cambridge University Press, 2004.

[5] A. V. Getling. *Rayleigh-Bénard Convection: Structures and Dynamics*. Singapore: World Scientific, 1998.

[6] E. L. Koschmieder. *Bénard cells and Taylor vortices*. Cambridge: Cambridge University Press, 1993.

[7] C. J. Chapman and M. R. E. Proctor. Nonlinear Rayleigh-Bénard convection between poorly conducting boundaries. *Journal of Fluid Mechanics*, 101:759–782, 1980.

[8] F. H. Busse. Non-linear properties of thermal convection. *Reports on Progress in Physics*, 41:1929–1967, 1978.

[9] R. E. Kelly and H. C. Hu. The onset of Rayleigh-Bénard convection in non-planar oscillatory flows. *Journal of Fluid Mechanics*, 249:373–390, 1993.

[10] M. S. Chana and P. G. Daniels. Onset of Rayleigh-Bénard convection in a rigid channel. *Journal of Fluid Mechanics*, 199:257–279, 1989.

[11] N. Shi, M. S. Emran, and J. Schumacher. Boundary layer structure in turbulent Rayleigh-Bénard convection. *Journal of Fluid Mechanics*, 706:5–33, 2012.

[12] J. D. Scheel, E. Kim, and K. R. White. Thermal and viscous boundary layers in turbulent Rayleigh-Bénard convection. *Journal of Fluid Mechanics*, 711:281–305, 2012.

[13] S. C. Hirata, L. S. B. Alves, N. Delenda, and M. N. Ouarzazi. Convective and absolute instabilities in Rayleigh-Bénard-Poiseuille mixed convection for viscoelastic fluids. *Journal of Fluid Mechanics*, 765:167–210, 2015.

[14] H. M. Park. Peculiarity in the Rayleigh-Bénard convection of viscoelastic fluids. *International Journal of Thermal Sciences*, 132:34–41, 2018.

[15] M. S. Aghighi, A. Ammar, C. Metivier, and M. Gharagozlu. Rayleigh-Bénard convection of casson fluids. *International Journal of Thermal Sciences*, 127:79–90, 2018.

[16] J. E. Wesfreid. Henri Bénard: Thermal convection and vortex shedding. *Comptes Rendus Mecanique*, 345:446–466, 2017.

[17] O. Thual. Zero-Prandtl number convection. *Journal of Fluid Mechanics*, 240:229–258, 1992.

[18] Y. Nandukumar and P. Pal. Instabilities and chaos in low-Prandtl number Rayleigh-Bénard convection. *Computers & Fluids*, 138:61–66, 2016.

[19] F. Chillà and J. Schumacher. New perspectives in turbulent Rayleigh-Bénard convection. *The European Physical Journal E*, 35:58, 2012.

[20] K. Q. Xia. Current trends and future directions in turbulent thermal convection. *Theoretical and Applied Mechanics Letters*, 3:052001, 2013.

[21] J. P. Lowman and G. T. Jarvis. Mantle convection models of continental collision and breakup incorporating finite thickness plates. *Physics of the Earth and Planetary Interiors*, 88:53–68, 1995.

[22] F. Wang, S. D. Huang, and K. Q. Xia. Thermal convection with mixed thermal boundary conditions: effects of insulating lids at the top. *Journal of Fluid Mechanics*, 817:1–11, 2017.

[23] C. W. Horton and J. F. T. Rogers. Convection currents in a porous medium. *Journal of Applied Physics*, 16:367–370, 1945.

[24] E. R. Lapwood. Convection of a fluid in a porous medium. *Mathematical Proceedings of the Cambridge Philosophical Society*, 44:508–521, 1948.

[25] P. Cheng. Convective heat transfer in porous layers by integral methods. *Letters in Heat and Mass Transfer*, 5:243–252, 1978.

[26] R. A. Wooding. Rayleigh instability of a thermal boundary layer in flow through a porous medium. *Journal of Fluid Mechanics*, 9:183–192, 1960.

[27] J. W. Elder. Steady free convection in a porous medium heated from below. *Journal of Fluid Mechanics*, 27:29–48, 1967.

[28] E. Palm, J. E. Weber, and O. Kvernvold. On steady convection in a porous medium. *Journal of Fluid Mechanics*, 54:153–161, 1972.

[29] D. A. Nield and A. Bejan. *Convection in Porous Media*. Cham: Springer, 2006.

[30] D. Rees. The onset of Darcy-Brinkman convection in a porous layer: an asymptotic analysis. *International Journal of Heat and Mass Transfer*, 45:2213–2220, 2002.

[31] A. Barletta and D. A. Nield. Instability of Hadley–Prats flow with viscous heating in a horizontal porous layer. *Transport in porous media*, 84:241–256, 2010.

[32] A. C. Baytas and I. Pop. Free convection in a square porous cavity using a thermal nonequilibrium model. *International Journal of Thermal Sciences*, 41:861–870, 2002.

[33] D. S. Rees. The convection of a bingham fluid in a differentially-heated porous cavity. *International Journal of Numerical Methods for Heat & Fluid Flow*, 26:879–896, 2016.

[34] F. Chen and C. F. Chen. Onset of finger convection in a horizontal porous layer underlying a fluid layer. *Journal of Heat Transfer*, 110:403–409, 1988.

[35] D. A. Nield. Onset of convection in a fluid layer overlying a layer of a porous medium. *Journal of Fluid Mechanics*, 81:513–522, 1977.

[36] D. R. Hewitt, J. A. Neufeld, and J. R. Lister. Stability of columnar convection in a porous medium. *Journal of Fluid Mechanics*, 737:205–231, 2013.

[37] K. Vafai. *Handbook of Porous Media*. New York: Crc Press, 2015.

[38] O. V. Trevisan and A. Bejan. Combined heat and mass transfer by natural convection in a porous medium. *Advances in Heat Transfer*, 20:315–352, 1990.

[39] H. Jeffreys. The stability of a layer of fluid heated below. *The London, Edinburgh, and Dublin Philosophical Magazine and Journal of Science*, 2:833–844, 1926.

[40] D. A. Nield. The thermohaline Rayleigh-Jeffreys problem. *Journal of Fluid Mechanics*, 29: 545–558, 1967.

[41] A. Mojtabi and M. C. Charrier-Mojta. Double-diffusive convection in porous media. *Handbook of Porous Media, Second Edition*, 2:287–338, 2005.

[42] B. T. Murray and C. F. Chen. Double-diffusive convection in a porous medium. *Journal of Fluid Mechanics*, 201:147–166, 1989.

[43] M. Mamou, P. Vasseur, and E. Bilgen. Double-diffusive convection instability in a vertical porous enclosure. *Journal of Fluid Mechanics*, 368:263–289, 1998.

[44] A. Bahloul, N. Boutana, and P. Vasseur. Double-diffusive and Soret-induced convection in a shallow horizontal porous layer. *Journal of Fluid Mechanics*, 491:325–352, 2003.

[45] S. K. Murthy, B. V. R. Kumar, P. Chandra, V. Sangwan, and M. Nigam. A study of double diffusive free convection from a corrugated vertical surface in a darcy porous medium under Soret and Dufour effects. *Journal of Heat Transfer*, 133:092601, 2011.

[46] M. Benzeghiba, S. Chikh, and A. Campo. Thermosolutal convection in a partly porous vertical annular cavity. *Journal of Heat Transfer*, 125:703–715, 2003.

[47] L. N. Da Costa, E. Knobloch, and N. O. Weiss. Oscillations in double-diffusive convection. *Journal of Fluid Mechanics*, 109:25–43, 1981.

[48] H. E. Huppert and D. R. Moore. Nonlinear double-diffusive convection. *Journal of Fluid Mechanics*, 78:821–854, 1976.

[49] T. Radko and D. P. Smith. Equilibrium transport in double-diffusive convection. *Journal of Fluid Mechanics*, 692:5–27, 2012.

[50] S. Mondal and P. Sibanda. Effects of buoyancy ratio on unsteady double-diffusive natural convection in a cavity filled with porous medium with non-uniform boundary conditions. *International Journal of Heat and Mass Transfer*, 85:401–413, 2015.

[51] N. Rudraiah and M. S. Malashetty. The influence of coupled molecular diffusion on double-diffusive convection in a porous medium. *Journal of Heat Transfer*, 108:872–876, 1986.

[52] N. Rudraiah and P. G. Siddheshwar. A weak nonlinear stability analysis of double diffusive convection with cross-diffusion in a fluid-saturated porous medium. *Heat and Mass Transfer*, 33:287–293, 1998.

[53] P. L. Quere, J. A. C. Humphrey, and F. S. Sherman. Numerical calculation of thermally driven two-dimensional unsteady laminar flow in cavities of rectangular cross section. *Numerical Heat Transfer*, 4:249–283, 1981.

[54] A. J. Chamkha and H. Al-Naser. Double-diffusive convection in an inclined porous enclosure with opposing temperature and concentration gradients. *International Journal of Thermal Sciences*, 40:227–244, 2001.

[55] G. Wang, Q. Wang, M. Zeng, and H. Ozoe. Numerical study of natural convection heat transfer in an inclined porous cavity with time-periodic boundary conditions. *Transport in Porous Media*, 74:293–309, 2008.

[56] O. Polat and E. Bilgen. Laminar natural convection in inclined open shallow cavities. *International Journal of Thermal Sciences*, 41:360–368, 2002.

[57] K. M. Khanafer and A. J. Chamkha. Hydromagnetic natural convection from an inclined porous square enclosure with heat generation. *Numerical Heat Transfer, Part A Applications*, 33:891–910, 1998.

[58] D. A. Nield and A. V. Kuznetsov. Local thermal non-equilibrium and heterogeneity effects on the onset of convection in a layered porous medium. *Transport in porous media*, 102: 1–13, 2014.

[59] D. A. Nield, A. V. Kuznetsov, A. Barletta, and M. Celli. The effects of double diffusion and local thermal non-equilibrium on the onset of convection in a layered porous medium: non-oscillatory instability. *Transport in Porous Media*, 107:261–279, 2015.

[60] S. Choi and J. A. Eastman. Enhancing thermal conductivity of fluids with nanoparticles. Technical report, Argonne National Lab., Illinois, USA, 1995.

[61] H. Masuda, A. Ebata, and K. Teramae. Alteration of thermal conductivity and viscosity of liquid by dispersing ultra-fine particles dispersion of AL_2O_2, SiO_2 and TiO_2 ultra-fine particles. *Netsu Bussei*, 7:227–233, 1993.

[62] J. Buongiorno. Convective transport in nanofluids. *Journal of Heat Transfer*, 128:240–250, 2006.

[63] D. Y. Tzou. Thermal instability of nanofluids in natural convection. *International Journal of Heat and Mass Transfer*, 51:2967–2979, 2008.

[64] A. V. Kuznetsov and D. A. Nield. Thermal instability in a porous medium layer saturated by a nanofluid: Brinkman model. *Transport in Porous Media*, 81:409–422, 2010.

[65] A. V. Kuznetsov and D. A. Nield. Effect of local thermal non-equilibrium on the onset of convection in a porous medium layer saturated by a nanofluid. *Transport in Porous Media*, 83:425–436, 2010.

[66] A. V. Kuznetsov and D. A. Nield. Natural convective boundary-layer flow of a nanofluid past a vertical plate: A revised model. *International Journal of Thermal Sciences*, 77:126–129, 2014.

[67] A. V. Kuznetsov and D. A. Nield. The ffect of local thermalnonequilibrium on the onset of convection in a porous medium layer saturated by a nanofluid: Brinkman model. *Journal of Porous Media*, 14:285–293, 2011.

[68] D. A. Nield and A. V. Kuznetsov. The onset of convection in a horizontal nanofluid layer of finite depth. *European Journal of Mechanics-B/Fluids*, 29:217–223, 2010.

[69] D. A. Nield and A. V. Kuznetsov. The Cheng-Minkowycz problem for natural convective boundary-layer flow in a porous medium saturated by a nanofluid. *International Journal of Heat and Mass Transfer*, 52:5792–5795, 2009.

[70] A. V. Kuznetsov and D. A. Nield. The onset of double-diffusive nanofluid convection in a layer of a saturated porous medium. *Transport in porous media*, 85:941–951, 2010.

[71] D. A. Nield and A. V. Kuznetsov. The onset of double-diffusive convection in a nanofluid layer. *International Journal of Heat and Fluid Flow*, 32:771–776, 2011.

[72] D. A. Nield and A. V. Kuznetsov. The onset of convection in a layer of a porous medium saturated by a nanofluid: Effects of conductivity and viscosity variation and cross-diffusion. *Transport in porous media*, 92:837–846, 2012.

[73] P. G. Siddheshwar and P. S. Titus. Nonlinear Rayleigh-Bénard convection with variable heat source. *Journal of Heat Transfer*, 135:122502, 2013.

[74] P. G. Siddheshwar, C. Kanchana, Y. Kakimoto, and A. Nakayama. Steady finite-amplitude Rayleigh-Bénard convection in nanoliquids using a two-phase model: Theoretical answer to the phenomenon of enhanced heat transfer. *Journal of Heat Transfer*, 139:012402, 2017.

[75] D. Yadav, G. S. Agrawal, and R. Bhargava. The onset of convection in a binary nanofluid saturated porous layer. *International Journal of Theoretical and Applied Multiscale Mechanics*, 2:198–224, 2012.

[76] M. Narayana, P. Sibanda, P. G. Siddheshwar, and G. Jayalatha. Linear and nonlinear stability analysis of binary viscoelastic fluid convection. *Applied Mathematical Modelling*, 37:8162–8178, 2013.

[77] S. Agarwal, P. Rana, and B. S. Bhadauria. Rayleigh–Bénard convection in a nanofluid layer using a thermal nonequilibrium model. *Journal of Heat Transfer*, 136:122501, 2014.

[78] D. A. Nield and A. V. Kuznetsov. The effect of vertical throughflow on thermal instability in a porous medium layer saturated by a nanofluid: a revised model. *Journal of Heat Transfer*, 137:052601, 2015.

[79] J. C. Umavathi and J. P. Kumar. Onset of convection in a porous medium layer saturated with an Oldroyd-B nanofluid. *Journal of Heat Transfer*, 139:012401, 2017.

[80] P. A. L. Narayana, P. S .N. Murthy, and R. S. R. Gorla. Soret-driven thermosolutal convection induced by inclined thermal and solutal gradients in a shallow horizontal layer of a porous medium. *Journal of Fluid Mechanics*, 612:1–19, 2008.

[81] D. A. S. Rees, A. P. Bassom, and P. G. Siddheshwar. Local thermal non-equilibrium effects arising from the injection of a hot fluid into a porous medium. *Journal of Fluid Mechanics*, 594:379–398, 2008.

[82] C. Siddheshwar, P. G .and Siddabasappa. Linear and weakly nonlinear stability analyses of two-dimensional, steady brinkman-bénard convection using local thermal non-equilibrium model. *Transport in Porous Media*, 120:605–631, 2017.

[83] D. A. S. Rees and A. P. Bassom. The onset of Darcy-Bénard convection in an inclined layer heated from below. *Acta Mechanica*, 144:103–118, 2000.

[84] J. S. Turner. *Buoyancy effects in fluids*. Cambridge: Cambridge University Press, 1979.

[85] N. Rudraiah. Double-diffusive magnetoconvection. *Pramana*, 27:233–266, 1986.

[86] W. Bian, P. Vasseur, E. Bilgen, and F. Meng. Effect of an electromagnetic field on natural convection in an inclined porous layer. *International Journal of Heat and Fluid Flow*, 17: 36–44, 1996.

[87] C. Revnic, T. Grosan, I. Pop, and D. B. Ingham. Magnetic field effect on the unsteady free convection flow in a square cavity filled with a porous medium with a constant heat generation. *International Journal of Heat and Mass Transfer*, 54:1734–1742, 2011.

[88] M. A. Mansour, A. J. Chamkha, R. A. Mohamed, M. M. A. El-Aziz, and S. E. Ahmed. Mhd natural convection in an inclined cavity filled with a fluid saturated porous medium with heat source in the solid phase. *Nonlinear Analysis: Modelling and Control*, 15:55–70, 2010.

[89] M. R. E. Proctor and N. O. Weiss. Magnetoconvection. *Reports on Progress in Physics*, 45: 1317, 1982.

[90] M. Narayana, S. N. Gaikwad, P. Sibanda, and R. B. Malge. Double diffusive magneto-convection in viscoelastic fluids. *International Journal of Heat and Mass Transfer*, 67: 194–201, 2013.

[91] D. Yadav, R. Bhargava, and G. S. Agrawal. Thermal instability in a nanofluid layer with a vertical magnetic field. *Journal of Engineering Mathematics*, 80:147–164, 2013.

[92] U. Gupta, J. Sharma, and V. Sharma. Instability of binary nanofluids with magnetic field. *Applied Mathematics and Mechanics*, 36:693–706, 2015.

[93] K. J. A. Van, A. H. Nielsen, J. J. Rasmussen, and B. Stenum. Shear flow instability in a rotating fluid. *Journal of Fluid Mechanics*, 387:177–204, 1999.

[94] C. Hunter and N. Riahi. Nonlinear convection in a rotating fluid. *Journal of Fluid Mechanics*, 72:433–454, 1975.

[95] S M Cox and P C Matthews. Instability of rotating convection. *Journal of Fluid Mechanics*, 403:153–172, 2000.

[96] S. Agarwal, B. S. Bhadauria, and P. G. Siddheshwar. Thermal instability of a nanofluid saturating a rotating anisotropic porous medium. *Special Topics & Reviews in Porous Media: An International Journal*, 2:53–64, 2011.

[97] R. Chand and G. C. Rana. On the onset of thermal convection in rotating nanofluid layer saturating a Darcy-Brinkman porous medium. *International Journal of Heat and Mass Transfer*, 55:5417–5424, 2012.

[98] D. Yadav, D. Lee, H. Cho, and J. Lee. The onset of double-diffusive nanofluid convection in a rotating porous medium layer with thermal conductivity and viscosity variation: a revised model. *Journal of Porous media*, 19:31–46, 2016.

[99] X. Liao, K. Zhang, and Y. Chang. On boundary-layer convection in a rotating fluid layer. *Journal of Fluid Mechanics*, 549:375–384, 2006.

[100] R. Chand and G. C. Rana. Magneto convection in a layer of nanofluid in porous medium a more realistic approach. *Journal of Nanofluids*, 4:196–202, 2015.

[101] U. Gupta, J. Ahuja, and R. K. Wanchoo. Magneto convection in a nanofluid layer. *International Journal of Heat and Mass Transfer*, 64:1163–1171, 2013.

[102] A. M. Soward. Thermal and magnetically driven convection in a rapidly rotating fluid layer. *Journal of Fluid Mechanics*, 90:669–684, 1979.

[103] J. J. Sanchez-Alvarez, E. C. Del Arco, and F. H. Busse. Onset of wall attached convection in a rotating fluid layer in the presence of a vertical magnetic field. *Journal of Fluid Mechanics*, 600:427–443, 2008.

[104] S. M. Cox and P. C. Matthews. New instabilities in two-dimensional rotating convection and magnetoconvection. *Physica D: Nonlinear Phenomena*, 149:210–229, 2001.

[105] D. Yadav, R. Bhargava, G.S. Agrawal, G. S. Hwang, J. Lee, and M. C. Kim. Magnetoconvection in a rotating layer of nanofluid. *Asia-Pacific Journal of Chemical Engineering*, 9:663–677, 2014.

[106] D. Yadav, R. Bhargava, and G. S. Agrawal. Numerical solution of a thermal instability problem in a rotating nanofluid layer. *International Journal of Heat and Mass Transfer*, 63: 313–322, 2013.

[107] C. T. Duba, M. Shekar, M. Narayana, and P. Sibanda. Soret and Dufour effects on thermohaline convection in rotating fluids. *Geophysical & Astrophysical Fluid Dynamics*, 110: 317–347, 2016.

[108] D. Yadav, J. Wang, R. Bhargava, J. Lee, and H. H. Cho. Numerical investigation of the effect of magnetic field on the onset of nanofluid convection. *Applied Thermal Engineering*, 103:1441–1449, 2016.

[109] G. Venezian. Effect of modulation on the onset of thermal convection. *Journal of Fluid Mechanics*, 35:243–254, 1969.

[110] M. N. Roppo, S. H. Davis, and S. Rosenblat. Bénard convection with time-periodic heating. *The Physics of Fluids*, 27:796–803, 1984.

[111] B. S. Bhadauria, P. G. Siddheshwar, and O. P. Suthar. Nonlinear thermal instability in a rotating viscous fluid layer under temperature/gravity modulation. *Journal of Heat Transfer*, 134:102502, 2012.

[112] P. Kiran and B. S. Bhadauria. Weakly nonlinear oscillatory convection in a rotating fluid layer under temperature modulation. *Journal of Heat Transfer*, 138:051702, 2016.

[113] B. S. Bhadauria. Combined effect of temperature modulation and magnetic field on the onset of convection in an electrically conducting-fluid-saturated porous medium. *Journal of Heat Transfer*, 130:052601, 2008.

[114] B. S. Bhadauria. Magnetofluidconvection in a rotating porous layer under modulated temperature on the boundaries. *Journal of Heat Transfer*, 129:835–843, 2007.

[115] B. S. Bhadauria. Time-periodic heating of Rayleigh-Bénard convection in a vertical magnetic field. *Physica Scripta*, 73:296, 2006.

[116] B. S. Bhadauria and P. Kiran. Chaotic and oscillatory magneto-convection in a binary viscoelastic fluid under g-jitter. *International Journal of Heat and Mass Transfer*, 84:610–624, 2015.

[117] P. G. Siddheshwar, B. S. Bhadauria, and A. Srivastava. An analytical study of nonlinear double-diffusive convection in a porous medium under temperature/gravity modulation. *Transport in Porous Media*, 91:585–604, 2012.

[118] O. P. Suthar, P. G. Siddheshwar, and B. S. Bhadauria. A study on the onset of thermally modulated Darcy-Bénard convection. *Journal of Engineering Mathematics*, 101:175–188, 2016.

[119] B. S. Bhadauria and P. Kiran. Weakly nonlinear oscillatory convection in a viscoelastic fluid saturating porous medium under temperature modulation. *International Journal of Heat and Mass Transfer*, 77:843–851, 2014.

[120] P. G. Siddheshwar, G. N. Sekhar, and G. Jayalatha. Effect of time-periodic vertical oscillations of the Rayleigh–Bénard system on nonlinear convection in viscoelastic liquids. *Journal of Non-Newtonian Fluid Mechanics*, 165:1412–1418, 2010.

[121] P. G. Siddheshwar and A. Abraham. Rayleigh-Benard convection in a dielectric liquid: imposed time-periodic boundary temperatures. *Chamchuri Journal of Mathematics*, 1:105–121, 2009.

[122] P. S. Stephen. Low viscosity magnetic fluid obtained by the colloidal suspension of magnetic particles, 1965. US Patent 3,215,572.

[123] R. E. Rosensweig. *Ferrohydrodynamics*. New York: Courier Corporation, 2013.

[124] B. A. Finlayson. Convective instability of ferromagnetic fluids. *Journal of Fluid Mechanics*, 40:753–767, 1970.

[125] L Schwab, U Hildebrandt, and K Stierstadt. Magnetic Bénard convection. *Journal of Magnetism and Magnetic Materials*, 39:113–114, 1983.

[126] P. J. Stiles and M. Kagan. Thermoconvective instability of a horizontal layer of ferrofluid in a strong vertical magnetic field. *Journal of Magnetism and Magnetic Materials*, 85:196–198, 1990.

[127] C. L. Russell, P. J. Blennerhassett, and P. J. Stiles. Large wave number convection in magnetized ferrofluids. *Journal of Magnetism and Magnetic Materials*, 149:119–121, 1995.

[128] I. S. Shivakumara, J. Lee, and C. E. Nanjundappa. Onset of thermogravitational convection in a ferrofluid layer with temperature dependent viscosity. *Journal of Heat Transfer*, 134: 012501, 2012.

[129] S. Venkatasubramanian and P. N. Kaloni. Effects of rotation on the thermoconvective instability of a horizontal layer of ferrofluids. *International Journal of Engineering Science*, 32: 237–256, 1994.

[130] S. Aniss, M. Belhaq, and M. Souhar. Effects of a magnetic modulation on the stability of a magnetic liquid layer heated from above. *Journal of Heat Transfer*, 123:428–433, 2001.

[131] C. E. Nanjundappa and I. S. Shivakumara. Effect of velocity and temperature boundary conditions on convective instability in a ferrofluid layer. *Journal of Heat Transfer*, 130: 104502, 2008.

[132] A. Sharma, P. K. Bharti, and R. G. Shandil. Linear stability of double-diffusive convection in a micropolar ferromagnetic fluid saturating a porous medium. *International Journal of Mechanical Sciences*, 49:1047–1059, 2007.

[133] R. Mittal and U. S. Rana. Effect of dust particles on a layer of micropolar ferromagnetic fluid heated from below saturating a porous medium. *Applied Mathematics and Computation*, 215:2591–2607, 2009.

[134] P. Vadasz. Stability of free convection in a rotating porous layer distant from the axis of rotation. *Transport in Porous Media*, 23:153–173, 1996.

[135] P. Vadasz and S. Olek. Transitions and chaos for free convection in a rotating porous layer. *International Journal of Heat and Mass Transfer*, 41:1417–1435, 1998.

[136] S. S. Motsa, P. Dlamini, and M. Khumalo. A new multistage spectral relaxation method for solving chaotic initial value systems. *Nonlinear Dynamics*, 72:265–283, 2013.

[137] C. Canuto, M. Y. Hussaini, A. Quarteroni, and J. A. Thomas. *Spectral Methods in Fluid Dynamics*. Berlin: Springer Science & Business Media, 2012.

[138] L. N. Trefethen. *Spectral Methods in MATLAB*. Philadelphia: Siam, 2000.

Appendix

A.1 Errata to Chapter 3

- Page 47, Line 1: "supreme" should be replaced with "great"
- Page 47, Line 4: "fluid" should be replaced with "fluids".
- Page 48, Last paragraph, line 8: "exchanges" should be replaced with "exchangers".
- Page 48, Last paragraph, line 11: "The recent" should be replaced with "The recently developed".
- Page 48, Last paragraph, line 12: the statement "compared to older methods such as the finite difference methods" should be removed.
- Page 49, Paragraph 1, line 5: the inequality "$T_h > T_c$" should be replaced with "$T_h < T_c$".
- Page 49, Paragraph 1, line 7: "momentum equation" should be replaced with "momentum equations".
- Page 49, Equation 6 and 7 : "$V = 0$" should be replaced with "$V = \mathbf{0}$", where $\mathbf{0}$ is zero vector.
- Page 51, Equations 15-21: "commas" should be inserted in equations 15-21.
- Page 55, Equation 45: "fullstop" should be inserted in equation 45

A.1 Errata to Chapter 4

- Page 68, Introduction, line 5: "Double diffusive" should be replaced with "Double-diffusive".
- Page 69, Paragraph 3, lines 5 and 12: "Double diffusive" should be replaced with "Double-diffusive".
- Page 69, Paragraph 4, 2nd from the last line: "contradictory" should be replaced with "contrary".
- Page 70, Paragraph 2, lines 1 and 3: "double diffusive" should be replaced with "Double-diffusive".
- Page 70, Section 2, line 4: "anticlockwise direction" should be replaced with "anticlockwise direction, see Fig.1".
- Page 70, Section 2, line 8 : the statement, "given as follows (see Fig.1)" should delete "(see Fig.1)"
- Page 70, Fig.1 : The angles ϕ and φ should be switched to ϕ being the angle of inclination of the magnetic field and φ being the angle of inclination of the square cavity.
- Page 70, Fig.1 : The derivative boundary conditions for C and T should be replaced with $\frac{dC}{dy} = \frac{dT}{dy} = 0$.
- Page 70, Fig.1: The zero velocity boundary conditions should be removed.
- Page 76, Equations 52 and 53: "fullstop" should be inserted in equation 52 and "comma" should be inserted in equation 53
- Page 78, Equations 58 and 61: "commas" should be inserted in equation 58 and 61
- Page 85, Fig.14: The values of "$\varphi = 135^\circ$" and "$\phi = 90^\circ$" should be replaced with"$\varphi = 90^\circ$" and "$\phi = 135^\circ$".

- Page 86, Conclusion 3: "The streamlines are seen to be weak when $\phi = 45^{\circ}$ but stronger ...." must change to "For a limited inclination angle of the magnetic angle ϕ, the streamlines are seen to be weak when $\phi = 45^{\circ}$, but stronger for higher values of ϕ that $\phi = 45^{\circ}$".

A.3 Errata to Chapter 5

- Page 91,Equation 2: The notation "$C_{V.H}$" should be replaced with "$C_{V,H}$"
- Page 91, Equation 6: "$\mathbf{M} = \frac{\mathbf{H}}{H}\mathbf{M}(M,T)$" should be replaced with "$\mathbf{M} = \frac{\mathbf{H}}{H} \cdot \mathbf{M}(M,T)$".
- Page 92, Equation 9: The parentheses) after Ω should be deleted it.
- Page 92, Equation 10 :"$V = 0$" should be replaced with "$V = \mathbf{0}$", where $\mathbf{0}$ is zero vector.
- Page 92, Equation 16: ζ' and w' should be denotes the vorticity and velocity in z-direction of the fluid.
- Page 94: "comma" should be inserted in the equation of the classical critical wavenumber
- Page 96, after Equation 78: "comma" should be inserted in equation after equation 78
- Page 97: "comma" should be inserted in the inequalities
- Page 97, Equation 86: "comma" should be inserted in equation 86
- Page 98: Equation 87-91: "commas" should be inserted in equations 87-91